Department of Electromagnetism and Physics of Matter &
Institute *Carlos I* for Theoretical and Computational Physics,
University of Granada, Spain.

Interplay between Network Topology and Dynamics in Neural Systems

Samuel Johnson

Ph.D. Thesis

Advisors: Joaquín J. Torres Agudo
& Joaquín Marro Borau

Granada, April 2011

Dedicated to my family

Acknowledgements

Aunque hay muchas más personas a las que estoy agradecido, por tantas cosas, de las que puedo enumerar en un espacio razonable, trataré de poner el umbral en algún sitio y mencionar explícitamente sólo a aquellas que me han ayudado de alguna manera directa con esta tesis. En primer lugar quiero hacer constar mi sincero agradecimiento a mis directores: Joaquín Torres no sólo es quien me introdujo al caos, los fractales, el SOC, las redes, la simulación... sino el que me mostró que la neurociencia es algo tan concreto y estudiable como la física estadística; Joaquín Marro, por su parte, al compartir conmigo su genial perspectiva sobre la ciencia y la complejidad, me ha abierto los ojos a toda una manera de ver el mundo. Miguel Ángel Muñoz ha sido también una influencia cientfífica importantísima, con su maravillosa combinación de talento y buen humor. Agradezco también a tod@s l@s demás compañer@s con quienes he trabajado y convivido estos años, tanto por lo que he aprendido de ellos como por los muchos buenos ratos: Pablo Hurtado, Pedro Garrido, Paco de los Santos, Antonio Lacomba, Elvira Romera, Ramón Contreras, Paco Ramos, Jesús Cortés, Juan Antonio Bonachela, Luca Donetti, José Manuel Martín, Omar al-Hammal, Jesús del Pozo, Carlos Espigares, Clara Guglieri, Pablo Sartori, Marina Manrique, Jordi Hidalgo, Virginia Domínguez, Jorge Mejías, Sebastiano de Franciscis, Alejandro Pinto, Leticia Rubio, Jordi Garces, Luca Sabino, Simone Pigolotti, Luís Seoane, Daniele Vilone y Miguel Ibáñez. Como bien sabéis, sois compañer@s mucho más que de trabajo, siéndolo también, según el caso, de piso, de grupo musical, de decrepitud, de juegos diversos, del alma... Por supuesto, hay otras personas con esta multiplicidad de roles a quienes sin embargo no voy a tratar de nombrar aquí: por favor, no penséis que es por falta de reconocimiento, sino por ahorrar papel y tinta, y porque de todas maneras seguramente no vayáis a leer esto.

I'm grateful to Mike Ramsey, Mohammed Boudjada and Helmut Rucker for treating me so well in Graz as well as introducing me to the world of research. Doy gracias a Marcelo del Castillo por invitarme a la UNAM y por ser, junto

con su familia y amig@s, tan buen anfitrión en México; a Ezequiel Albano, Gabriel Baglietto, Belén Moglia, Nara Guisoni y Luis Diambra por tratarme tan bien en La Plata; and to Nick Jones and Sumeet Agarwal for making me so welcome in Oxford. I am also grateful to all the people who have helped in one way or another with my research, be it reading manuscripts, providing data, suggesting ideas, or simply with stimulating conversations. I'm probably leaving many deserving people out when I mention Dante Chialvo, Álex Arenas, Ginestra Bianconi, Yamir Moreno, Jennifer Dunne, Alberto Pascual, Víctor Eguíluz, Sasha Goltsev, Gorka Zamora, Lars Rudolf, Sabine Hilfiker, Tiago Peixoto, Ole Paulsen and Peter Latham. También estoy agradecido a Juan Soler, Alberto Prieto, Juan Calvo, Pilar Guerrero, Irene Mendoza, Estrella Ryan, Luna Álvarez, Javier (Chancly) Pascual, Nikolina Dimitrov, Felisa Torralba y Caroline de Cannart por su diversa ayuda. Three members of my family who have been particularly influential on my scientific interests and helpful in various ways are my uncle Dave Jones, my grandfather Tony Jones, and my aunt Sue Ziebland.

Cécile Poirier, qui as été avec moi pendant la plus part de ces dernières quatre ans, tu m'as fait surmonter tant d'obstacles et m'as aidé tellement que je n'ai vraiment pas de mots pour te remercier assez. And the mental freedom and emotional basis I need to undertake this or any other project is grounded in the unconditional support and love from my parents, Jenni and Alan, and my sisters, Jazz and Abby. Thanks so much to all of you.

Finally, thanks are also due to the government of the United States for its perseverance in attempting to crush the news organization Wikileaks, whose continual publication of enlightening documents so often kept me from working on this thesis; and to myself, for at all times resisting the temptation of perfectionism when writing this up – as the reader will no doubt observe.

"To say that a man is made up of certain chemical elements is a satisfactory description only for those who intend to use him as a fertilizer."

Hermann Joseph Muller

"Je n'avais pas besoin de cette hypothèse-là."

Pierre-Simon Laplace

"Research is what I'm doing when I don't know what I'm doing."

Werner von Braun

Abstract

This thesis is a compendium of research which brings together ideas from the fields of Complex Networks and Computational Neuroscience to address two questions regarding neural systems:
1) How the activity of neurons, via synaptic changes, can shape the topology of the network they form part of, and
2) How the resulting network structure, in its turn, might condition aspects of brain behaviour.
Although the emphasis is on neural networks, several theoretical findings which are relevant for complex networks in general are presented – such as a method for studying network evolution as a stochastic process, or a theory that allows for ensembles of correlated networks, and sets of dynamical elements thereon, to be treated mathematically and computationally in a model-independent manner. Some of the results are used to explain experimental data – certain properties of brain tissue, the spontaneous emergence of correlations in all kinds of networks... – and predictions regarding statistical aspects of the central nervous system are made. The mechanism of Cluster Reverberation is proposed to account for the near-instant storage of novel information the brain is capable of.

Preamble: The Ant, the Grasshopper and Complexity

Once upon a time, in a charming and peaceful little valley, a grasshopper sat under the shade of a sunflower, idly strumming up a tune, when a young worker ant came into view. The grasshopper watched as she trundled her way laboriously up an incline under the weight of a large piece of leaf. When she was close enough, he hailed her:

'Ahoy there, friend. I hope I won't seem tactless if I point out what a singularly cumbersome bit of leaf you have there. Would you not rather put it down for a while and join me for a quick jam session? You could bang along on some twigs or something.'

'Thank you for the offer, but I must continue on my way,' replied the ant, glancing up in slight surprise at being thus addressed.

'Oh, what a pity,' the grasshopper rejoined. 'And where, if I may be so bold as to inquire, would you be taking your rather unappetising ration of cellulose?'

'Well, I can't say I really know... I just follow this trail of pheromones I've come across. I'm sure it's for some noble purpose though.'

'Ah, that must be reassuring. And I suppose when you get to wherever it is you don't know you're going you intend to eat your bit of leaf...'

'Oh no, I can't digest something like this – who do you take me for?'

'You can't? Well, how strange...'

'What's strange?'

'However did an animal evolve which, instead of engaging in biologically reasonable (not to mention enjoyable) activities, such as playing music to attract sexual partners, prefers to lug useless bits of leaf about? How on earth can that serve to spread your genes?'

'I'm not interested in music or sex, whatever those are. I just follow simple rules, like all my identical sisters. You could say we're automata.'

'Thanks, I was going to but wasn't sure whether you'd be offended. Well, let

me wish you an agreeable day of toil, you frigid little automaton.'

With that, the grasshopper gave a big leap into the air, slightly exasperated by the folly so often displayed by his fellow insects. Looking down, he spotted a few more ants, all carrying leaves in the same direction as the one he had just met. Intrigued, he fluttered slightly higher (since grasshoppers can, actually, fly, if not all that well). He realised the ants were all heading for a nest some way off. In fact, there were many ant trails leading to various sources of food. It dawned on the grasshopper that although the individual ants were just boring little morons idiotically following rules, the nest as a whole was managing to find the closest leaves, bring them back along optimal routes, and feed them to its plantations of fungi. The colony was behaving like an intelligent organism, in some respects not so different from he himself, who functioned thanks to the cells of his body – each with the same genome, like the ants – cooperating through the obedience to relatively simple rules.

This thought impressed the grasshopper very much, driving him to flutter even higher so as to see things in greater perspective. From there he considered the apparently fragile web of trophic, parasitical and symbiotic interactions linking all the living beings in the valley – a network which nonetheless must have evolved a particularly robust structure not to shatter at the first environmental fluctuation. He became so enthralled by the idea of such complexity on one scale emerging from simplicity on another that he didn't even pay any attention to an attractive young grasshopperess making her wanton way just below him. Instead, he couldn't help fearing that a butterfly he noticed gently flapping his wings would probably set off a hurricane somewhere. As he flew ever higher, he began to see snowflakes glide by, overwhelmingly intricate and beautiful patterns self-organised out of the simplest little water molecules. Finally he was so high that he began to reflect on how the very stellar systems, galaxies, clusters, superclusters, filaments of galaxies... – of which his whole world was but an infinitesimal component – also interacted with each other via the simple rules of gravity and pressure to form objects marvellous beyond conception.

What he didn't notice until it was too late, as he left behind the cosy protection of the atmosphere, was how ultraviolet sunlight and ionising cosmic rays were steadily burning his wings each to a crisp. Beginning to fall, he

only hoped he would have time to consider the several morals to his tragic tale.

After a while spent plummeting to his doom he realised that, the freefall terminal velocity and life expectancy of a grasshopper being what they respectively were, he would most likely die peacefully of old age somewhere along his way down – never again contemplating his Edenic valley except, like some prophetic locust, from afar.

Contents

List of Figures

List of Tables

Chapter 1

Resumen en español

Paradigma de sistema complejo y el peor comprendido de nuestros órganos, el cerebro es, esencialmente, una inmensa red de células que se comunican entre sí mediante señales electro-químicas. Este trabajo recoge y desarrolla ideas del joven campo de las Redes Complejas para tratar de mejorar nuestro entendimiento acerca del comportamiento colectivo complejo que puede emerger en las redes de neuronas a partir de dinámicas individuales relativamente sencillas.

El Capítulo 2 es una breve introducción a las Redes Complejas y a la Neurociencia Computacional. Se describe, entre otras cosas, el modelo de Hopfield de red neuronal atractora, en que cada nodo representa una neurona y las sinapsis son representadas por los enlaces. Este sistema puede almacenar información, en forma de patrones o configuraciones concretas de neuronas activas e inactivas, en los *pesos sinápticos*; es decir, en la intensidad con la que la actividad de una neurona influye sobre sus vecinas. Si, para representar un patrón dado, dos neuronas vecinas han de adoptar el mismo estado (activo o inactivo), se refuerza la interacción entre ambas, mientras que se debilita en caso contrario. Repitiendo esta operación para cada pareja conectada de neuronas y para cada patrón, estos patrones se convierten en los estados que minimizan la energía total (atractores de la dinámica), y el sistema evoluciona siempre hacia el patrón que más se parezca a su estado inicial. Este mecanismo, llamado de *memoria asociativa*, es la responsable del almacenaje y la recuperación de información tanto en modelos más realistas de medios neuronales, como en muchos aparatos artificiales que desempeñan tareas tales como la identificación y la clasificación de imágenes. Además, hoy en día existen evidencias experimentales suficientes para asegurar que algo parecido ocurre en el cerebro: mediante los procesos bioquímicos de potenciación de

largo plazo (LTP, por sus siglas en inglés) y depresión de largo plazo (LTD), las sinapsis modifican gradualmente sus conductancias durante el aprendizaje.

El Capítulo 3 aborda el problema de cómo puede desarrollarse una red con el tipo de estructuras que se observa en el cerebro. Para ello se formaliza como un proceso estocástico una red que evoluciona mediante cambios probabilísticos que dependen de cualquier manera de información local y global de los grados (números de vecinos) de los nodos, tal como se hace en la Ref. (Johnson et al., 2010a). Se considera que estas suposiciones son relevantes para el caso del cerebro ya que la arborización y la atrofia sinápticas dependen de la actividad eléctrica de la neurona en cuestión, que a su vez puede estar relacionada con el número de vecinos que tenga, y con la densidad sináptica media en la red. Se demuestra cómo esta situación viene descrita por una ecuación de Fokker-Planck, y se aplica a dos conjuntos de datos reales neurofisiológicos: por una parte, la curvas de *poda sináptica* (fuerte reducción de la densidad sináptica que sufre el córtex durante la infancia) de autopsias humanas pueden explicarse con unas suposiciones mínimas; por otra, varias magnitudes estadísticas de la red del anélido C. Elegans (distribución de grados, perfil de correlaciones, *clustering* o agrupamiento y camino mínimo medio) emergen con cierta precisión y de manera natural justo en la transición de fase que presenta el modelo. Esto da fuerza a la idea de que el sistema nervioso optimiza su rendimiento colocándose cerca de un punto crítico. Un caso parecido, en que los enlaces de la red, en vez de desaparecer o aparecer, son redirigidos estocásticamente, presentado en la Ref. (Johnson et al., 2009b), se describe en el Apéndice A.

El resto de la tesis se centra en los efectos que pueden tener sobre el comportamiento colectivo de sistemas de neuronas las características topológicas descritas en el Capítulo 3. Se sabe que la heterogeneidad de la distribución de grados de la red suele tener una influencia significativa en la dinámica de elementos conectados mediante sus enlaces. En el caso de redes neuronales de Hopfield, Torres *et al.* (Torres et al., 2004) demostraron que, en redes *libres de escala* (que son altamente heterogéneas), el rendimiento aumenta con la heterogeneidad. El Capítulo 4 examina el mismo efecto en una red neuronal que incluye otro ingrediente biológico: la *depresión sináptica*, gracias a la cual se observa una transición entre una fase de memoria estática a otra en que el sistema salta caóticamente entre los patrones guardados. Resulta que cerca de este punto crítico (el famoso Borde del Caos) la red es capaz de realizar una tarea dinámica necesaria para los seres vivos: reconocer, de entre varios patrones que tenga almacenados, uno dado que se le "enseñe" y retenerlo in-

definidamente después. Como demostramos en la Ref. (Johnson et al., 2008), la heterogeneidad de la distribución de grados de la red acerca el punto crítico a una región del espacio de parámetros en que apenas hay depresión sináptica. Teniendo en cuenta que esta depresión empeora la capacidad de memoria del sistema, se concluye que una red altamente heterogénea es la óptima para realizar este tipo de tarea dinámica. Las redes funcionales medidas en el córtex humano durante tareas del estilo adopta la red libre de escala más heterogéna posible, por lo que cabe la hipótesis de que el cerebro esté maximizando así su rendimiento.

Otra propiedad altamente estudiada de las redes complejas es la existencia de correlaciones entre los grados de nodos vecinos. Cuando dichas correlaciones son positivas (nodos muy conectados se suelen conectar con otros que también tienen muchos vecinos, y los que tienen pocos con otros parecidos) se dice que la red es *asortativa*; mientras que es *disasortativa* si las correlaciones son negativas (los que tienen muchas conexiones se conectan, preponderantemente, con los que tienen pocas). Curiosamente, se había observado que por lo general las redes sociales (por ejemplo, redes de colaboraciones profesionales o de contactos sexuales) son asortativas, mientras que prácticamente todas las demás (genéticas, tróficas, proteicas, de transportes, de palabras, Internet, la Web...) son significativamente disasortativas. Aunque se había estudiado los efectos de estas correlaciones en varios sistemas, las técnicas matemáticas y computacionales para ello padecían de inconvenientes que restaban generalidad a los resultados. Para solventar esto, en el Capítulo 5 se describe un nuevo método para particionar el espacio de las fases de redes en regiones de correlaciones iguales, una técnica que permite tanto análisis teórico como computacional de este tipo de sistemas. Utilizando este método junto con ideas de Teoría de la Información se demuestra también el resultado principal de la Ref. (Johnson et al., 2010b): que la disasortatividad es el estado "natural" (en cuanto a situación de equlibrio) de las redes heterogéneas, lo cual explica la preponderancia en la realidad de este tipo de configuraciones. La preferencia de los humanos por agregarse en función de propiedades similares sería la explicación de que las redes sociales se encuentren fuera del equilibrio, en regiones asortativas del espacio de fases.

En el Capítulo 6 se aplica el método del Capítulo 5 al caso de una red neuronal de Hopfield que no sólo presenta heterogeneidad, sino también correlaciones nodo-nodo. Se encuentra, como ya fue descrito en la Ref. (de Franciscis et al., 2011), que estos sistemas pueden aumentar de manera notable su

robustez frente a ruido gracias a las correlaciones positivas. De nuevo, esto parece encajar, al menos cualitativamente, con resultados experimentales que han encontrado redes funcionales en el córtex humano altamente asortativas.

Hemos dicho que las redes neuronales pueden aprender gracias a una apropiada modificación de los pesos sinápticos mediante LTP y LTD, lo que explica la memoria de largo plazo. Pero estos procesos bioquímicos ocurren en un tiempo característico de al menos minutos. Los modelos de memoria de corto plazo, que ocurren en escalas de tiempo menores, suelen dar por hecho que la información que se utiliza está de antemano almacenada en el cerebro, y que el sujeto realizando la tarea sólo ha de activar y mantener de alguna manera la configuración correcta (como en el Capítulo 4). Pero es fácil darse cuenta de que esto no puede ser el caso para cualquier tarea: basta mirar algo totalmente nuevo por un instante, cerrar los ojos, y pensar en lo que se ha visto. Los únicos modelos de memoria de corto plazo existentes que no requieren aprendizaje sináptico se basan en que cada neurona mantenga de alguna manera la información que le corresponde (típicamente gracias a una serie de procesos sub-celulares). Pero al no emerger la memoria como propiedad colectiva del sistema, sino como suma de memorias individuales, estos modelos padecen de una gran falta de robustez frente a ruido. Y, lejos de presentar un comportamiento individual fiable, las neuronas se caracterizan justamente por ser células de una alta variabilidad, con tendencia a disparar de manera más o menos aleatoria. En el Capítulo 7 se propone un mecanismo, llamado *Cluster Reverberation* (CR), o Reverberación de Grupo, gracias al cual incluso sistemas como redes con unidades simples, binarias, como en el modelo de Hopfield pueden almacenar información instantáneamente sin necesidad de aprendizaje sináptico, y de una manera que puede ser todo lo robusto frente a ruido como se quiera (Johnson et al., 2011). Para ello el sistema aprovecha la existencia de estados metastables (situaciones que minimizan la energía del sistema localmente, sin corresponder al mínimo global) y como consecuencia aparecen transitorios en la dinmica de la actividad neuronal cuyas propiedades son consecuencia inmediata de las características de la topología subyacente y que es del tipo de las descritas anteriormente en el Capítulo 3 y en experimentos, esto es, el grado de agrupamiento o la modularidad de la red. Básicamente, grupitos densamente interconectados de neuronas pueden mantener un estado conjunto de alta o baja actividad, en promedio. Considerando cada grupito como un elemento funcional elemental, en vez de cada neurona, se consigue la aparición de las propiedades requeridas. Es más, algunas otras características

de la memoria de corto plazo emergen de manera natural de este mecanismo. En particular, se demuestra que la información se pierde gradualmente con el tiempo según una ley aproximadamente potencial, como ha sido descrito en experimentos psicofísicos.

En conclusión, las principales aportaciones originales de esta Tesis son:

- Métodos analíticos y computacionales para estudiar redes evolutivas (Johnson et al., 2009b, 2010a) y redes con correlaciones nodo-nodo (Johnson et al., 2010b; de Franciscis et al., 2011).
- Una respuesta a la pregunta de por qué la mayoría de las redes reales son disasortativas (Johnson et al., 2010b).
- Propiedades topológicas que pueden optimizar el rendimiento de redes neuronales (Johnson et al., 2008; de Franciscis et al., 2011).
- Un mecanismo que pudiera estar detrás de la memoria de corto plazo (Johnson et al., 2011).

Chapter 2

Where we are and where we'd like to go

2.1 From bridges to brains

Strolling through the streets of Königsberg, a young Immanuel Kant may have wondered whether, as some hoped, a path could be found that would take him once and only once over each of the city's celebrated seven bridges and back to where he started. In 1736 Leonard Euler pointed out that for this or any other problem of the kind all that mattered was which land masses were connected to each other, and by how many bridges. In other words, the situation could be captured by a graph, as in Fig. 2.1, in which each land mass is represented by a node (also called vertex) and each bridge by a link (or edge). He showed that in the case of Königsberg no such walk could be found, since an "Eulerian cycle" in a connected graph exists if and only if the degrees of all nodes are even numbers – the degree of a node being its number of edges (Euler, 1736). And thus was Graph Theory born.

For over two centuries, the graphs people were interested in were precisely defined objects, usually sufficiently small to be drawn on a piece of paper. But in the late nineteen fifties, mathematicians began to study *random graphs* – i.e., defined only by some random generation process – perhaps with a view to better dealing with ever-growing communications networks (Bollobás, 2001). E. N. Gilbert considered a situation in which there are n nodes and each pair is connected by an edge with probability q (Gilbert, 1959). For different values of these parameters, he was able to obtain the likelihood of the graph being connected (that is, of there being a path joining any two nodes). A similar model was proposed by Paul Erdös and Alfréd Rényi: each of all the possible graphs

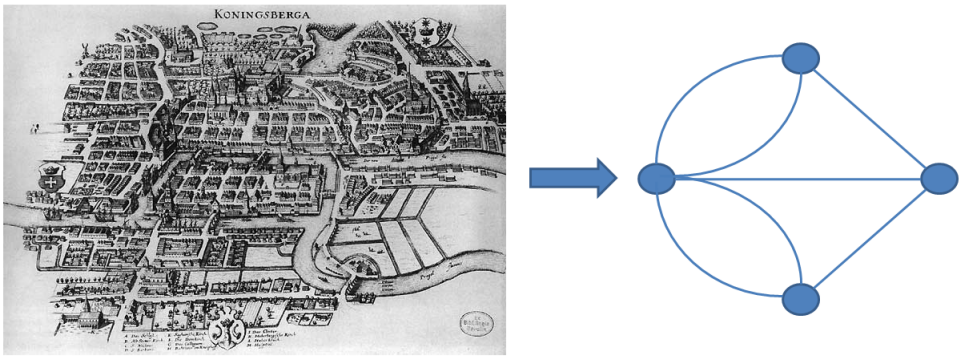

Figure 2.1: The problem of the Seven Bridges of Königsberg can be reduced to a graph in which nodes and edges represent land masses and bridges, respectively.

with n nodes and m edges had an equal chance of being "picked" (Erdös and Rényi, 1959). In fact, a given graph will be generated with equal probability in either scenario, so the descriptions are equivalent, and usually known as the Erdös-Rényi (ER) model. It is simple to see that if one were to average over many graphs generated by either of these processes, the degrees would follow a binomial distribution – tending, for large n, to a Poisson distribution. That is, $p(k)$ is symmetrically centred around its mean value and drops off exponentially – where k_i is the degree of node i. An interesting phenomenon that can be observed using the ER model is that of percolation. If we measure the size Φ of the *largest connected component* (that is, of the highest number of nodes in the graph forming a connected subgraph) we obtain at different values of the probability q (or, equivalently, of $m = \frac{1}{2}qn^2$), we see that there is a critical value, $q_c = 1/n$, above which Φ/n does not vanish for high n – that is, there will usually exist a connected subgraph of a size comparable to that of the whole system. This passing from one situation (or phase) to another, each characterised by some qualitatively different characteristic, is known in physics as a *phase transition*. In this case, it is a second-order transition, since the control parameter Φ varies continuously (and not abruptly, as in first-order transitions), and has innumerable applications. For instance, the nodes might be people susceptible to some disease, trees which may be set on fire, or oil bubbles in a porous medium. The epidemic will spread, the forest will burn, or the oil will be extractable if the density of edges – contagious contact, fire-conducting proximity, or links between pores – is over the critical value.

In his 1929 short story *Chains* (*Láncszemek*, in the original Hungarian) Frigyes Karinthy suggested that the number of people in a chain of acquaintances grows exponentially with size, and thus that very few steps are needed to join anyone with any other person. This Small World idea was taken up in 1967 by Stanley Milgram, who performed a series of experiments that, while somewhat less controversial than his well-known obedience-to-authority explorations, have nonetheless been widely discussed (Milgram, 1967). He and his colleagues sent various letters to random people with the request to attempt to send them on to a particular individual many thousands of miles away, plus the constraint that this had to be done via people with whom the sender was on first-name terms. Many of the letters reached their destination, after having been sent on by a surprisingly small number of intervening people. This was later popularised as the Six Degrees of Separation – the famous idea that any two people are linked by a path of only six acquaintances. Within the connected component of an ER random graph any two nodes are also joined by a short path – of the order of the logarithm of the number of nodes. However, this is less surprising, since these networks are not *clustered*; that is, they do not have the property typical of social networks whereby "the friends of my friends are (also likely to be) my friends." In 1998, Duncan Watts and Steven Strogatz put forward a network model which took this feature into account. They considered a ring of n nodes, each connected to their k nearest neighbours (they set $k = 4$). Each edge was then broken from one of its nodes and rewired to some other random node with a probability p. Thus, $p = 0$ leaves the ring intact, while $p = 1$ changes it into an ER random graph. Two magnitudes were measured for different values of p: the mean-minimum-path length, l, and the clustering coefficient, C. The first is simply an average over all pairs of nodes of the minimum-paths connecting them. The latter can be seen as the probability that two neighbours of a given node are directly connected to each other. For $p = 0$, the clustering is high ($C = \frac{1}{2}$) and independent of the network size, while the mean minimum path scales with n ($l \simeq n/8$). At the other extreme, $p = 1$ yields a vanishingly small clustering ($C = k/n$) but short paths ($l \simeq \ln n / \ln k$). The most interesting case is found at intermediate values of p. As p grows from zero, l falls very rapidly to a value close to the random case, but C does not present this drop until a much higher value is reached. Watts and Strogatz called this intermediate zone the Small-World region, since everyone is highly-interconnected while much of the local structure is conserved. They suggested that this is actually a property of many

real networks (as has since turned out to be the case (Newman, 2003c)), most especially of social networks – in which C is often several orders of magnitude greater than if the graph were random, while l is not much larger than in such a case. As the authors point out, it is essential to take this feature into account for the study of, say, epidemics.

Another feature of networks which is quite ubiquitous in the real world is that degree distributions are highly heterogeneous; in fact, they often follow power-laws, $p(k) \sim k^{-\gamma}$, with γ a positive constant typically between 2 and 3. Such networks are nowadays referred to as *scale free*. In the nineteen fifties, Herbet Simon showed that these distributions come about when "the rich get richer" (Simon, 1955). Applying this idea to the case of scientific citations, Derek de Solla Price proposed the first known model of a scale-free network, in which nodes represent papers and edges are citations (de S. Price, 1965). Each node has an in-degree (the number of papers citing it) and an out-degree (papers it cites). That is, the network is *directed*, since edges have a direction. Assuming that the probability a paper has of being cited by a new one is proportional to the number already citing it (its in-degree), the network is built up through the gradual addition of nodes, the neighbours of these being chosen according to their existing in-degrees. Price showed analytically that such a mechanism leads to an in-degree distribution $p(k) \sim k^{-(2+1/m)}$, with m a parameter of the model equivalent to the mean degree[1]. He called this mechanism *cumulative advantage*. Somewhat ironically – considering that Price, with a PhD in history from Cambridge, is best known as the father of scientometrics – this work was mostly ignored by the scientific community. The model was rediscovered in 1999 by Albert-László Barabási and Reka Albert, with the difference that they considered the network to be undirected (Barabási and Albert, 1999). They coined the term *preferential attachment* for the rich-get-richer mechanism, which is now generally assumed to be behind the formation of most scale-free networks (although other mechanisms exist (Caldarelli et al., 2002; Krapivsky et al., 2000; Newman, 2005)). Among many interesting consequences of such degree heterogeneity, Mark Newman showed that the clustering and mean-minimum-path length are respectively higher and lower than in homogeneous networks, making all scale-free networks to some extent small worlds (Newman, 2003b). It also has important consequences for dynamical processes taking place among elements on the network, such as the

[1]Note that in a directed network, the mean in-degree and mean out-degree coincide.

synchronisation of coupled oscillators (Barahona and Pecora, 2002).

As mentioned above, networks can be made up of separate components such that no path exists between nodes in different subgraphs. This is an extreme case of *community structure*. However, what is usually more interesting is the fact that communities may exist such that there is a higher density of edges within them than without, even if the network is connected (Girvan and Newman, 2002). These communities are also at times called modules or clusters (although this can create some confusion with the related but distinct idea of clustering referred to above). Given a network, one can make a partition – that is, divide the nodes up into groups – and calculate what proportion of the edges fall within these, compared with the random expectation. This measure is called the modularity of this partition, and sometimes one speaks of the modularity of a graph referring to that of the partition for which this value is maximum. Determining the community structure of empirical networks can often provide useful insights into aspects of the systems. For instance, the communities may correspond to functional groups in a metabolic network, or groups of people who share some trait. However, there are many problems related to making this kind of measurement. For one thing, there are so many possible partitions that even an ER random graph can have a fairly high modularity due simply to statistical fluctuations (Reichardt and Bornholdt, 2006). Then there is the fact that community structure can exist on may different levels – that is, the groups considered can be of any size – so one must usually consider a hierarchy of modules (Arenas et al., 2006). Furthermore, finding an optimal partition is an NP-Complete problem (Garey and Johnson, 1979), which makes comparing the modularity of each possible partition intractable in all but very small networks. For these and other reasons, in recent years much work has gone into finding efficient algorithms to determine the community structure of networks, albeit approximately (Girvan and Newman, 2002; Donetti and Muñoz, 2004; Blondel et al., 2008) – as well as into comparing the results offered by each approach (L. Danon et al., 2005).

Finally, another feature of networks worth mentioning arises when the nodes of a network are endowed with some property and this is reflected by the layout of the edges: the situation is called a *mixing pattern* (Newman, 2002, 2003a). For instance, people might tend to choose sexual partners who share certain characteristics, such as mother-tongue or self-defined race. In these cases the network is *assortative*, since nodes of a kind assort, or group together. However, if the property in question were, say, gender, then the same

graphs would be *disassortative* if most of the relations were heterosexual. In these cases the property can be considered discrete, but it can be continuous – for instance, people might assort according to age. An interesting case is when the property in question is the degree of each node, since it is then an entirely topological issue. The extent to which the degrees of neighbouring nodes are correlated – as given, for example, by Pearson's correlation coefficient (Newman, 2002) – is then a measure of the *assortativity* of the graph, being positive for assortative networks and negative for disassortative ones. It turns out that there is a striking universality in the nature of the degree-degree correlations displayed by real-world networks, whether natural or artificial: social networks, like the ones just described, tend to be assortative, while almost all other kinds of network are disassortative (Pastor-Satorras et al., 2001; Newman, 2003c). Often specific functional constraints can be found to justify correlations of one or other kind, but in Chapter 5 of this thesis the purely topological explanation put forward in Ref. (Johnson et al., 2010b) is described. In any case, the degree-degree correlations of a network can play a significant role in the behaviour of processes taking place thereon. For example, assortative networks have lower percolation thresholds and are more robust to targeted attack (Newman, 2003a), while disassortative ones make for more stable ecosystems and seem to be more synchronizable (Brede and Sinha).

All the aspects of networks mentioned in this brief overview, as well as many others, have been shown to be relevant for a wide range of complex systems (Albert and Barabási, 2002; Newman, 2003c; Boccaletti et al., 2006). Among these is the brain, a paradigm of complexity as well as the least understood of our organs. However, research focusing on how the collective behaviour of neural systems, as observed in mathematical models, is influenced by the topology of the underlying network is relatively scarce. This is perhaps due in part to the attention that other biological properties of the nervous system have tended to draw from the Computational Neuroscience community. Thanks to the flurry of activity that the field of Complex Networks has been enjoying over the last decade, this is a particularly good moment to undertake a more systematic analysis of how dynamics and topology are related in this kind of systems.

2.2 Neural networks in neuroscience

Ever since the publication of Santiago Ramón y Cajal's drawings of neurons – in his words, those "mysterious butterflies of the soul" – it has been clear that the nervous system is composed of a large number of such cells connected to one another to form a network (y Cajal, 1995). Long axons, ending in terminals which form synapses to the dendrites which branch out from neighbouring neurons, transmit *action potentials* (APs) – changes in the cellular membrane voltage – and enable neurons somehow to cooperate and give rise the astonishing emergent phenomenon called thought. One of these APs is formed each time the membrane electric potential of a neuron surpasses a threshold value, leading to the opening of a great many voltage-dependent ionic gates between the cell and the extra-cellular medium. In turn, the membrane potential of a given neuron is constantly affected by action potentials arriving from neighbouring neurons, and thus an extremely complex web of cellular signalling is achieved.

The first model neuron was proposed by McCulloch and Pitts (1943). This was simply an element that would return a Heaviside step function of the sum of its inputs. Sets of such "artificial neurons" could be used to implement any logical gate. Shortly after this, another important suggestion was made, this time by the psychologist Donald Hebb. Attempting to relate Pavlovian conditioning experiments with cellular plasticity, he conjectured, in 1949, the existence of some biological mechanism that would lead to neurons which repeatedly fired (i.e., let off action potentials) together becoming more strongly coupled (Hebb, 1949). The initiation and propagation of action potentials in individual neurons was first modelled mathematically by Alan L. Hodgkin and Andrew Huxley in 1952 by means of a set of nonlinear ordinary differential equations which took into account the various ion fluxes (Hodgkin and Huxley, 1952).

However, the concept of a neural network (as understood in theoretical and computational neuroscience) was partly inspired by mathematical models of *spin systems*. The first of these was the Ising model, put forward in 1920 by Wilhelm Lenz and studied by Ernst Ising with a view with a view to understanding phase transitions and magnets (Onsager, 1944; Brush, 1967). It was known that the spin of electrons conferred a magnetic moment to individual atoms, but it wasn't clear how exactly a very many such spins could self-organise into a large body producing a net magnetic field. By considering an infinite set of entities (spins) with possible values plus or minus one (up

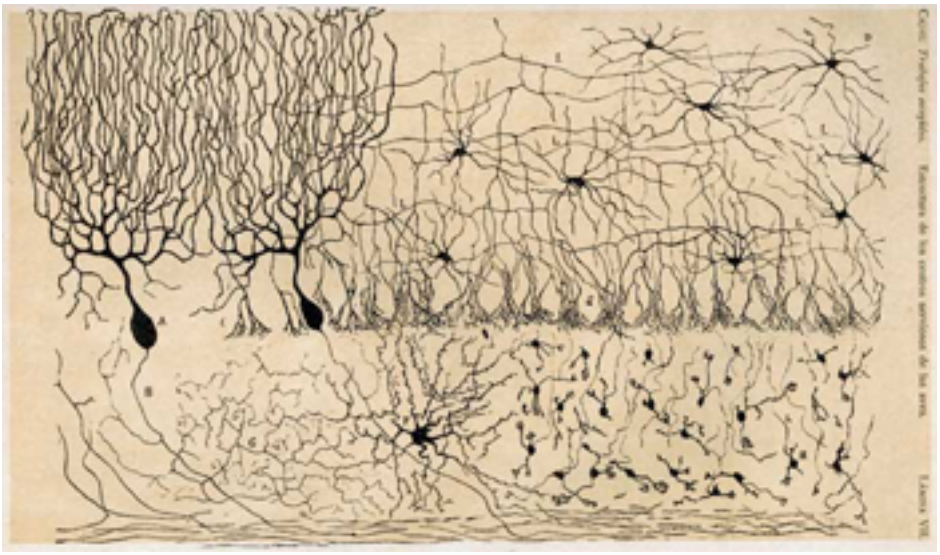

Figure 2.2: Drawing of the cells of the chick cerebellum, from "Estructura de los centros nerviosos de las aves", Madrid, 1905. Notice how the neurons make up a complex network of synaptic interactions.

or down, say) which, when placed at the nodes of a lattice, interact in such a way that energy is lowest when neighbours are aligned, and a temperature parameter to govern the extent of random fluctuations, it was eventually shown that, below a certain critical temperature (in two or more dimensions), symmetry is spontaneously broken and most of the spins end up aligned (Baxter, 1982). This *ferromagnetic* solution comes about and is then maintained because it has a lower energy than any other configuration of spins. Subsequent models, in particular that of Sherrington and Kirkpatrick (1975), incorporated inhomogeneities in the coupling strengths such that there was no longer a configuration which simultaneously minimized all interaction energies, leading to frustrated states (spin-glasses).

These ideas were put together, by Amari (1972) and then by Hopfield (1982), in the first neural network models to exhibit the mechanism known as *associative memory*. Each model neuron was placed at the node of a network, originally assumed to be fully connected (all nodes connected to all the rest), and followed a dynamics which can be seen either as that of Ising spins or of McCulloch-Pitts neurons. However, a noise parameter usually referred to as "temperature" by analogy with spin systems could be included to allow for non-deterministic behaviour. By setting the interaction strengths (synaptic weights) not randomly, as in the Sherrington-Kirkpatrick model, but according

to the Hebb rule referred to above, information could be stored and retrieved by the system. More specifically, a set of particular *patterns*, or configurations of positive and negative elements (firing and non-firing neurons), are recorded in the following way: for each pattern, one looks at each pair of neurons and adds a quantity to the weight of the synapse joining them if the pattern in question requires them to be in the same state, and subtracts it when they should be opposite. In this way, the minimum energy configurations correspond to the stored patterns, which therefore become attractors of the dynamics: if the temperature is not too heigh to destroy all order, the system will evolve towards whichever of these patterns most resembles the initial configuration it is placed in. Figure 2.3 illustrates how this mechanism works for a system such that the firing and non-firing neurons represent black and white pixels of a bitmap image.

Thanks to associative memory, if we were to store, say, a set of photos of various people and then "show" the network a different picture of one of the same subjects, it would be able to retrieve the correct identity. Not only is this mechanism used nowadays in technology capable of performing tasks such as pattern discrimination and classification, but it is widely considered to underlie our own capacity for learning and recalling information. There is evidence from neuronal readouts that this is so (Amit, 1995), and not long ago, *in vivo* experiments finally established that learning is indeed related to the processes of long term potentiation (LTP) and depression (LTD) – by which synapses between neurons that fire nearly simultaneously gradually increase or decrease their conductance depending on the interval of time elapsed (Gruart et al., 2006; Roo et al., 2008).

The neural network models studied nowadays generally include more realistic dynamics both for the neurons and for the synapses, taking into account a variety of cellular and subcellular processes (Amit, 1989; Torres and Varona, 2010). For example, the fact that the conductance of synapses in reality depends on their workload has been found to enable a network to switch from one pattern to another – either spontaneously or as a reaction to sensory stimuli – providing a means for the performance of dynamic tasks (Cortes et al., 2006; Holcman and Tsodyks, 2006); this result also seems to agree well with physiological data (Korn and Faure, 2003). In fact, there is evidence that the brain somehow maintains itself close to a boundary – called, in physics, a critical point – between an ordered and a chaotic regime (Eguíluz et al., 2005; Chialvo, 2004; Chialvo et al., 2008; Bonachela et al., 2010; Torres and Varona,

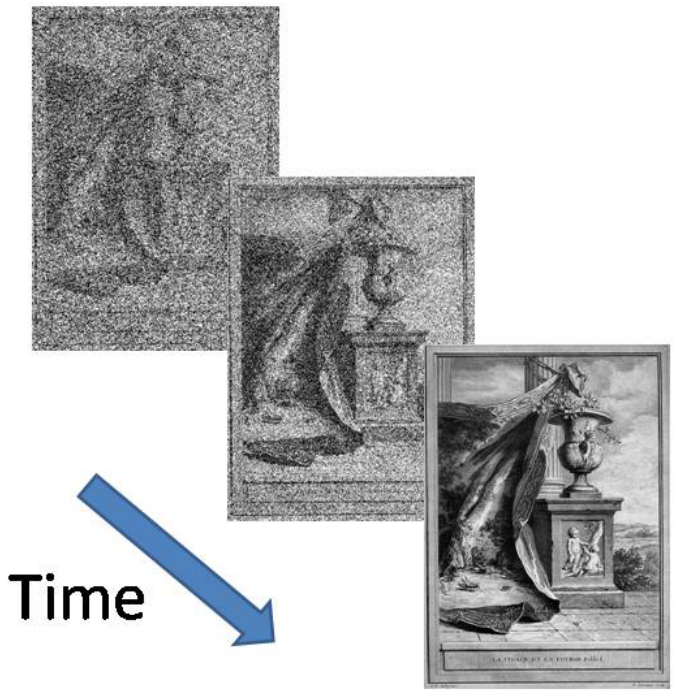

Figure 2.3: In the Hopfield neural-network model, the interaction strengths (representing synaptic weights) store information in the form of particular patterns, or configurations of firing neurons, which become attractors of the dynamics. Whatever the initial state of the system, it will always evolve towards one of these patterns, thus allowing for the storage and retrieval of information. The mechanism, known as *associative memory*, is thought to be at the basis of memory in the brain. In this case, the network is "remembering" an illustration by Jean-Baptiste Oudry for Jean de la Fontaine's fable *La Cigale et la Fourmi*.

2010). This would be in line with research that shows how certain useful properties – such as the computational capacity of some neural-network models (Bertschinger and Natschläger, 2004), or the dynamic range of sensitivity to stimuli in sensory systems (Kinouchi and Copelli, 2006) – are optimised at this "edge of chaos (Chialvo, 2006)".

That these models should actually reflect, albeit in an enormously simplified way, what actually goes on in our brains tends to fit in quite well with intuitive expectations – to the extent that so-called *connectionist* models seem to be gradually becoming the accepted paradigm in relevant areas of psychology and philosophy (Marcus and G.F., 2001; Frank, 1997). For instance, from

this point of view the way in which the recollection of a particular detail often evokes, almost instantly, a whole landscape of sensations and emotions makes sense, since these concepts will have been stored in some way as the same pattern. Also, the fact that new memories are recorded in synapses which were already being used to store previous information would seem to explain why memories tend to fade slowly with time, yet can still be recalled, at least to some extent, when a particular thought in some sense overlaps with (reminds one of) one of them. When this happens, the old memory springs to mind and, if held there for long enough, can be refreshed via long term potentiation and depression – although interaction with other patterns or with current stimuli may well modify the refreshed information. Similarly, previous information influences the storing of new memories, leading to the well known fact that we tend to "see" things the way we expect them to be.

It seems, then, that the basic mechanisms behind the ability of our brains to remember things, at least when the information is stored slowly enough for the biochemical processes of LTP and LTD to be at work (long-term memory), are now understood. Not only are the implications of such knowledge far-reaching in themselves. The way in which it was developed is also particularly notworthy. More or less sketchy ideas from areas as diverse as behavioural psychology, neurophysiology and theoretical physics were brought together in order to come up with a minimal mathematical model capable of manifesting the sought-after phenomenon of information retrieval as a consequence of the known properties of a great many simple elements. This kind of research can at first seem more like a mathematical game than anything to do with nitty-gritty reality. But the fact the basic mechanism of associative memory has since borne up to decades of experimenting and theoretical probing reveals how insightful it can actually be. It is likely that other features of brain function – short-term memory, information processing or emotional tagging, to name but the first few that spring to mind – will eventually be thrown under a similar light. In fact, we can expect the nature of even such an elusive and intimate phenomenon as consciousness some day to become clear. After all, the explanations behind other emergent properties of matter which in their day seemed almost mystical, such as temperature or life, are now well understood.

2.3 A declaration of intent

As Zora Neale Hurston put it, "Research is formalized curiosity. It is poking and prying with a purpose." But there are many possible purposes, and even more different ways of poking and prying. The motivation behind the work presented here is to understand how the phenomena we observe in certain systems on a macroscopic scale can come about from interactions of their many relatively simple constituent elements. In the case of neural systems, it seems reasonable to assume that these basic elements are neurons, and that it is thanks to the cooperation of a great many of these cells that such organs are able to think and feel. The human brain – with about 100 billion neurons connected by 100 trillion synapses – being the most complex system we know of, an enormous degree of simplification will be required for our description to be of any use to this purpose. (In fact, if we could somehow simulate a brain in all detail, the result would be just as unfathomable as the original object, however exciting the activity may prove for other reasons.) The physiology of the neuron is nowadays quite well understood. However, just as the properties of atoms or transistors that are key to understanding phase transitions or the workings of a microchip are, respectively, magnetic interactions and voltage-dependent gating, we must try to ascertain exactly which neuronal features are necessary for the macroscopic behaviour we are interested in to occur. One way to do this is to start by considering only the most basic characteristics and explore what non-trivial phenomena emerge from these, allowing us then to add new ingredients one at a time to pinpoint the relevant ones. In this line, we consider large sets of Hopfield's simple binary model neurons to study how network properties are related to collective behaviour.

This work is laid out as follows. Chapter 3 deals with development. The appearance and disappearance of edges in a network (growth and death of synapses, in the case of the brain) is formalised as a stochastic process and studied in a general setting (Johnson et al., 2009b, 2010a). It turns out that many of the topological features observed in experiments are well modelled in this way – which to some extent justifies, *a posteriori*, our initial assumptions. The following chapters describe particular phenomena that emerge as a direct consequence of some of those topological features: *degree heterogeneity* in conjunction with synaptic depression improves the performance of dynamical tasks (Johnson et al., 2008) (Chapter 4); *assortativity* serves to enhance a neural network's robustness to noise (de Franciscis et al., 2011) (Chapter 6); and *clustering* or *modularity* can lead to metastable states with certain properties

essential for some short-term memory abilities (properties hitherto lacking in previous models) (Johnson et al., 2011) (Chapter 7). Thanks to the extreme simplicity of the basic elements we are considering, we are able not only to simulate but also to understand mathematically how exactly the interesting phenomena emerge. This makes it possible to predict, to some extent, which extra ingredients *will not* invalidate the results if they are taken into account explicitly.

Some of the work has a more general scope than the study of neural networks. In particular, the equations obtained in Chapter 3 can be applied to any network that evolves under the influence of probabilistic addition and deletion of edges. And the method put forward in Chapter 5 for the study of correlated networks can be used not just for analysing particular models, as we go on to do in Chapter 6, but to solve many other problems – such as that of the ubiquity of *disassortative* networks in nature and technology (Johnson et al., 2010b), or how the property of nestedness typical of ecosystems is related to other topological characteristics (c.f. Appendix C).

To sum up, the aim of the thesis is **to shed light on how cellular dynamics can lead to the complex network structures of neural systems, and, in its turn, in what ways this topology can influence, optimise and determine the collective behaviour of such systems.**

The main contributions made are:

- An analytical method to study the evolution of networks governed by a combination of local and global stochastic rules.
- A mathematical and computational technique for the study of correlated networks in a model-independent way.
- Possible biological justifications for two non-trivial features of the topology of the human cortex: heterogeneity of the degree distribution and high assortativity.
- An answer to the long-standing question of why most networks are disassortative.
- Cluster Reverberation: the first mechanism proposed which would allow neural systems to store information instantaneously in a robust manner.

Chapter 3

Evolving networks and the development of neural systems

The highly heterogeneous degree distributions of most empirical networks is assumed in many cases to arise from some form of cummulative advantage, or preferential attachment. However, the origin of various other topological features is often not clear and attributed to specific functional requirements. We show how it is possible to analyse a very general scenario in which nodes gain or lose edges according to arbitrary functions of local and/or global degree information. Applying our method to two rather different examples of brain development – synaptic pruning in humans and the neural network of the worm *C. Elegans* – we find that simple biologically motivated assumptions lead to very good agreement with experimental data. In particular, many nontrivial topological features of the worm's brain arise naturally at a critical point.

3.1 Introduction

The conceptual simplicity of a *network* – a set of nodes, some pairs of which connected by edges – often suffices to capture the essence of cooperation in complex systems. Ever since Barabási and Albert presented their evolving network model (Barabási and Albert, 1999), in which linear preferential attachment leads asymptotically to a scale-free degree distribution (the degree, k, of a node being its number of neighbouring nodes), there have been many variations or refinements to the original scenario (Albert and Barabási, 2000; G. Bianconi and Barabási, 2001; Krapivsky et al., 2000; Bianconi and Barabási, 2001; Park et al., 2005; Ree, 2007) (see also the review by Boccaletti et al. (2006)). In Ref. (Johnson et al., 2009b), we show how topological phase tran-

sitions and scale-free solutions can emerge in the case of nonlinear rewiring in fixed-size networks, and this work is summarized in Appendix A. In Ref. (Johnson et al., 2010a) we extend our scope to more general and realistic situations, considering the evolution of networks making only minimal assumptions about the attachment/detachment rules. In fact, all we assume is that these probabilities factorize into two parts: a local term that depends on node degree, and a global term, which is a function of the mean degree of the network. This is the work described in this chapter.

Our motivation can be found in the mechanisms behind many real-world networks, but we focus, for the sake of illustration, on the development of biological neural networks, where nodes represent neurons and edges play the part of synaptic interaction (Amit, 1989; Sporns et al., 2004; Torres and Varona, 2010). Experimental neuroscience has shown that enhanced electric activity induces synaptic growth and dendritic arborization (Lee et al., 1980; Frank, 1997; Klintsova and Greenough, 1999; Roo et al., 2008). Since the activity of a neuron depends on the net current received from its neighbours, which tends to be higher the more neighbours it has, we can see node degree as a proxy for this activity – accounting for the local term alluded to above. On the other hand, synaptic growth and death also depend on concentrations of various molecules, which can diffuse through large areas of tissue and therefore cannot in general be considered local. A feature of brain development in many animals is *synaptic pruning* – the large reduction in synaptic density undergone throughout infancy. Chechik et al. (1999, in press) have shown that via an elimination of less needed synapses, this can reduce the energy consumed by the brain (which in a human at rest can account for a quarter of total energy used) while maintaining near optimal memory performance. Going on this, we will take the mean degree of the network – or mean synaptic density – to reflect total energy consumption, hence the global terms in our attachment/detachment rules (Johnson et al., 2009a).

An alternative approach would be to consider some kind of model neurons explicitly and couple the probabilities of synaptic growth and death to neuronal dynamic variables, such as local and global fields. In an Amari-Hopfield network, for example, the expected value of the field (total incoming current) at node i is proportional to i's degree (Torres et al., 2004), the total current (energy consumption) in the network therefore being proportional to the mean degree; qualitatively, these observations are likely to hold also in more realistic situations (Magistretti, 2009), although relations need not

be linear. Co-evolving networks of this sort are currently attracting attention, with dynamics such as Prisoner's Dilemma (Poncela et al., 2008), Voter Model (Vazquez et al., 2008) or Random Walkers (Antiqueira et al., 2009). Although we consider this line of work particularly interesting, for generality and analytical tractability we opt here to use only topological information for the attachment/detachment rules, although our results can be applied to any situation in which the dynamical states of the elements at the nodes can be functionally related to degrees[1].

Following a brief general analysis, we show how appropriate choices of functions induce the system to evolve towards heterogeneous (sometimes scale-free) networks while undergoing synaptic pruning in quantitative agreement with experiments. At the same time, degree-degree correlations emerge naturally, thus making the resulting networks *disassortative* – as tends to be the case for most biological networks – and leading to realistic small-world parameters.

3.2 Basic considerations

Consider a simple undirected network with N nodes defined by the adjacency matrix $\hat{a}$, the element $\hat{a}_{ij}$ representing the existence or otherwise of an edge between nodes i and j. Each node can be characterized by its degree, $k_i = \sum_j \hat{a}_{ij}$. Initially, the degrees follow some distribution $p(k, t = 0)$ with mean $\kappa(t)$. We wish to study the evolution of networks in which nodes can gain or lose edges according to stochastic rules which only take into account local and global information on degrees. So as to implement this in the most general way, we will assume that at every time step, each node has a probability of gaining a new edge, P_i^{gain}, to a random node; and a probability of losing a randomly chosen edge, P_i^{lose}. We assume these factorize as $P_i^{\text{gain}} = u(\kappa)\pi(k_i)$ and $P_i^{\text{lose}} = d(\kappa)\sigma(k_i)$, where u, d, π and σ can be arbitrary functions, but impose nothing else other than normalization.

For each edge that is withdrawn from the network, two nodes decrease in degree: i, chosen according to $\sigma(k_i)$, and j, a random neighbour of i's; so there is an added effective probability of loss $k_j/(\kappa N)$. Similarly, for each edge placed in the network, not only l chosen according to $\pi(k_l)$ increases its degree;

[1]For instance, the stationary distribution of walkers used for edge dynamics by Antiqueira et al. (2009) is actually obtained purely from topological information, although it can only be written in terms of local degrees for undirected networks.

a random node m will also gain, with the consequent effective probability N^{-1} (though see[2]). Let us introduce the notation $\tilde{\pi}(k) \equiv \pi(k) + N^{-1}$ and $\tilde{\sigma}(k) \equiv \sigma(k) + k/(\kappa N)$. Network evolution can now be seen as a *one step process* (van Kampen, 1992) with transition rates $u(\kappa)\tilde{\pi}(k)$ and $d(\kappa)\tilde{\sigma}(k)$. The expected value for the increment in a given $p(k,t)$ at each time step (which we equate with a temporal derivative) defines a master equation for the degree distribution (Johnson et al., 2009b):

$$\begin{aligned}\frac{\mathrm{d}p(k,t)}{\mathrm{d}t} = u(\kappa)\,\tilde{\pi}(k-1)p(k-1) + d(\kappa)\,\tilde{\sigma}(k+1)p(k+1) \\ - \left[u(\kappa)\,\tilde{\pi}(k) + d(\kappa)\,\tilde{\sigma}(k)\right] p(k,t).\end{aligned} \tag{3.1}$$

Assuming now that $p(k,t)$ evolves towards a stationary distribution, $p_{\mathrm{st}}(k)$, then this must necessarily satisfy detailed balance since it is a one step process (van Kampen, 1992); i.e., the flux of probability from k to $k+1$ must equal the flux from $k+1$ to k, for all k (Marro and Dickman). This condition (sufficient for Eq. (3.1) to be zero) can be written as

$$\frac{\partial p_{\mathrm{st}}(k)}{\partial k} = \left[\frac{u(\kappa_{\mathrm{st}})}{d(\kappa_{\mathrm{st}})}\frac{\tilde{\pi}(k)}{\tilde{\sigma}(k+1)} - 1\right] p_{\mathrm{st}}(k), \tag{3.2}$$

where we have substituted a difference for a partial derivative and $\kappa_{\mathrm{st}} \equiv \sum_k k p_{\mathrm{st}}(k)$. Setting π and σ so as to be normalized to one (i.e., $\sum_k p(k)\pi(k) = \sum_k p(k)\sigma(k) = 1$, $\forall t$), which is equivalent to saying that at each time step exactly $u(\kappa)$ nodes are chosen to gain edges and $d(\kappa)$ to lose them, then in the stationary state we will have $u(\kappa_{\mathrm{st}}) = d(\kappa_{\mathrm{st}})$ since the total number of edges will be conserved. From Eq. (3.2) we can see that $p_{\mathrm{st}}(k)$ will have an extremum at some value k_e if it satisfies $\tilde{\pi}(k_e) = \tilde{\sigma}(k_e + 1)$. k_e will be a maximum (minimum) if the numerator in Eq. (3.2) is smaller (greater) than the denominator for $k > k_e$, and viceversa for $k < k_e$. Assuming, for example, that there is one and only one such k_e, then a maximum implies a relatively homogeneous distribution, while a minimum means $p_{\mathrm{st}}(k)$ will be split in two, and therefore highly heterogeneous. More intuitively, if for nodes with large enough k there is a higher probability of gaining edges than of losing them, the degrees of these nodes will grow indefinitely, leading to heterogeneity. If, on the other hand, highly connected nodes always lose more edges than they gain, we will

[2]We are ignoring the small corrections that arise because $j \neq i$ and $l \neq m$, which in any case would disappear if self-connections were allowed.

obtain quite homogeneous networks. From this reasoning we can see that a particularly interesting case (which turns out to be critical) is that in which $\pi(k)$ and $\sigma(k)$ are such that

$$\tilde{\pi}(k) = \tilde{\sigma}(k) \equiv v(k), \quad \forall k. \tag{3.3}$$

According to Eq. (3.2), Condition (3.3) means that for large k, $\partial p_{st}(k)/\partial k \to 0$, and $p_{st}(k)$ flattens out – as for example a power-law does.

The standard Fokker-Planck approximation for the one step process defined by Eq. (3.1) is (van Kampen, 1992):

$$\begin{aligned}\frac{\partial p(k,t)}{\partial t} = \frac{1}{2}\frac{\partial^2}{\partial k^2}\left\{\left[d(\kappa)\tilde{\sigma}(k) + u(\kappa)\tilde{\pi}(k)\right]p(k,t)\right\} \\ + \frac{\partial}{\partial k}\left\{\left[d(\kappa)\tilde{\sigma}(k) - u(\kappa)\tilde{\pi}(k)\right]p(k,t)\right\}.\end{aligned} \tag{3.4}$$

For transition rates which meet Condition (3.3), Eq. (3.4) can be written as:

$$\begin{aligned}\frac{\partial p(k,t)}{\partial t} = \frac{1}{2}\left[d\left(\kappa\right) + u\left(\kappa\right)\right]\frac{\partial^2}{\partial k^2}\left[v(k)p(k,t)\right] \\ + \left[d\left(\kappa\right) - u\left(\kappa\right)\right]\frac{\partial}{\partial k}\left[v(k)p(k,t)\right].\end{aligned} \tag{3.5}$$

Ignoring boundary conditions, the stationary solution must satisfy, on the one hand, $v(k)p_{\mathrm{st}}(k) = Ak + B$, so that the diffusion is stationary, and, on the other, $u(\kappa_{\mathrm{st}}) = d(\kappa_{\mathrm{st}})$, to cancel out the drift. For this situation to be reachable from any initial condition, $u(\kappa)$ and $d(\kappa)$ must be monotonous functions, decreasing and increasing respectively.

3.3 Synaptic pruning

As a simple example, we will first consider global probabilities which have the linear forms:

$$u[\kappa(t)] = \frac{n}{N}\left(1 - \frac{\kappa(t)}{\kappa_{\max}}\right) \quad \text{and} \quad d[\kappa(t)] = \frac{n}{N}\frac{\kappa(t)}{\kappa_{\max}}, \tag{3.6}$$

where n is the expected value of the number of additions and deletions of edges per time step, and $\kappa_{\max}$ is the maximum value the mean degree can have. This choice describes a situation in which the higher the density of synapses, the less likely new ones are to sprout and the more likely existing ones are to atrophy – a situation that might arise, for instance, in the presence of a finite quantity

of nutrients. Again taking into account that π and σ are normalized to one, summing over $P_i^{\text{gain}} - P_i^{\text{lose}}$ we find that the expected increment in $\kappa(t)$ is

$$\langle \frac{\Delta\kappa(t)}{\Delta t} \rangle = 2\{u[\kappa(t)] - d[\kappa(t)]\} = 2\frac{n}{N}\left[1 - 2\frac{\kappa(t)}{\kappa_{\max}}\right]$$

(independently of the local probabilities). Therefore, the mean degree will increase or decrease exponentially with time, from $\kappa(0)$ to $\frac{1}{2}\kappa_{\max}$. Assuming that the initial condition is, say, $\kappa(0) = \kappa_{\max}$, and expressing the solution in terms of the *mean synaptic density* – i.e., $\rho(t) \equiv \kappa(t)N/(2V)$, with V the total volume considered – we have

$$\rho(t) = \rho_{\text{f}}\left(1 + e^{-t/\tau_{\text{p}}}\right), \tag{3.7}$$

where we have defined $\rho_{\text{f}} \equiv \rho(t \to \infty)$ and the time constant for pruning is $\tau_{\text{p}} = \rho_{\text{f}}N/n$. This equation was fitted in Fig. 3.1 to experimental data on layers 1 and 2 of the human auditory cortex[3] obtained during autopsies by Huttenlocher and Dabholkar (1997).

It seems reasonable to assume that the initial overgrowth of synapses is due to the transient existence of some kind of growth factors. If we account for these by including a nonlinear, time-dependent term $g(t) \equiv a\exp(-t/\tau_{\text{g}})$ in the probability of growth, i.e., $u[\kappa(t), t] = (n/N)[1 - \kappa(t)/\kappa_{\max} + g(t)]$, leaving $d[\kappa(t)]$ as before, we find that $\rho(t)$ becomes

$$\rho(t) = \rho_{\text{f}}\left[1 + e^{-t/\tau_{\text{p}}} - \left(1 + e^{-t_0/\tau_{\text{p}}}\right)e^{-\frac{t-t_0}{\tau_{\text{g}}}}\right], \tag{3.8}$$

where t_0 is the time at which synapses begin to form ($t = 0$ corresponds to the moment of conception) and τ_{g} is the time constant related to growth. The inset in Fig. 3.1 shows the best fit to the auditory cortex data. Since the contour conditions ρ_{f} and (for Eq. (3.8)) t_0 are simply taken as the value of the last data point and the time of the first one, in each case, the time constants τ_{p} and τ_{g} are the only parameters needed for the fit.

3.4 Phase transitions

The drift-like evolution of the mean degree we have just illustrated with the example of synaptic pruning is independent of the local probabilities $\pi(k)$

[3] Data points for three particular days (smaller symbols) are omitted from the fit, since we believe these must be from subjects with inherently lower synaptic density.

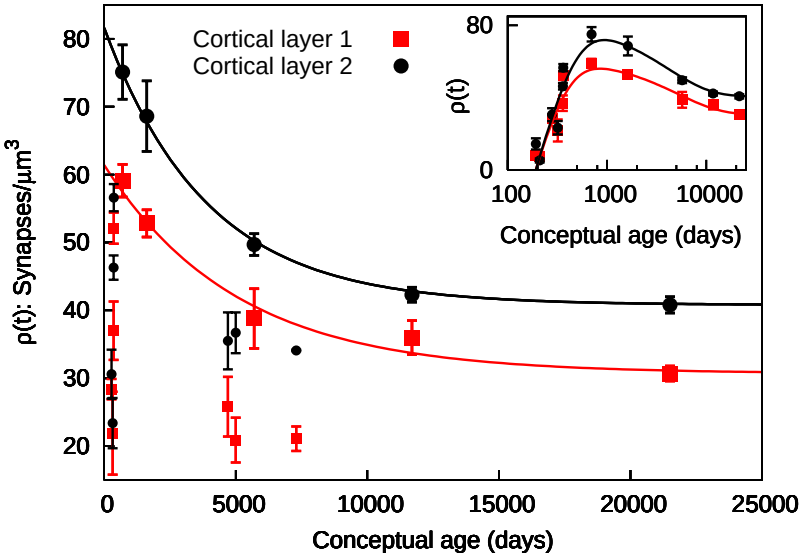

Figure 3.1: Synaptic densities in layers 1 (red squares) and 2 (black circles) of the human auditory cortex against time from conception. Data from Huttenlocher and Dabholkar (1997), obtained by directly counting synapses in tissues from autopsies. Lines follow best fits to Eq. (3.7), where the parameters were: for layer 1, $\tau_{\rm p} = 5041$ days; and for layer 2, $\tau_{\rm p} = 3898$ days (for $\rho_{\rm f}$ we have used the last data pints: 30.7 and 40.8 synapses/μm^3, for layers 1 and 2 respectively). Data pertaining to the first year and to days 4700, 5000 7300, shown with smaller symbols, where omitted from the fit. Assuming the existence of transient growth factors, we can include the data points for the first year in the fit by using Eq. (3.8). This is done in the inset (where time is displayed logarithmically). The best fits were: for layer 1, $\tau_{\rm g} = 151.0$ and $\tau_{\rm p} = 5221$; and for layer 2, $\tau_{\rm g} = 191.1$ and $\tau_{\rm p} = 4184$, all in days (we have approximated t_0 to the time of the first data points, 192 days).

and $\sigma(k)$. The effect of these is rather in the diffusive behaviour which can lead, as mentioned, either to homogeneous or to heterogeneous final states. A useful bounded order parameter to characterize these phases is therefore $m \equiv \exp\left(-\sigma^2/\kappa^2\right)$, where $\sigma^2 = \langle k^2 \rangle - \kappa^2$ is the variance of the degree distribution ($\langle \cdot \rangle \equiv N^{-1} \sum_i (\cdot)$ represents an average over nodes). We will use $m_{\rm st} \equiv \lim_{t\to\infty} m(t)$ to distinguish between the different phases, since $m_{\rm st} = 1$ for a regular network and $m_{\rm st} \to 0$ for one following a highly heterogeneous distribution. Although there are particular choices of probabilities which lead to Eq. (3.5), these are not the only critical cases, since the transition from

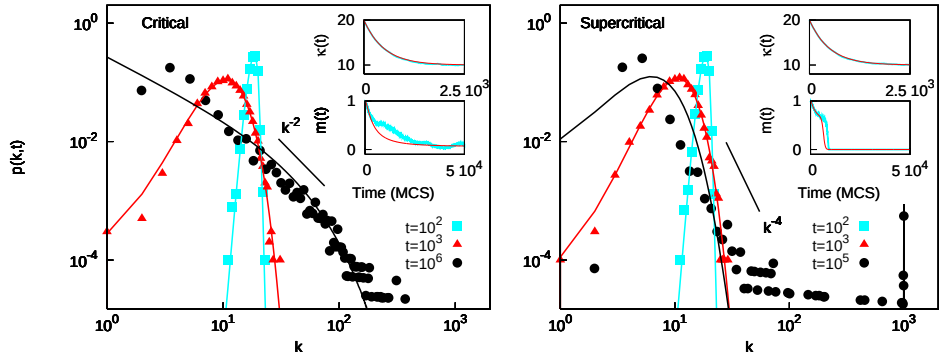

Figure 3.2: Evolution of the degree distributions of networks beginning as regular random graphs with $\kappa(0) = 20$ in the critical (top) and supercritical (bottom) regimes. Local probabilities are $\sigma(k) = k/(\langle k\rangle N)$ in both cases, and $\pi(k) = 2\sigma(k) - N^{-1}$ and $\pi(k) = k^{3/2}/(\langle k^{3/2}\rangle N)$ for the critical and supercritical ones, respectively. Global probabilities as in Eq. (3.6), with $n = 10$ and $\kappa_{\max} = 20$. Symbols in the main panels correspond to $p(k,t)$ at different times as obtained from MC simulations. Lines result from numerical integration of Eq. (3.1). Insets show typical time series of κ and m. Light blue lines are from MC simulations and red lines are theoretical, given by Eq. (3.7) and Eq. (3.1), respectively. $N = 1000$.

homogeneous to heterogeneous stationary states can come about also with functions which never meet Condition (3.3). Rather, this is a classic topological phase transition, the nature of which depends on the choice of functions (Park and Newman, 2004; Burda et al., 2004; Derényi et al., 2004) .

Evolution of the degree distribution is shown in Fig. 3.2 for critical and supercritical choices for the probabilities, as given by MC simulations (starting from regular random graphs) and contrasted with theory. (The subcritical regime is not shown since the stationary state has a distribution similar to the ones at $t = 10^3$ MCS in the other regimes.) The disparity between the theory and the simulations for the final distributions is due to the build up of certain correlations not taken into account in our analysis. This is because the existence of some very highly connected nodes reduces the probability of there being very low degree nodes. In particular, if there are, say, x nodes connected to the rest of the network, then a natural cutoff, $k_{min} = x$, emerges. Note that this occurs only when we restrict ourselves to simple networks, i.e., with only one edge allowed for each pair of nodes. This topological phase transition is shown in Fig. 3.3, where $m_{\rm st}$ is plotted against parameter α for global

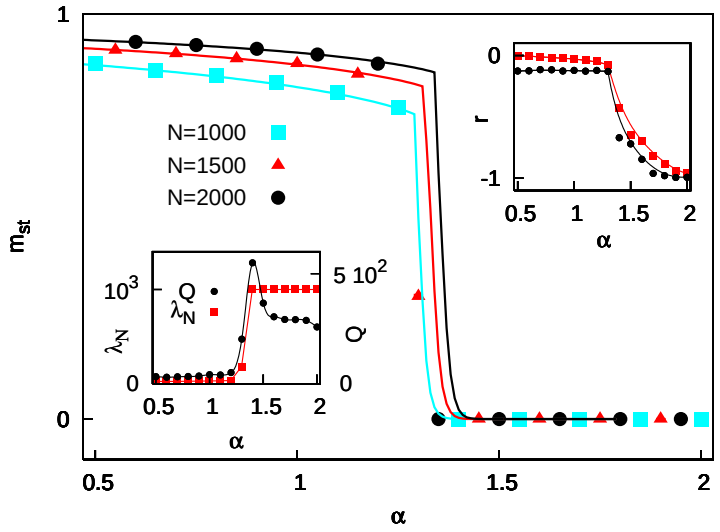

Figure 3.3: Phase transitions in $m_{\rm st}$ for $\pi(k) \sim k^\alpha$ and $\sigma(k) \sim k$, and $u(\kappa)$ and $d(\kappa)$ as in Eq. (3.6). $N = 1000$ (blue squares), 1500 (red triangles) and 2000 (black circles); $\kappa(0) = \kappa_{\rm max} = 2n = N/50$. Corresponding lines are from numerical integration of Eq. (3.1). The bottom left inset shows values of the highest eigenvalue of the Laplacian matrix (red squares) and of $Q = \lambda_N/\lambda_2$ (black circles), a measure of unsynchronizability; $N = 1000$. The top right inset shows transitions for the same parameters in the final values of Pearson's correlation coefficient r (see Section 3.5), both for only one edge allowed per pair of nodes (red squares) and without this restriction (black circles).

probabilities as in Eq. (3.6) and local ones $\pi(k) \sim k^\alpha$ and $\sigma(k) \sim k$. This situation corresponds to one in which edges are eliminated randomly while nodes have a power-law probability of sprouting new ones (note that power-laws are good descriptions of a variety of monotonous response functions, yet only require one parameter). Although, to our knowledge, there are not yet enough empirical data to ascertain what degree distribution the structural topology of the human brain follows, it is worth noting that its functional topology, at the level of brain areas, has been found to be scale-free with an exponent very close to 2 (Eguíluz et al., 2005).

In general, most other measures can be expected to undergo a transition along with its variance. For instance, highly heterogeneous networks (such as scale-free ones) exhibit the small-world property, characterized by a high *clustering coefficient,* $C \gg \langle k \rangle/N$, and a low *mean minimum path,* $l \sim \ln(N)$ (Watts and Strogatz, 1998). A particularly interesting topological feature of

a network is its *synchronizability* – i.e., given a set of oscillators placed at the nodes and coupled via the edges, how wide a range of coupling strengths will result in them all becoming synchronized. Barahona and Pecora showed analytically that, for linear oscillators, a network is more synchronizable the lower the relation $Q = \lambda_N/\lambda_2$ – where λ_N and λ_2 are the highest and lowest non-zero eigenvalues of the Laplacian matrix ($\hat{\Lambda}_{ij} \equiv \delta_{ij}k_i - \hat{a}_{ij}$), respectively (Barahona and Pecora, 2002). The bottom left inset in Fig. 3.3 displays the values of Q and λ_N obtained for the different stationary states. There is a peak in Q at the critical point. It has been argued that this tendency of heterogeneous topologies to be particularly unsynchronizable poses a paradox given the wide prevalence of scale-free networks in nature, a problem that has been deftly got around by considering appropriate weighting schemes for the edges (Motter et al., 2005; Chavez et al., 2005) (see also[4], and the review by Arenas et al. (2008a)). However, there is no generic reason why high synchronizability should always be desirable. In fact, it has recently been shown that heterogeneity can improve the dynamical performance of model neural networks precisely because the fixed points are easily destabilised (Johnson et al., 2008) (as well as conferring robustness to thermal fluctuations and improving storage capacity (Torres et al., 2004)). This makes intuitive sense, since, presumably, one would not usually want all the neurons in one's brain to be doing exactly the same thing. Therefore, this point of maximum *unsynchronizability* at the phase transition may be a particularly advantageous one.

On the whole, we find that three classes of network – homogeneous, scale-free (at the critical point) and ones composed of starlike structures, with a great many small-degree nodes connected to a few hubs – can emerge for any kind of attachment/detachment rules. It follows that a network subject to some sort of optimising mechanism, such as Natural Selection for the case of living systems, could thus evolve towards whichever topology best suits its requirements by tuning these microscopic actions.

3.5 Correlations

Most real networks have been found to exhibit degree-degree correlations, also known as *mixing* by degree (Pastor-Satorras et al., 2001; Newman, 2003c).

[4]Using pacemaker nodes, scale-free networks have also been shown to emerge via rules which maximize synchrony (Sendina-Nadal et al., 2008).

They can thus be classified as *assortative*, when the degree of a typical node is positively correlated with that of its neighbours, or *disassortative,* when the correlation is negative. This property has important implications for network characteristics such as connectedness and robustness (Newman, 2002, 2003a). A useful measure of this phenomenon is Pearson's correlation coefficient applied to the edges (Newman, 2003c,a; Boccaletti et al., 2006): $r = ([k_l k'_l] - [k_l]^2)/([k_l^2] - [k_l]^2)$, where k_l and k'_l are the degrees of each of the two nodes pertaining to edge l, and $[\cdot] \equiv (\langle k \rangle N)^{-1} \sum_l (\cdot)$ represents an average over edges; $|r| \leq 1$. Writing $\sum_l (\cdot) = \sum_{ij} \hat{a}_{ij} (\cdot)$, r can be expressed in terms of averages over nodes:

$$r = \frac{\langle k \rangle \langle k^2 k_{nn}(k) \rangle - \langle k^2 \rangle^2}{\langle k \rangle \langle k^3 \rangle - \langle k^2 \rangle^2}, \tag{3.9}$$

where $k_{nn}(k)$ is the mean nearest-neighbour-degree function; i.e., if $k_{nn,i} \equiv k_i^{-1} \sum_j \hat{a}_{ij} k_j$ is the mean degree of the neighbours of node i, $k_{nn}(k)$ is its average over all nodes such that $k_i = k$. Whereas most social networks are assortative ($r > 0$) – due, probably, to mechanisms such as homophily (Newman, 2003c) – almost all other networks, whether biological, technological or information-related, seem to be generically disassortative. The top right inset in Fig. 3.3 displays the stationary value of r obtained in the same networks as in the main panel and lower inset. It turns out that the heterogeneous regime is disassortative, the more so the larger α. (Note that a completely homogeneous network cannot have degree-degree correlations, since all degrees are the same.) It is known that the restriction of having at most one edge per pair of nodes induces disassortativity (Park and Newman, 2003; Maslov et al., 2004). However, in our case this is not the sole origin of the correlations, as can also be seen in the same inset of Fig. 3.3, where we have plotted r for networks in which we have lifted the restriction and allowed any number of edges per pair of nodes. In fact, when multiple edges are allowed, the correlations are slightly stronger. As we shall discuss in Chapter 5, there is a general entropic reason for heterogeneous networks, in their equilibrium state (i.e., in the absence of correlating mechanisms), to become disassortative (Johnson et al., 2010b). But neither is this here the case, since the networks generated are driven from equilibrium by the mechanisms of preferential attachment and detachment.

To understand how these specific correlations come about, consider a pair of nodes (i, j), which, at a given moment, can either be occupied by an edge or unoccupied. We will call the expected times of permanence for occupied and unoccupied states τ_{ij}^{o} and τ_{ij}^{u}, respectively. After sufficient evolution time (so

that occupancy becomes independent of the initial state[5]), the expected value of the corresponding element of the adjacency matrix, $E(\hat{a}_{ij}) \equiv \hat{\epsilon}_{ij}$, will be

$$\hat{\epsilon}_{ij} = \frac{\tau_{ij}^{\mathrm{O}}}{\tau_{ij}^{\mathrm{O}} + \tau_{ij}^{\mathrm{U}}}.$$

If p_{ij}^{+} (p_{ij}^{-}) is the probability that (i,j) will become occupied (unoccupied) given that it is unoccupied (occupied), then $\tau_{ij}^{\mathrm{O}} \sim 1/p_{ij}^{-}$ and $\tau_{ij}^{\mathrm{U}} \sim 1/p_{ij}^{+}$, yielding

$$\hat{\epsilon}_{ij} = \left(1 + \frac{p_{ij}^{-}}{p_{ij}^{+}}\right)^{-1}.$$

Taking into account the probability that each node has of gaining or losing an edge, we obtain[6]: $p_{ij}^{+} = u(\langle k \rangle) N^{-1} [\pi(k_i) + \pi(k_j)]$ and $p_{ij}^{-} = d(\langle k \rangle)[\sigma(k_i)/k_i + \sigma(k_j)/k_j]$. Then, assuming that the network is sparse enough that $p_{ij}^{-} \gg p_{ij}^{+}$ (since the number of edges is much smaller than the number of pairs), and particularising for power-law local probabilities $\pi(k) \sim k^{\alpha}$ and $\sigma(k) \sim k^{\beta}$, the expected occupancy of the pair is

$$\hat{\epsilon}_{ij} \simeq \frac{p_{ij}^{+}}{p_{ij}^{-}} = \frac{u(\langle k \rangle)}{d(\langle k \rangle)} \frac{\langle k^{\beta} \rangle}{\langle k^{\alpha} \rangle N} \left(\frac{k_i^{\alpha} + k_j^{\alpha}}{k_i^{\beta-1} + k_j^{\beta-1}} \right).$$

Considering the stationary state, when $u(\langle k \rangle) = d(\langle k \rangle)$, and for the case of random deletion of edges, $\beta = 1$ (so that the only nonlinearity is due to α), the previous expression reduces to

$$\hat{\epsilon}_{ij} \simeq \frac{\langle k \rangle}{2\langle k^{\alpha} \rangle N} \left(k_i^{\alpha} + k_j^{\alpha} \right). \tag{3.10}$$

(Note that this matrix is not consistent term by term, since $\sum_j \hat{\epsilon}_{ij} \neq k_i$, although it is globally consistent: $\sum_{ij} \hat{\epsilon}_{ij} = \langle k \rangle N$.) The nearest-neighbour-degree function is now

$$k_{nn}(k_i) = \frac{1}{k_i} \sum_j \hat{\epsilon}_{ij} k_j = \frac{\langle k \rangle}{2\langle k^{\alpha} \rangle} (\langle k \rangle k_i^{\alpha-1} + \langle k^{\alpha+1} \rangle k_i^{-1})$$

(a decreasing function for any α), with the result that Pearson's coefficient becomes

$$r = \frac{1}{\langle k^{\alpha} \rangle} \left(\frac{\langle k \rangle^3 \langle k^{\alpha+1} \rangle - \langle k^2 \rangle^2 \langle k^{\alpha} \rangle}{\langle k \rangle \langle k^3 \rangle - \langle k^2 \rangle^2} \right). \tag{3.11}$$

[5] Note that this will always happen eventually since the process is ergodic.

[6] Again, we are ignoring corrections due to the fact that i is necessarily different from j.

More generally, one can understand the emergence of these correlations in the following way. For the network to become heterogeneous, we must have $\pi(k) + N^{-1} \geq \sigma(k) + k/(\langle k \rangle N)$ for large enough k, so that highly connected nodes do not lose more edges than they can acquire (see Section 3.2). This implies that $\pi(k)$ must be increasing and approximately linear or superlinear. The expected value of the degree of a node i, chosen according to $\pi(k_i)$, is then $E(k_i) = N^{-1} \sum_k \pi(k) k \gtrsim \langle k^2 \rangle / \langle k \rangle$, while that of its new, randomly chosen neighbour, j, is only $E(k_j) = \langle k \rangle$. This induces disassortative correlations which can never be compensated by the breaking of edges between nodes whose expected degree values are $N^{-1} \sum_k \sigma(k) k$ and $\langle k^2 \rangle / \langle k \rangle$ if $\sigma(k)$ is an increasing function. It thus ensues that a scenario such as the one analysed in this paper will never lead to assortative networks except for some cases in which $\sigma(k)$ is a decreasing function – meaning that less connected nodes should be more likely to lose edges. Assortativity could, however, arise if there were some bias also on the node chosen to be i's neighbour, e.g. on the postsynaptic neuron – which is precisely what happens in most social networks, where individuals do not generally choose their friends, partners, etc. randomly. Although there seem to be other reasons for the ubiquity of disassortative networks in nature (Johnson et al., 2010b), it is possible that the generality of the scenario studied here may also play a part.

We can use the expected value matrix $\hat{\epsilon}$ to estimate other magnitudes. For example, the clustering coefficient, as defined by Watts and Strogatz (Watts and Strogatz, 1998), is an average over nodes of C_i, with C_i the proportion of i's neighbours which are connected to each other; so its expected value is $E(C_i) = \hat{\epsilon}_{jl}$ conditioned to j and l being neighbours of i's. This means that, on average, we can make the approximation that

$$k_j = k_l = \langle k_{nn} \rangle = \frac{\langle k \rangle}{2\langle k^\alpha \rangle} [\langle k \rangle \langle k^{\alpha-1} \rangle + \langle k^{\alpha+1} \rangle \langle k^{-1} \rangle].$$

Substituting this value in Eq. (3.10), and taking into account that one edge of j's and one of l's are taken up by i, we have

$$C \simeq \frac{\langle k \rangle}{\langle k^\alpha \rangle N} (\langle k_{nn} \rangle - 1)^\alpha. \tag{3.12}$$

For a rough estimate of the mean minimum path (the minimum path between two nodes being the smallest number of edges one has to follow to get from one to the other), we can proceed as Albert and Barabási (2002). For a given node, let us define the number of nearest neighbours, z_1, next-nearest neighbours, z_2, and in general mth neighbours, z_m. Using the relation $z_m = z_1 \left(z_2/z_1\right)^{m-1}$,

and assuming that the network is connected and can be obtained in l steps, this yields

$$1 + \sum_{1}^{l} z_m = N. \tag{3.13}$$

On average, $z_1 = \langle k \rangle$ and $z_2 = \langle k \rangle [(1 - C)\langle k_{nn} \rangle - 1]$ (since for each second nearest neighbour, one edge goes to the reference node and a proportion C to mutual neighbours). Now, if $N \gg z_1$ and $z_2 \gg z_1$, Eq. (3.13) leads to

$$l \simeq 1 + \frac{\ln(N/\langle k \rangle)}{\ln[(1 - C)\langle k_{nn} \rangle - 1]}. \tag{3.14}$$

3.6 The C. Elegans neural network

There exists a biological neural network which has been entirely mapped (although not, to the best of our knowledge, at different stages of development) – that of the much-investigated worm *C. Elegans* (White et al., 1986; Watts and Strogatz, 1998). With a view to testing whether such a network could arise via simple stochastic rules of the kind we are here considering, we ran simulations for the same number of nodes, $N = 307$, and (stationary) mean degree, $\langle k \rangle = 14.0$ (in the simple, undirected representation of the network). Using the global probabilities given by Eq. (3.6) and local ones $\pi(k) \sim k^{\alpha}$ and $\sigma(k) \sim k$ (as in Fig. 3.3), we obtain a surprising result. Precisely at the critical point, $\alpha = \alpha_c \simeq 1.35$, there are some remarkable similarities between the biological network and the ones produced by the model.

Figure 3.4 displays the degree distributions, both for the empirical network and for the average (stationary) simulated network corresponding to the critical point, while the top inset shows the mean-nearest-neighbour degree function $k_{nn}(k)$ for the same networks. Both $p(k)$ and $k_{nn}(k)$ of the simulated networks can be seen to be very similar to those measured in the biological one. Furthermore, as is displayed in Table 3.1, the clustering coefficient obtained in simulation is almost the same as the empirical one. The mean minimum path is similar though slightly smaller in simulation, probably due to the worm's brain having modules related to functions (Arenas et al., 2008b). Finally, Pearson's coefficient is also in fairly good agreement, although the simulated networks are actually a bit more disassortative. It should, however, be stressed that the simulation results are for averages over 100 runs, while the biological system is equivalent to a single run; given the small number of neurons, statistical fluctuations can be fairly large, so one should refrain from attributing too much

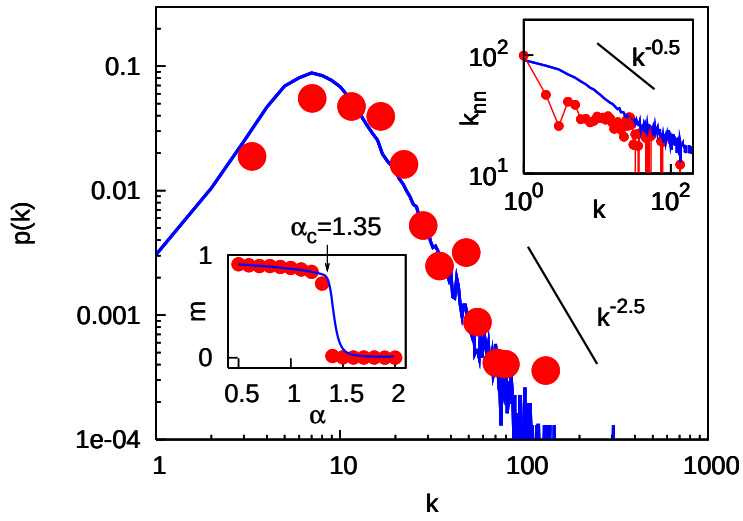

Figure 3.4: Degree distribution (binned) of the *C. Elegans* neural network (circles) (White et al., 1986) and that obtained with MC simulations (line) in the stationary state ($t = 10^5$ steps) for an equivalent network in which edges are removed randomly ($\beta = 1$) at the critical point ($\alpha = 1.35$). $N = 307$, $\kappa_{\rm st} = 14.0$, averages over 100 runs. Global probabilities as in Eq. (3.6). The slope is for $k^{-5/2}$. Top right inset: mean-neighbour-degree function $k_{nn}(k)$ as measured in the same empirical network (circles) and as given by the same simulations (line) as in the main panel. The slope is for $k^{-1/2}$. Bottom left inset: $m_{\rm st}$ of equivalent network for a range of α, both from simulations (circles) and as obtained with Eq. (3.1). (See also Table 3.1.)

importance to the precise values obtained – at least until we can average over 100 worms. Table 3.1 also shows the values of C, l and r both as estimated form the theory laid out in Section 3.5, and for the equivalent network in the *configuration model* (Newman, 2003c) – generally taken as the null model for heterogeneous networks, where the probability of an edge existing between nodes i and j is $k_i k_j/(\langle k\rangle N)$. It is clear that whereas the configuration-model predictions deviate substantially from the magnitudes measured in the *C. Elegans* neural network, the growth process we are here considering accounts for them quite well. It is interesting that it should be at the critical point that a structural topology so similar to the empirical one emerges, since it seems that the brain's functional topology may also be related to a critical point (Chialvo, 2004; Chialvo et al., 2008).

	Experiment	Simulation	Theory	Config.
C	0.28	0.28	0.23	0.15
l	2.46	2.19	1.86	1.96
r	-0.163	-0.207	-0.305	-0.101

Table 3.1: Values of small-world parameters C and l, and Pearson's correlation coefficient r, as measured in the neural network of the worm *C. Elegans* (White et al., 1986), and as obtained from simulations in the stationary state ($t = 10^5$ steps) for an equivalent network at the critical point when edges are removed randomly – i.e., for $\alpha = 1.35$ and $\beta = 1$. $N = 307$, $\kappa_{\rm st} = 14.0$; averages over 100 runs and global probabilities as in Eq. (3.6). Theoretical estimates correspond to Eqs. (3.12), (3.14) and (3.11) applied to the networks generated by the same simulations. The last column lists the respective *configuration model* values: C and l are obtained theoretically as in (Newman, 2003c), while r, from MC simulations as in (Maslov et al., 2004), is the value expected due to the absence of multiple edges. (See also Fig. 3.4.)

3.7 Discussion

With this work we have attempted, on the one hand, to extend our understanding of evolving networks so that any choice of transition probabilities dependent on local and/or global degrees can be treated analytically, thereby obtaining some model-independent results; and on the other, to illustrate how such a framework can be applied to realistic biological scenarios. For the latter, we have used two examples relating to two rather different nervous systems:
i) synaptic pruning in humans, for which the use of nonlinear global probabilities reproduces the initial increase and subsequent depletion in synaptic density in good accord with experiments – to the extent that nonmonotonic data points spanning a lifetime can be very well fitted with only two parameters; and
ii) the structure of the *C. Elegans* neural network, for which it turns out that by only considering the numbers of nodes and edges, and imposing random deletion of edges and power-law probability of growth, the critical point leads

to networks exhibiting many of the worm's nontrivial features – such as the degree distribution, small-world parameters, and even level of disassortativity.

These examples indicate that it is not far-fetched to contemplate how many structural features of the brain or other networks – and not just the degree distributions – could arise by simple stochastic rules like the ones considered; although, undoubtedly, other ingredients such as natural modularity (Arenas et al., 2008b), a metric (Kaiser and Hilgetag, 2004) or functional requirements (Sporns et al., 2004) can also be expected to play a role in many instances. We hope, therefore, that the framework laid out here – in which for simplicity we have assumed the network to be undirected and to have a fixed size, although generalizations are straightforward – may prove useful for interpreting data from a variety of fields. It would be particularly interesting to try to locate and quantify the biological mechanisms assumed to be behind this kind of network dynamics.

Chapter 4

Bringing on the Edge of Chaos with heterogeneity

The collective behaviour of systems of coupled excitable elements, such as neurons, has been shown to depend significantly on the heterogeneity of the degree distribution of the underlying network of interactions. For instance, broad – in particular, scale-free – distributions have been found to improve static memory performance in neural-network models. Here we look at the influence of degree heterogeneity in a neural network which, due to the effect of synaptic depression (a kind of fatigue of the interaction strengths), exhibits chaotic behaviour. Not only can the existence of a chaotic phase be related to neurophysiological experiments; it allows the system to perform a class of dynamic pattern-recognition tasks. We find first of all that, as has been described in a few other systems, optimal performance is achieved close to the phase transition – i.e., at the so-called *Edge of Chaos*. Furthermore, we obtain a functional relationship between the level of synaptic depression required to bring on chaos and the heterogeneity of the degree distribution. This result points to a clear advantage of low-exponent scale-free networks, and suggests an explanation for their apparent ubiquity in certain biological systems.

4.1 Exciting cooperation

Excitable systems allow for the regeneration of waves propagating through them, and may thus respond vigorously to weak stimulus. The brain and other parts of the nervous system are well–studied paradigms, and forest fires with constant ignition of trees and autocatalytic reactions in surfaces, for instance, also share some of the basics (Bak et al., 1990; Meron, 1992; Lindner et al.,

2004; Izhikevich, 2007; Arenas et al., 2008a). The fact that signals are not gradually damped by friction in these cases is a consequence of cooperation among many elements in a nonequilibrium setting. These systems can be seen as large networks of nodes that are "excitable". This admits various realizations, but typically means that each element has a threshold and a refractory time between consecutive responses – a behaviour that impedes thermal equilibrium.

Some brain tasks can be simulated with mathematical neural networks. As described in Chapter 2, these consist of neurons – often modelled as variables which are as simple as possible while still able to display the essence of the cooperative behaviour of interest[1] – connected by edges representing synapses (Amari, 1972; Hopfield, 1982; Amit, 1989; Torres and Varona, 2010). If the edges are weighted according to some prescription – such as the Hebb rule (Hebb, 1949) – which saves information from a set of given patterns of activity (particular configurations of active and inactive neurons), these patterns become attractors of the phase-space dynamics. Therefore, the system is then able to retrieve the stored patterns; this mechanism is known as *associative memory*. Actual neural systems do much more than just recalling a memory and staying there, however. That is, one should expect dynamic instabilities or some other destabilizing mechanism. This expectation is reinforced by recent experiments suggesting that synapses undergo rapid changes with time which may both determine brain tasks (Abbott et al., 1997; Tsodyks et al., 1998; Hilfiker et al., 1999; Pantic et al., 2002) and induce irregular and perhaps chaotic activity (Barrie et al., 1996; Korn and Faure, 2003).

One may argue that the observed rapid changes (which have been found to cause "synaptic depression" and/or "facilitation" on the time scale of milliseconds (Tsodyks et al., 1998; Pantic et al., 2002) – i.e., much faster than the plasticity processes whereby synapses *store* patterns (Malenka and Nicoll, 1999)) may simply correspond to the characteristic behaviour of single excitable elements. Furthermore, a fully-connected network which describes cooperation among such excitable elements has recently been shown to exhibit both attractors and chaotic instabilities (Marro et al., 2008). The work described here, first reported by Johnson et al. (2008), extends and generalizes this study to conclude on the influence of the excitable network topology on

[1]Several studies have already shown that binary neurons can capture the essence of cooperation in many more complex settings. See, for instance, (Pantic et al., 2002) in the case of integrate and fire neuron models of pyramidal cells.

dynamic behaviour. We show, in particular, an interesting correlation between certain wiring topology and optimal functionality.

4.2 The Fast-Noise model

Consider N binary nodes ($s_i = \pm 1$) and the adjacency matrix, $\hat{a}_{ij} = 1, 0$, which indicates the existence or not of an edge between nodes $i, j = 1, 2, ..., N$. Let there be a set of M patterns, $\xi_i^\nu = \pm 1$, $\nu = 1, ...M$ (which we generate here at random), and assume that they are "stored" by giving each edge a base weight $\overline{\omega_{ij}} = N^{-1} \sum_\nu \xi_i^\nu \xi_j^\nu$. Actual weights are dynamic, however, namely, $\omega_{ij} = \overline{\omega_{ij}} x_j$ where x_j is a stochastic variable. Assuming the limit in which this varies in a time scale infinitely smaller than the one for node dynamics, we can consider a stationary distribution such as $P(x_j|S) = q\delta(x_j - \Xi_j) + (1-q)\delta(x_j - 1)$, $S = \{s_j\}$, for instance. This amounts to assuming that, at each time step, every connection has a probability q of altering its weight by a factor Ξ_j which is a function (to be determined) of the local *field* at j, defined as the net current arriving to j from other nodes. This choice differs essentially from the one used by Marro et al. (2008), where q depends on the global degree of order and Ξ_j is a constant independent of j.

Assume independence of the noise at different edges, and that the transition rate for the stochastic changes is

$$\frac{\bar{c}\,(S \to S^i)}{\bar{c}\,(S^i \to S)} = \prod_{j/\hat{a}_{ij}=1} \frac{\int dx_j P(x_j|S)\Psi(u_{ij})}{\int dx_j P(x_j|S^i)\Psi(-u_{ij})},$$

where $u_{ij} \equiv s_i s_j x_j \overline{\omega_{ij}} T^{-1}$, $\Psi(u) = \exp\left(-\frac{1}{2}u\right)$ to have proper contour conditions, T is a "temperature" or stochasticity parameter, and S^i stands for S after the change $s_i \to -s_i$. (This formalism and its interpretation is described in detail by Marro and Dickman.) We define the *effective local fields* $h_i^{\text{eff}} = h_i^{\text{eff}}(S, T, q)$ via $\prod_j \varphi_{ij}^- / \varphi_{ij}^+ = \exp\left(-h_i^{\text{eff}} s_i / T\right)$, where $\varphi_{ij}^\pm \equiv q \exp\left(\pm \Xi_j v_{ij}\right) + (1-q)\exp\left(\pm v_{ij}\right)$, with $v_{ij} = \frac{1}{2}\hat{a}_{ij} u_{ij}$. Effective weights ω_{ij}^{eff} then follow from $h_i^{\text{eff}} = \sum_j \omega_{ij}^{\text{eff}} s_j \hat{a}_{ij}$. To obtain an analytical expression, we linearize around $\overline{\omega_{ij}} = 0$ (a good approximation when $M \ll N$), which yields

$$\omega_{ij}^{\text{eff}} = \left[1 + q\left(\Xi_j - 1\right)\right] \overline{\omega_{ij}}.$$

In order to fix Ξ_j here, we first introduce the overlap vector $\overrightarrow{m} = (m^1, ...m^M)$, with $m^\nu \equiv N^{-1} \sum_i \xi_i^\nu s_i$, which measures the correlation between the current configuration and each of the stored patterns, and the *local* one $\overrightarrow{m_j}$ of components $m_j^\nu \equiv \langle k \rangle^{-1} \sum_l \xi_l^\nu s_l \hat{a}_{jl}$, where $\langle k \rangle$ is the mean node connectivity, i.e.,

the average of $k_i = \sum_j \hat{a}_{ij}$. We then assume, for any $q \neq 0$, that the relevant factor is $\Xi_j = 1 + \zeta(h_j^\nu)(\Phi - 1)/q$, with

$$\zeta(h_j^\nu) = \frac{\chi^\alpha}{1 + M/N} \sum_\nu |h_j^\nu|^\alpha,$$

where $\chi \equiv N/\langle k \rangle$ and $\alpha > 0$ is a parameter. This comes from the fact that the field at node j can be written as a sum of components from each pattern, namely, $h_j = \sum_\nu^M h_j^\nu$, where

$$h_j^\nu = \xi_j^\nu N^{-1} \sum_i \hat{a}_{ij} \xi_i^\nu s_i = \chi^{-1} \xi_j^\nu m_j^\nu.$$

Our choice for Ξ_j, which amounts to assuming that the "fatigue" at a given edge increases with the field at the preceding node j (and allows to recover the fully–connected limit described by Marro et al. (2008) if $\alpha = 2$), finally leads to

$$\omega_{ij}^{\text{eff}} = [1 + (\Phi - 1)\zeta_j(\overrightarrow{m_j})]\, \overline{\omega_{ij}}.$$

Varying Φ one sets the nature of the weights. That is, $0 < \Phi < 1$ corresponds to resistance (*depression*) due to heavy local work, while the edge facilitates – i.e., tends to increase the effect of the signal under the same situation – for $\Phi > 1$. (The action of the edge is reversed for negative Φ.) We performed Monte Carlo simulations using standard parallel updating with the effective rates $\bar{c}\,(S \to S^i)$ computed using the latter effective weights.

4.3 Edge of Chaos

It is possible to solve the single pattern case ($M = 1$) under a mean-field assumption, which is a good approximation for large enough connectivity. That is, we may substitute the matrix $\hat{a}_{ij}$ by its mean value over network realizations to obtain analytical results that are independent of the underlying disorder. Imagine that each node hosts k_i *half–edges* according to a distribution $p(k)$, the total number of half–edges in the network being $\langle k \rangle N$. Choose a node i at random and randomly join one of its half–edges to an available free half–edge. The probability that this half–edge ends at node j is $k_j / (\langle k \rangle N)$. Once all the nodes have been linked up, the expected value (as a quenched average over network realizations) for the number of edges joining nodes i and j is[2]

[2] Assuming one edge at most between any two nodes, $\hat{a}_{ij} = 0, 1$, the value will be slightly smaller, but it is easy to prove that this is also a good approximation if the network has a *structural cut-off*: $k_i < \sqrt{\langle k \rangle N}$, $\forall i$.

$E(\hat{a}_{ij}) = k_i k_j / (\langle k \rangle N)$. This expression, which can be seen as a definition of the so-called *configuration model* for complex networks (Newman, 2003c), is valid for random networks with a given degree sequence (or, in practise, a given degree distribution) that have zero degree-degree correlations between neighbours (Johnson et al., 2010b). Using the notation $\eta_i \equiv \xi_i s_i$, we have $m_j = \chi \langle \eta_i \hat{a}_{ij} \rangle_i = \frac{\chi}{N} \sum_i \eta_i \hat{a}_{ij}$. Because node activity is not statistically independent of connectivity (Torres et al., 2004), we must define a new set of overlap parameters, analogous to m and m_j. That is, $\mu_n \equiv \langle k_i^n \eta_i \rangle_i / \langle k^n \rangle$ and the local versions $\mu_n^j \equiv \chi \langle k_i^n \eta_i \hat{a}_{ij} \rangle_i / \langle k^n \rangle$. After using $\hat{a}_{ij} = E(\hat{a}_{ij})$, one obtains the relation $\mu_n^i = \langle k^{n+1} \rangle k_i \mu_{n+1} / (\langle k^n \rangle \langle k \rangle^2)$. Inserting this expression into the definition of μ_n, and substituting $\langle s_i \rangle = \tanh[T^{-1} h_i^{eff}(S)]$ (for large N), standard mean-field analysis yields

$$\mu_n(t+1) = \frac{1}{\langle k^n \rangle} \left\langle k^n \tanh M_{T,\Phi}(k,t) \right\rangle_k ,$$

where the last quantity is defined as

$$M_{T,\Phi} = \frac{k}{TN} \left[\mu_1(t) + (\Phi - 1) \frac{\langle k^{\alpha+1} \rangle}{\langle k \rangle^{\alpha+1}} |\mu_1(t)|^\alpha \mu_{\alpha+1}(t) \right] .$$

This is a two-dimensional map which is valid for any random topology of distribution $p(k)$. Note that the macroscopic magnitude of interest is $\mu_0 = m \equiv |\overrightarrow{m}|$.

A main consequence of this is the existence of a critical temperature, T_c, under very general conditions. More specifically, as T is decreased, the overlap m describes a second–order phase transition from a disordered or, say, "paramagnetic" phase to an ordered ("ferromagnetic") phase which exhibits associative memory. The mean-field temperature at which this transition occurs is

$$T_c = \frac{\langle k^2 \rangle}{\langle k \rangle N}.$$

On the other hand, the map reduces to

$$\mu_n(t+1) = \text{sign} \left\{ \mu_n(t) \left[1 + (\Phi - 1) \frac{\langle k^{\alpha+1} \rangle}{\langle k \rangle^{\alpha+1}} \right] \right\}$$

for $T = 0$. This implies the existence at $\Phi = \Phi_0$, where

$$\Phi_0 = 1 - \frac{\langle k \rangle^{\alpha+1}}{\langle k^{\alpha+1} \rangle},$$

of a transition as Φ is decreased from the ferromagnetic phase to a new phase in which periodic hopping between the attractor and its negative occurs. This

is confirmed by the Monte Carlo simulations for $M > 1$; that is, the hopping is also among different attractors for finite T. The simulations also indicate that this transition washes out at low enough finite temperature. Instead, Monte Carlo evolutions show that, for a certain range of Φ values, the system activity then exhibits chaotic behaviour.

The transition from ferromagnetic to chaotic states is a main concern hereafter. Our interest in this regime follows from several recent observations concerning the relevance of chaotic activity in a network. In particular, it has been shown that chaos might be responsible for certain states of attention during brain activity (Torres et al., 2008, 2009), and that some network properties such as the computational capacity (Bertschinger and Natschläger, 2004) and the dynamic range of sensitivity to stimuli (de Assis and Copelli, 2008) may become optimal at the *Edge of Chaos* in a variety of settings.

We next note that the critical values T_c and Φ_0 only depend on the moments of the generic distribution $p(k)$, and that the ratio $\langle k^a\rangle/\langle k\rangle^a$, $a > 1$, is a convenient way of characterizing heterogeneity. We studied in detail two particular types of connectivity distributions with easily tunable heterogeneity; that is, networks with $\langle k\rangle N/2$ edges randomly distributed with $p\,(k)$ such that the heterogeneity depends on a single parameter. Our first case is the bimodal distribution, $p(k) = \frac{1}{2}\delta(k - k_1) + \frac{1}{2}\delta(k - k_2)$ with parameter $\Delta = (k_2 - k_1)/2 = \langle k\rangle - k_1 = k_2 - \langle k\rangle$. Our second case is the *scale–free* distribution, $p(k) \sim k^{-\gamma}$, which does not have any characteristic size but k is confined to the limits, k_0 and $k_m \leq \min(k_0 N^{\frac{1}{\gamma-1}}, N - 1)$ for finite N. Notice that the network in this case gets more homogeneous as γ is increased[3], and that this kind of distribution seems to be most relevant in nature (Newman, 2003c; Boccaletti et al., 2006). In particular, it seems important to mention that the *functional* topology of the human brain, as defined by correlated activity between small clusters of neurons, has been shown to correspond to this case with exponent $\gamma \simeq 2$ (Eguíluz et al., 2005). (It has not yet been possible to ascertain the brain's *structural* topology experimentally, but there is some evidence that function reflects structure at least to some extent (Zhou et al., 2006b). Furthermore, it has been suggested, based on indirect methods, that the structural connectivity of cat and macaque brains, at the level of brain areas, may indeed be scale free (Kaiser et al., 2007) – and in any

[3]The distribution is truncated and therefore not strictly scale free for $\gamma < 2$. However, nature shows examples for which γ is slightly larger than 1, so we consider the whole range here.

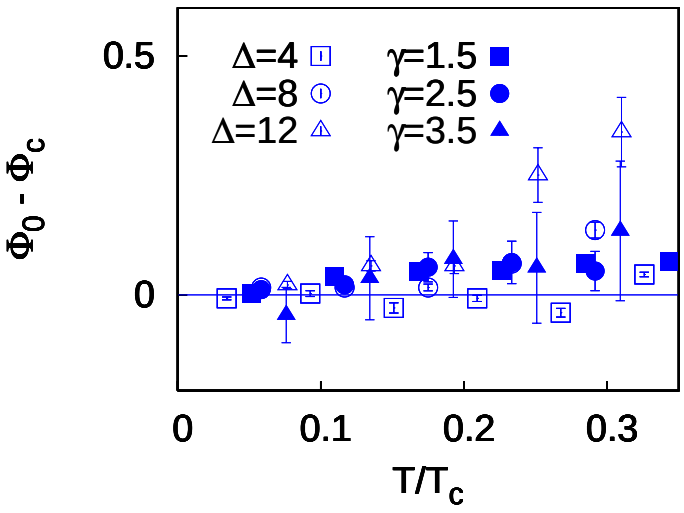

Figure 4.1: The temperature dependence of the difference between the values for the fatigue at which the ferromagnetic–periodic transition occurs, as obtained analytically for $T = 0$ (Φ_0) and from MC simulations at finite T (Φ_c). The critical temperature is calculated as $T_c = \langle k^2 \rangle \left(\langle k \rangle N \right)^{-1}$ for each topology. Data are for bimodal distributions with varying Δ and for scale–free topologies with varying γ, as indicated. Here, $\langle k \rangle = 20$, $N = 1600$ and $\alpha = 2$. Standard deviations, represented as bars in this graph, were shown to drop with $N^{-1/2}$ (not depicted).

case displays significantly higher heterogeneity than that of, say, Erdős–Rényi random graphs.)

We obtained the critical value of the fatigue, $\Phi_c(T)$, from Monte Carlo simulations at finite temperature T. These indicate that chaos never occurs for $T \gtrsim 0.35 T_c$. On the other hand, a detailed comparison of the value Φ_c with Φ_0 – as obtained analytically for $T = 0$ – indicates that $\Phi_c \simeq \Phi_0$.

Figure 4.1 illustrates the "error" $\Phi_0 - \Phi_c(T)$ for different topologies. This shows that the approximation $\Phi_c \simeq \Phi_0$ is quite good at low T for any of the cases examined. Therefore, assuming the critical values for the main parameters, T_c and Φ_0, as given by our map, we conclude that the more heterogeneous the distribution of connectivities of a network is, the lower the amount of fatigue, and the higher the critical temperature, needed to destabilize the dynamics. As an example of this interesting behaviour, consider a network with $\langle k \rangle = \ln(N)$, and dynamics according to $\alpha = 2$. If the distribution were

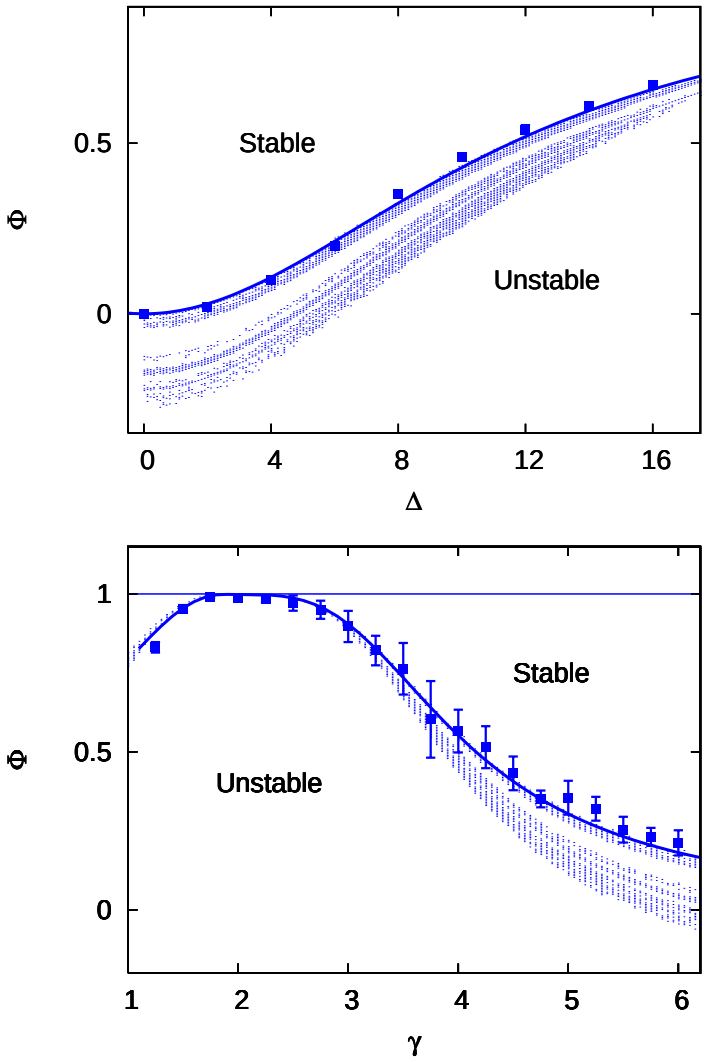

Figure 4.2: The critical fatigue values Φ_0 (solid lines) and Φ_c from MC averages over 10 networks (symbols) with $T = 2/N$, $\langle k \rangle = 20$, $N = 1600$, $\alpha = 2$. The dots below the lines correspond to changes of sign of the Lyapunov exponent as given by the iterated map, which qualitatively agree with the other results. This is for bimodal and scale–free topologies, as indicated.

regular, the critical values would be $T_c = \ln(N)/N$ (which goes to zero in the thermodynamic limit) and $\Phi_0 = 0$. However, a scale–free topology with the same number of edges and $\gamma = 2$ would yield $T_c = 1$ and $\Phi_0 = 1 - 2(\ln N)^3/N^2$ (which goes to 1 as $N \to \infty$).

Figure 6.5 illustrates, for two topologies, the phase diagram of the ferromagnetic–chaotic transition. Most remarkable is the plateau observed in the *Edge-of-*

Chaos or transition curve for scale–free topologies around $\gamma \simeq 2$, for which very little fatigue, namely, $\Phi \lesssim 1$ which corresponds to slight *depression*, is required to achieve chaos. The limit $\gamma \to \infty$ corresponds to $\langle k \rangle$–regular graphs (equivalent to $\Delta = 0$). If γ is reduced, k_m increases and k_0 decreases. The network is truncated when $k_m = N$. It follows that a value of γ exits at which k_0 cannot be smaller, so that k_m must drop to preserve $\langle k \rangle$. This explains the fall in Φ_c as $\gamma \to 1$.

Assuming that the "ferromagnetic phase" here corresponds to a *synchronous state*, our results are in qualitative agreement with the ones obtained recently for coupled oscillators (Nishikawa et al., 2003; Zhou et al., 2006a). As a matter of fact, the range of coupling strengths which allow for stability of synchronous states in these systems has been shown to depend on the spectral gap of the Laplacian matrix (Barahona and Pecora, 2002), implying that the more heterogeneous a topology is, the more easily activity can become unstable. It should be emphasized, however, that the dynamics we are considering here does not come within the scope of the formalism used to derive these results, since activity at node i depends on the local field at node j.

4.4 Network performance

As a further illustration of our findings, we monitored the performance as a function of topology during a simulation of pattern recognition. That is, we "showed" the system a pattern, say ν chosen at random from the set of M previously stored, every certain number of time steps. This was performed in practice by changing the field at each node for one time step, namely, $h_i \to h_i + \delta\xi^\nu$, where δ measures the intensity of the input signal. Ideally, the network should remain in this configuration until it is newly stimulated. The performance may thus be estimated from a temporal average of the overlap between the current state and the input pattern, $\langle m^\nu \rangle_{time}$. This is observed to simply increase monotonically with Δ for the bimodal case. The scale–free case, however, as illustrated in Fig. 4.3, shows how the task is better performed the closer to the Edge of Chaos the network is. This is because the system is then easily destabilized by the stimulus while being able to retrieve a pattern with accuracy. Figure 4.3 also shows that the best performance for the scale–free topology when $\Phi = 1$, i.e., in the absence of any fatigue, definitely occurs around $\gamma = 2$.

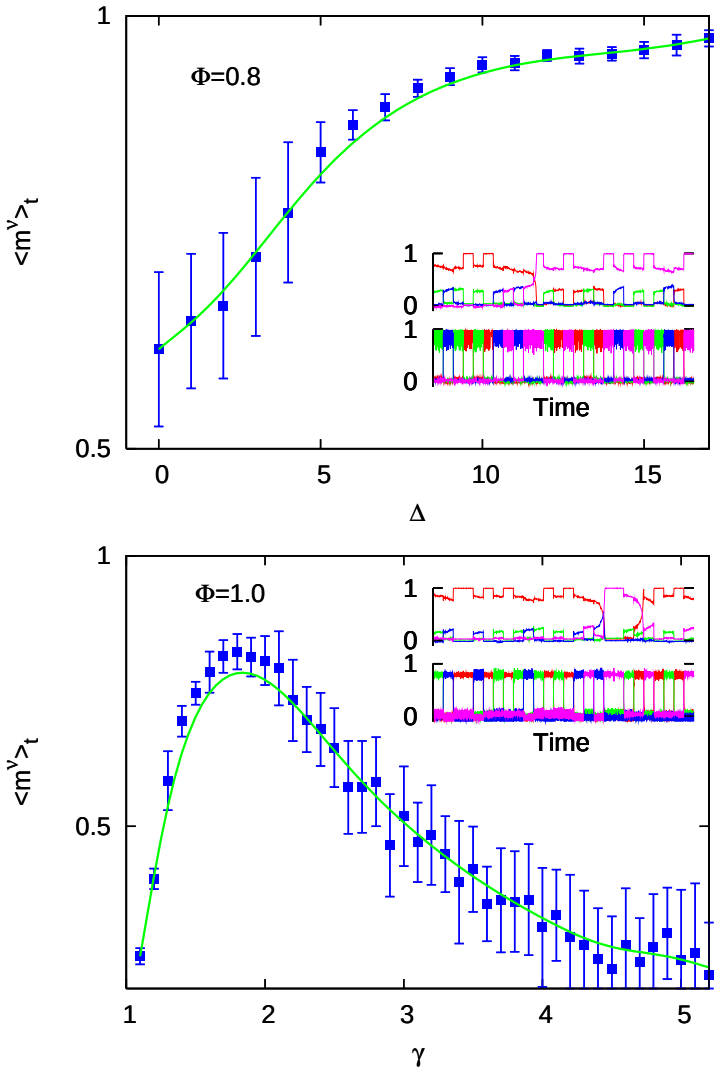

Figure 4.3: Network "performance" (see the main text) against Δ for bimodal topologies (above) and against γ for scale–free topologies (below). $\Phi = 0.8$ for the first case and $\Phi = 1$ in the second. Averages over 20 network realizations with stimulation every 50 MC steps for 2000 MC steps, $\delta = 5$ and $M = 4$; other parameters as in Fig. 6.5. Inset shows sections of typical time series of m^ν for $\Delta = 10$ (above) and $\gamma = 4$ (below); the corresponding stimulus for pattern ν is shown underneath.

4.5 Discussion

The model network we have studied is one of the simplest relevant situations one may conceive. In particular, as emphasized above, we are greatly simplyfieng the elements at the nodes (neurons) as binary variables. However, our

assumption of dynamic connections which depend on the local fields in such a simple scenario happens to show that a close relation may exist between topological heterogeneity and function, thus suggesting this may indeed be a relevant property for a realistic network efficiently to perform certain high level tasks. In a similar way to networks shown previously to be useful for pattern recognition and family identification (Cortes et al., 2005), our system retrieves memory patterns with accuracy in spite of noise, and yet it is easily destabilized so as to change state in response to an input signal – without requiring excessive *fatigue* for the purpose. There is a relation between the amount Φ of fatigue and the value of γ for which performance is maximized. One may argue that the plateau of "good" behaviour shown around $\gamma \simeq 2$ for scale–free networks with $\Phi \lesssim 1$ (Fig. 6.5) is a possible justification for the supposed tendency of certain systems in nature to evolve towards this topology. It may also prove useful for implementing some artificial networks.

Chapter 5

Correlated networks and natural disassortativity

An intriguing feature of complex networks is the ubiquity of strong negative degree-degree correlations between neighbouring nodes – the only exceptions being social systems, which tend to be *assortative* instead of *disassortative*. With the double purpose of addressing this mystery and uncovering the effects of correlations on network behaviour, we put forward a method which allows for the model-independent study of ensembles of correlated networks. We go on to show, by means of an information theory approach, that the expected value of correlations for a network at equilibrium (i.e., in the absence of specific correlating mechanisms) is not, as had been supposed, uncorrelated, but rahter disassortative. It turns out that the correlations of some networks are in excellent agreement with our predictions, while others, with known correlating or anticorrelating mechanisms, indeed appear to have been driven from their equilibrium points as expected. Therefore, our approach not only provides a parsimonious topological answer to a long-standing question, but also a neutral model against which to contrast experimental data to determine whether mechanisms must be sought to account for observed correlations. We go on to use our method, in Chapter 6, to study the influence of assortativity on neural-network dynamics.

5.1 Assortativity of networks

Complex networks, whether natural or artificial, have non-trivial topologies which are usually studied by analysing a variety of measures, such as the degree distribution, clustering, average paths, modularity, etc. (Albert and

Barabási, 2002; Dorogovtsev and Mendes, 2003; Pastor-Satorras and Vespignani, 2004; Newman, 2003c; Boccaletti et al., 2006) The mechanisms which lead to a particular structure and their relation to functional constraints are often not clear and constitute the subject of much debate (Newman, 2003c; Boccaletti et al., 2006). When nodes are endowed with some additional "property," a feature known as *mixing* or *assortativity* can arise, whereby edges are not placed between nodes completely at random, but depending in some way on the property in question. If similar (dissimilar) nodes tend to wire together, the network is said to be *assortative* (*disassortative*) (Newman, 2002, 2003a).

An interesting situation is when the property taken into account is the degree of each node – i.e., the number of neighbouring nodes connected to it. It turns out that a high proportion of empirical networks – whether biological, technological, information-related or linguistic – are disassortatively arranged (high-degree nodes, or hubs, are preferentially linked to low-degree neighbours, and viceversa) while social networks are usually assortative. Such degree-degree correlations have important consequences for network characteristics such as connectedness and robustness (Newman, 2002, 2003a).

However, while assortativity in social networks can be explained taking into account homophily (Newman, 2002, 2003a) or modularity (Newman and Park, 2003), the widespread prevalence and extent of disassortative mixing in most other networks remains somewhat mysterious. Maslov *et al.* found that the restriction of having at most one edge per pair of nodes induces some disassortative correlations in heterogeneous networks (Maslov et al., 2004), and Park and Newman showed how this analogue of the Pauli exclusion principle leads to the edges following Fermi statistics (Park and Newman, 2003) (see also (Capocci and Colaiori, 2006)). However, this restriction is not sufficient to fully account for empirical data. In general, when one attempts to consider computationally all the networks with the same distribution as a given empirical one, the mean assortativity is not necessarily zero (Holme and Zhao, 2007). But since some "randomization" mechanisms induce positive correlations and others negative ones (Farkas et al., 2004; Johnson et al., 2010a), it is not clear how the phase space can be properly sampled numerically.

In this chapter we develop a method for the study of correlated networks which is model-independent, and describe the main result of Ref. (Johnson et al., 2010b) – namely, that there is a general reason, consistent with empirical data, for the "natural" mixing of most networks to be disassortative. Using an information-theory approach we find that the configuration which can be

expected to come about in the absence of specific additional constraints turns out not to be, in general, uncorrelated. In fact, for highly heterogeneous degree distributions such as those of the ubiquitous scale-free networks, we show that the expected value of the mixing is usually disassortative: there are simply more possible disassortative configurations than assortative ones. This result provides a simple topological answer to a long-standing question. Let us caution that this does *not* imply that all scale-free networks are disassortative, but only that, in the absence of further information on the mechanisms behind their evolution, this is the neutral expectation.

5.2 The entropy of network ensembles

The topology of a network is entirely described by its adjacency matrix $\hat{a}$; the element $\hat{a}_{ij}$ represents the number of edges linking node i to node j (for undirected networks, $\hat{a}$ is symmetric). Among all the possible microscopically distinguishable configurations a set of L edges can adopt when distributed among N nodes, it is often convenient to consider the set of configurations which have certain features in common – typically some macroscopic magnitude, like the degree distribution. Such a set of configurations defines an *ensemble*. In a seminal series of papers Bianconi has determined the partition functions of various ensembles of random networks and derived their statistical-mechanics entropy (Bianconi, 2008, 2009; Anand and Bianconi, 2009). This allows the author to estimate the probability that a random network with certain constraints has of belonging to a particular ensemble, and thus assess the relative importance of different magnitudes and help discern the mechanisms responsible for a given real-world network. For instance, she shows that scale-free networks arise naturally when the total entropy is restricted to a small finite value. Here we take a similar approach: we obtain the Shannon information entropy encoded in the distribution of edges. As we shall see, both methods yield the same results (Jaynes, 1957; Anand and Bianconi, 2009), but for our purposes the Shannon entropy is more tractable.

The Shannon entropy associated with a probability distribution p_m is

$$s = -\sum_m p_m \ln(p_m),$$

where the sum extends over all possible outcomes m. For a given pair of nodes (i, j), p_m can be considered to represent the probability of there being m edges between i and j. For simplicity, we shall focus here on networks such

that $\hat{a}_{ij}$ can only take values 0 or 1, although the method is applicable to any number of edges allowed. In this case, we have only two terms: $p_1 = \hat{\epsilon}_{ij}$ and $p_0 = 1 - \hat{\epsilon}_{ij}$, where $\hat{\epsilon}_{ij} \equiv E(\hat{a}_{ij})$ is the expected value of the element $\hat{a}_{ij}$ given that the network belongs to the ensemble of interest. The entropy associated with pair (i, j) is then

$$s_{ij} = -\left[\hat{\epsilon}_{ij} \ln(\hat{\epsilon}_{ij}) + (1 - \hat{\epsilon}_{ij}) \ln(1 - \hat{\epsilon}_{ij})\right],$$

while the total entropy of the network is $S = \sum_{ij}^{N} s_{ij}$:

$$S = -\sum_{ij}^{N} \left[\hat{\epsilon}_{ij} \ln(\hat{\epsilon}_{ij}) + (1 - \hat{\epsilon}_{ij}) \ln(1 - \hat{\epsilon}_{ij})\right]. \tag{5.1}$$

Since we have not imposed symmetry of the adjacency matrix, this expression is in general valid for directed networks. For undirected networks, however, the sum is only over $i \leq j$, with the consequent reduction in entropy.

For the sake of illustration, we shall estimate the entropy of the Internet at the autonomous system (AS) level and compare it with the values obtained in (Bianconi, 2008, 2009; Anand and Bianconi, 2009) assuming the network belongs to two different ensembles: the fully random graph, or Erdős-Rényi (ER) ensemble, and the *configuration* ensemble with a scale-free degree distribution ($p(k) \sim k^{-\gamma}$) (Newman, 2003c) and structural cutoff, $k_i < \sqrt{\langle k \rangle N}$, $\forall i$ (Bianconi, 2008, 2009; Anand and Bianconi, 2009) ($\langle k \rangle$ is the mean degree). In this example, we assume the network to be sparse enough to expand the term $\ln(1-\hat{\epsilon}_{ij})$ in Eq. (5.1) and keep only linear terms. This reduces Eq. (5.1) to

$$S_{sparse} \simeq -\sum_{ij}^{N} \hat{\epsilon}_{ij}[\ln(\hat{\epsilon}_{ij}) - 1] + O(\hat{\epsilon}_{ij}^2).$$

In the ER ensemble, each of N nodes has an equal probability of receiving each of $\frac{1}{2}\langle k \rangle N$ undirected edges. So, writing $\hat{\epsilon}_{ij}^{ER} = \langle k \rangle / N$, we have

$$S_{ER} = -\frac{1}{2}\langle k \rangle N \left[\ln\left(\langle k \rangle / N\right) - 1\right].$$

The configuration ensemble, which imposes a given degree sequence $(k_1, ...k_N)$, is defined via the expected value of the adjacency matrix (Newman, 2003c; Johnson et al., 2008):

$$\hat{\epsilon}_{ij}^{c} = k_i k_j / (\langle k \rangle N).$$

This value leads to

$$S_c = \langle k \rangle N[\ln(\langle k \rangle N) + 1] - 2N\langle k \ln k \rangle,$$

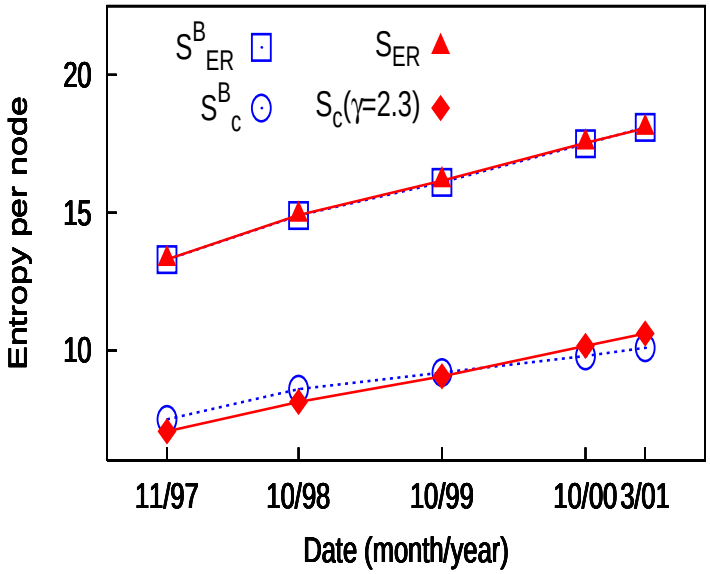

Figure 5.1: Evolution of the Internet at the AS level. Empty (blue) squares and circles: entropy per node of randomized networks in the fully random and in the configuration ensembles, as obtained by Bianconi (hence the "B" superscription) (Bianconi, 2008, 2009; Anand and Bianconi, 2009). Filled (red) triangles and diamonds: Shannon entropy for an ER network and a scale-free one with $\gamma = 2.3$, respectively.

where $\langle\cdot\rangle \equiv N^{-1}\sum_i(\cdot)$ stands for an average over nodes.

Fig. 5.1 displays the entropy per node obtained in (Bianconi, 2008, 2009; Anand and Bianconi, 2009) for the first two levels of approximation (ensembles) to the Internet at the AS level, first taking into account only the numbers of nodes N and edges $L = \frac{1}{2}\langle k\rangle N$, and then also the degree sequence. Alongside these, we plot the Shannon entropy both for an ER random network, (which coincides exactly with Bianconi's expression), and for a scale-free network with $\gamma = 2.3$ (the slight disparity arising from this exponent's changing a little with time).

5.3 Entropic origin of disassortativity

We shall now go on to analyse the effect of degree-degree correlations on the entropy. In the configuration ensemble, the expected value of the mean degree

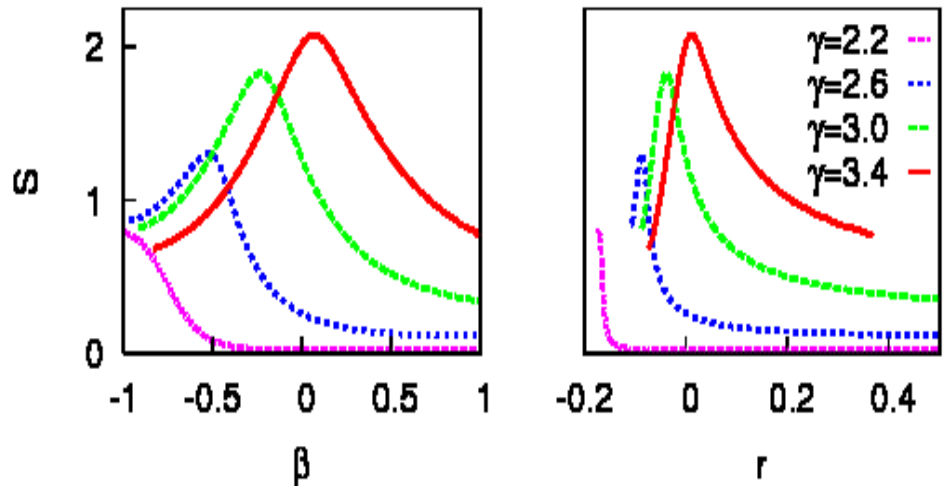

Figure 5.2: Shannon entropy of correlated scale-free networks against parameter β (left panel) and against Pearson's coefficient r (right panel), for various values of γ (increasing from bottom to top). $\langle k\rangle = 10$, $N = 10^4$.

of the neighbours of a given node is

$$k_{nn,i} = k_i^{-1} \sum_j \hat{\epsilon}^c_{ij} k_j = \frac{\langle k^2\rangle}{\langle k\rangle},$$

which is independent of k_i. However, as mentioned above, real networks often display degree-degree correlations, with the result that $k_{nn,i} = k_{nn}(k_i)$. If $k_{nn}(k)$ increases (decreases) with k, the network is assortative (disassortative). A measure of this phenomenon is Pearson's coefficient applied to the edges (Newman, 2003c, 2002, 2003a; Boccaletti et al., 2006):

$$r = \frac{[k_l k'_l] - [k_l]^2}{[k_l^2] - [k_l]^2},$$

where k_l and k'_l are the degrees of each of the two nodes belonging to edge l, and $[\cdot] \equiv (\langle k\rangle N)^{-1} \sum_l(\cdot)$ is an average over edges. Writing $\sum_l(\cdot) = \sum_{ij} \hat{a}_{ij}(\cdot)$, r can be expressed as

$$r = \frac{\langle k\rangle\langle k^2 k_{nn}(k)\rangle - \langle k^2\rangle^2}{\langle k\rangle\langle k^3\rangle - \langle k^2\rangle^2}. \tag{5.2}$$

The ensemble of all networks with a given degree sequence $(k_1, ...k_N)$ contains a subset for all members of which $k_{nn}(k)$ is constant (the configuration ensemble), but also subsets displaying other functions $k_{nn}(k)$. We can identify each one

of these subsets (regions of phase space) with an expected adjacency matrix $\hat{\epsilon}$ which simultaneously satisfies the following conditions:

$$\textbf{i)} \quad \sum_j k_j \hat{\epsilon}_{ij} = k_i k_{nn}(k_i),\ \forall i, \text{ and}$$

$$\textbf{ii)} \quad \sum_j \hat{\epsilon}_{ij} = k_i,\ \forall i \text{ (for consistency)}.$$

An ansatz which fulfils these requirements is any matrix of the form

$$\hat{\epsilon}_{ij} = \frac{k_i k_j}{\langle k \rangle N} + \int d\nu \frac{f(\nu)}{N} \left[\frac{(k_i k_j)^\nu}{\langle k^\nu \rangle} - k_i^\nu - k_j^\nu + \langle k^\nu \rangle \right], \tag{5.3}$$

where $\nu \in \mathbb{R}$ and the function $f(\nu)$ is in general arbitrary, although depending on the degree sequence it shall here be restricted to values which maintain $\hat{\epsilon}_{ij} \in [0,1]$, $\forall i,j$. This ansatz yields

$$k_{nn}(k) = \frac{\langle k^2 \rangle}{\langle k \rangle} + \int d\nu f(\nu) \sigma_{\nu+1} \left[\frac{k^{\nu-1}}{\langle k^\nu \rangle} - \frac{1}{k} \right] \tag{5.4}$$

(the first term being the result for the configuration ensemble), where $\sigma_{b+1} \equiv \langle k^{b+1} \rangle - \langle k \rangle \langle k^b \rangle$. In practice, one could adjust Eq. (5.4) to fit any given function $k_{nn}(k)$ and then wire up a network with the desired correlations: it suffices to throw random numbers according to Eq. (5.3) with $f(\nu)$ as obtained from the fit to Eq. (5.4)[1]. To prove the uniqueness of a matrix $\hat{\epsilon}$ obtained in this way (i.e., that it is the only one compatible with a given $k_{nn}(k)$) assume that there exists another valid matrix $\hat{\epsilon}' \neq \hat{\epsilon}$. Writting $\hat{\epsilon}'_{ij} - \hat{\epsilon}_{ij} \equiv h(k_i, k_j) = h_{ij}$, then **i**) implies that $\sum_j k_j h_{ij} = 0$, $\forall i$, while **ii**) means that $\sum_j h_{ij} = 0$, $\forall i$. It follows that $h_{ij} = 0$, $\forall i,j$.

In many empirical networks, $k_{nn}(k)$ has the form $k_{nn}(k) = A + Bk^\beta$, with $A, B > 0$ (Boccaletti et al., 2006; Pastor-Satorras et al., 2001) – the mixing being assortative (disassortative) if β is positive (negative). Such a case is fitted by Eq. (5.4) if

$$f(\nu) = C \left[\delta(\nu - \beta - 1) \frac{\sigma_2}{\sigma_{\beta+2}} - \delta(\nu - 1) \right],$$

[1] Although, as with the configuration ensemble, it is not always possible to wire a network according to a given $\hat{\epsilon}$.

with C a positive constant, since this choice yields

$$k_{nn}(k) = \frac{\langle k^2 \rangle}{\langle k \rangle} + C\sigma_2 \left[\frac{k^\beta}{\langle k^{\beta+1} \rangle} - \frac{1}{\langle k \rangle} \right]. \tag{5.5}$$

After plugging Eq. (5.5) into Eq. (5.2), one obtains:

$$r = \frac{C\sigma_2}{\langle k^{\beta+1} \rangle} \left(\frac{\langle k \rangle \langle k^{\beta+2} \rangle - \langle k^2 \rangle \langle k^{\beta+1} \rangle}{\langle k \rangle \langle k^3 \rangle - \langle k^2 \rangle^2} \right). \tag{5.6}$$

Inserting Eq. (5.3) in Eq. (5.1), we can calculate the entropy of correlated networks as a function of β and C – or, by using Eq. (5.6), as a function of r. Particularizing for scale-free networks, then given $\langle k \rangle$, N and γ, there is always a certain combination of parameters β and C which maximizes the entropy; we shall call these β^* and C^*. For $\gamma \lesssim 5/2$ this point corresponds to $C^* = 1$. For higher γ, the entropy can be slightly higher for larger C. However, for these values of γ, the assortativity r of the point of maximum entropy obtained with $C = 1$ differs very little from the one corresponding to β^* and C^* (data not shown). Therefore, for the sake of clarity but with very little loss of accuracy, in the following we shall generically set $C = 1$ and vary only β in our search for the level of assortativity, r^*, that maximizes the entropy given $\langle k \rangle$, N and γ. Note that $C = 1$ corresponds to removing the linear term, proportional to $k_i k_j$, in Eq. (5.3), and leaving the leading non-linearity, $(k_i k_j)^{\beta+1}$, as the dominant one.

Fig. 5.2 displays the entropy curves for various scale-free networks, both as functions of β and of r: *depending on the value of γ, the point of maximum entropy can be either assortative or disassortative*. This can be seen more clearly in Fig. 5.3, where r^* is plotted against γ for scale-free networks with various mean degrees $\langle k \rangle$. The values obtained by Park and Newman (Park and Newman, 2003) as those resulting from the one-edge-per-pair restriction are also shown for comparison: notice that whereas this effect alone cannot account for the Internet's correlations for any γ, entropy considerations would suffice if $\gamma \simeq 2.1$. As shown in the inset, the results are robust in the large system-size limit.

Since most networks observed in the real world are highly heterogeneous, with exponents in the range $\gamma \in (2, 3)$, it is to be expected that these should display a certain disassortativity – the more so the lower γ and the higher $\langle k \rangle$. In Fig. 5.4 we test this prediction on a sample of empirical, scale-free networks quoted in Newman's review (Newman, 2003c) (p. 182). For each case, we found the value of r that maximizes S according to Eq. (5.1), after inserting Eq. (5.3) with the quoted values of $\langle k \rangle$, N and γ. In this way, we obtained

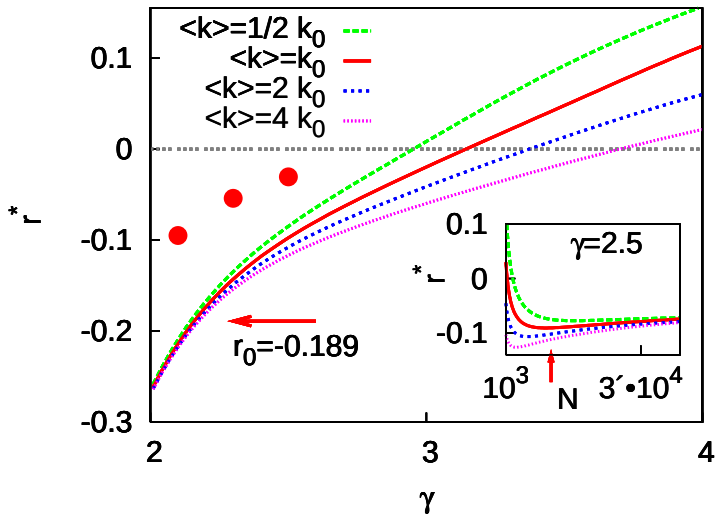

Figure 5.3: Lines from top to bottom: r at which the entropy is maximized, r^*, against γ for random scale-free networks with mean degrees $\langle k\rangle = \frac{1}{2}$, 1, 2 and 4 times $k_0 = 5.981$, and $N = N_0 = 10697$ nodes (k_0 and N_0 correspond to the values for the Internet at the AS level in 2001 (Park and Newman, 2003), which had $r = r_0 = -0.189$). Symbols are the values obtained in (Park and Newman, 2003) as those expected solely due to the one-edge-per-pair restriction (with k_0, N_0 and $\gamma = 2.1$, 2.3 and 2.5). Inset: r^* against N for networks with fixed $\langle k\rangle/N$ (same values as the main panel) and $\gamma = 2.5$; the arrow indicates $N = N_0$.

the expected assortativity for six networks, representing: a peer-to-peer (P2P) network, metabolic reactions, the nd.edu domain, actor collaborations, protein interactions, and the Internet (see (Newman, 2003c) and references therein). For the metabolic, Web domain and protein networks, *the values predicted are in excellent agreement with the measured ones*; therefore, no specific anticorrelating mechanisms need to be invoked to account for their disassortativity. In the other three cases, however, the predictions are not accurate, so there must be additional correlating mechanisms at work. Indeed, it is known that small routers tend to connect to large ones (Pastor-Satorras et al., 2001), so one would expect the Internet to be more disassortative than predicted, as is the case[2] – an effect that is less pronounced but still detectable in the more

[2]However, as Fig. 5.3 shows, if the Internet exponent were the $\gamma = 2.2 \pm 0.1$ reported in (Pastor-Satorras et al., 2001) rather than $\gamma = 2.5$, entropy would account more fully for

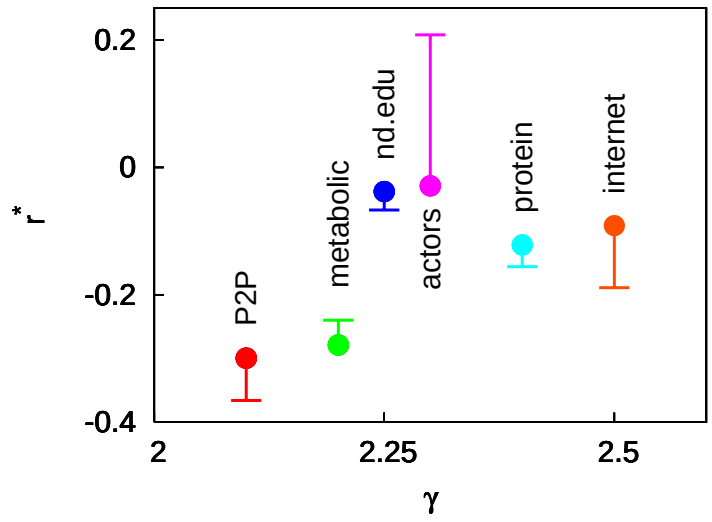

Figure 5.4: Level of assortativity that maximizes the entropy, r^*, for various real-world, scale-free networks, as predicted theoretically by Eq. (5.1) (circles) and as directly measured (horizontal lines), against exponent γ.

egalitarian P2P network. Finally, as is typical of social networks, the actor graph is significantly more assortative than predicted, probably due to the homophily mechanism whereby highly connected, big-name actors tend to work together (Newman, 2002, 2003a).

5.4 To sum up...

We have shown how the ensemble of networks with a given degree sequence can be partitioned into regions of equally correlated networks and found, using an information-theory approach, that the largest (maximum entropy) region, for the case of scale-free networks, usually displays a certain disassortativity. Therefore, in the absence of knowledge regarding the specific evolutionary forces at work, this should be considered the most likely state. Given the accuracy with which our approach can predict the degree of assortativity of certain empirical networks *with no a priori information thereon*, we suggest this as a neutral model to decide whether or not particular experimental data require specific mechanisms to account for observed degree-degree correlations.

these correlations.

Chapter 6

Enhancing robustness to noise via assortativity

As we saw in Chapter 4, the performance of attractor neural networks depends crucially on the heterogeneity of the underlying topology's degree distribution. We take this analysis a step further by examining the effect of degree-degree correlations – or assortativity – on neural-network behaviour. In Chapter 5 we described a method for studying correlated networks and dynamics thereon, both analytically and computationally, which is independent of how the topology may have evolved. We now make use of this to show how the robustness to noise is greatly enhanced in assortative (positively correlated) neural networks, especially if it is the hub neurons that store the information.

6.1 Background

For a dozen years or so now, the study of complex systems has been heavily influenced by results from network science – which one might regard as the fusion of graph theory with statistical physics (Newman, 2003c; Boccaletti et al., 2006). Phenomena as diverse as epidemics (Watts and Strogatz, 1998), cellular function (Süel et al., 2006), power-grid failures (Buldyrev et al., 2010) or internet routing (Boguñá et al., 2010), among many others (Arenas et al., 2008a), depend crucially on the structure of the underlying network of interactions. One of the earliest systems to have been described as a network was the brain, which is made up of a great many neurons connected to each other by synapses (y Cajal, 1995; Amit, 1989; Abbott and Kepler, 1990; Torres and Varona, 2010). Mathematically, the first neural networks combined the Ising model (Baxter, 1982) with the Hebb learning rule (Hebb, 1949) to reproduce,

very successfully, the storage and retrieval of information (Amari, 1972; Hopfield, 1982; Amit, 1995). Neurons were simplified to binary variables (like Ising spins) representing firing or non-firing cells. By considering the trivial fully-connected topology, exact solutions could be reached, which at the time seemed more important than attempting to introduce biological realism. Subsequent work has tended to focus on considering richer dynamics for the cells rather than on the way in which these are interconnected (Vogels et al., 2005; Torres et al., 2007; Mejias et al., 2010). However, the topology of the brain – whether at the level of neurons and synapses, cortical areas or functional connections – is obviously far from trivial (Amaral et al., 2000; Sporns et al., 2004; Eguíluz et al., 2005; Arenas et al., 2008b; Bullmore and Sporns, 2009; Johnson et al., 2010a).

The number of neighbours a given node in a network has is called its degree, and much attention is paid to degree distributions since they tend to be highly heterogeneous for most real networks. In fact, they are often approximately scale-free (i.e., described by power laws) (Newman, 2003c; Boccaletti et al., 2006; Peretto, 1992; Barabási and Oltvai, 2004). By including this topological feature in a Hopfield-like neural-network model, Torres *et al.* Torres et al. (2004) found that degree heterogeneity increases the system's performance at high levels of noise, since the hubs (high degree nodes) are able to retain information at levels well above the usual critical noise. To prove this analytically, the authors considered the *configurational ensemble* of networks (the set of random networks with a given degree distribution but no degree-degree correlations) and showed that Monte Carlo (MC) simulations were in good agreement with mean-field analysis, despite the approximation inherent to the latter technique when the network is not fully connected. A similar approach can also be used to show how heterogeneity may be advantageous for the performance of certain tasks in models with a richer dynamics (Johnson et al., 2008). It is worth mentioning that this influence of the degree distribution on dynamical behaviour is found in many other settings, such as the more general situation of systems of coupled oscillators (Barahona and Pecora, 2002).

Another property of empirical networks that is quite ubiquitous is the existence of correlations between the degrees of nodes and those of their neighbours (Pastor-Satorras et al., 2001; Newman, 2002, 2003a). If the average degree-degree correlation is positive the network is said to be *assortative*, while it is called *disassortative* if negatively correlated. Most heterogeneous networks are

disassortative (Newman, 2003c), which, as described in Chapter 5, seems to be because this is in some sense their equilibrium (maximum entropy) state given the constraints imposed by the degree distribution (Johnson et al., 2010b). However, there are probably often mechanisms at work which drive systems from equilibrium by inducing different correlations, as appears to be the case for most social networks, in which nodes (people) of a kind tend to group together. This feature, known as *assortativity* or *mixing by degree*, is also relevant for processes taking place on networks. For instance, assortative networks have lower percolation thresholds and are more robust to targeted attack (Newman, 2003a), while disassortative ones make for more stable ecosystems and are – at least according to the usual definition – more synchronizable (Brede and Sinha).

The approach usually taken when studying correlated networks computationally is to generate a network from the configuration ensemble and then introduce correlations (positive or negative) by some stochastic rewiring process (Maslov et al., 2004). A drawback of this method, however, is that results may well then depend on the details of this mechanism: there is no guarantee that one is correctly sampling the phase space of networks with given correlations. For analytical work, some kind of hidden variables from which the correlations originate are often considered (Caldarelli et al., 2002; Söderberg, 2002; Boguñá and Pastor-Satorras, 2003; Fronczak and Fronczak, 2006) – an assumption which can also be used to generate correlated networks computationally (Boguñá and Pastor-Satorras, 2003). This can be a very powerful method for solving specific network models. However, it may not be appropriate if one wishes to consider all possible networks with given degree-degree correlations, independently of how these may have arisen. In this chapter, we get round the problem by making use of the method put forward by Johnson et al. (2010b) (and described in Chapter 5) whereby the ensemble of all networks with given correlations can be considered theoretically without recurring to hidden variables (de Franciscis et al., 2011). Furthermore, we show how this approach can be used computationally to generate random networks that are representative of the ensemble of interest (i.e., they are model-independent). In this way, we study the effect of correlations on a simple neural network model and find that assortativity increases performance in the face of noise – particularly if it is the hubs that are mainly responsible for storing information (and it is worth mentioning that there is experimental evidence suggestive of a main functional role played by hub neurons in the brain (Morgan and Soltesz,

2008; Bonifazi et al., 2009)). The good agreement between the mean-field analysis and our MC simulations bears witness both to the robustness of the results as regards neural systems, and to the viability of using this method for studying dynamics on correlated networks.

6.2 Preliminary considerations

6.2.1 Model neurons on networks

The attractor neural network model put forward by Hopfield (Hopfield, 1982) consists of N binary neurons, each with an activity given by the dynamic variable $s_i = \pm 1$. Every time step (MCS), each neuron is updated according to the stochastic transition probability $P(s_i \to \pm 1) = \frac{1}{2}\left[1 \pm \tanh\left(h_i/T\right)\right]$ (parallel dynamics), where the field h_i is the combined effect on i of all its neighbours, $h_i = \sum_j \hat{w}_{ij} s_j$, and T is a noise parameter we shall call *temperature*, but which represents any kind of random fluctuations in the environment. This is the same as the Ising model for magnetic systems, and the transition rule can be derived from a simple interaction energy such that aligned variables s (spins) contribute less energy than if they were to take opposite values. However, this system can store P given configurations (*memory patterns*) $\xi_i^\nu = \pm 1$ by having the interaction strengths (*synaptic weights*) set according to the Hebb rule (Hebb, 1949): $\hat{w}_{ij} \propto \sum_{\nu=1}^{P} \xi_i^\nu \xi_j^\nu$. In this way, each pattern becomes an attractor of the dynamics, and the system will evolve towards whichever one is closest to the initial state it is placed in. This mechanism is called *associative memory*, and is nowadays used routinely for tasks such as image identification. What is more, it has been established that something similar to the Hebb rule is implemented in nature via the processes of long-term potentiation and depression at the synapses (Malenka and Nicoll, 1999; Roo et al., 2008; Rodríguez-Moreno and Paulsen, 2008; Kwag and Paulsen, 2009), and this phenomenon is indeed required for learning (Gruart et al., 2006).

To take into account the topology of the network, we shall consider the weights to be of the form $\hat{w}_{ij} = \hat{\omega}_{ij}\hat{a}_{ij}$, where the element $\hat{a}_{ij}$ of the adjacency matrix represents the number of directed edges (usually interpreted as synapses in a neural network) from node j to node i, while $\hat{\omega}$ stores the patterns, as before:

$$\hat{\omega}_{ij} = \frac{1}{\langle k \rangle} \sum_{\nu=1}^{P} \xi_i^\nu \xi_j^\nu .$$

For the sake of coherence with previous work, we shall assume $\hat{a}$ to be sym-

metric (i.e., the network is undirected), so each node is characterized by a single degree $k_i = \sum_j \hat{a}_{ij}$. However, all results are easily extended to directed networks – in which nodes have both an *in* degree, $k_i^{\text{in}} = \sum_j \hat{a}_{ij}$, and an *out* degree, $k_i^{\text{out}} = \sum_j \hat{a}_{ji}$ – by bearing in mind it is only a neuron's pre-synaptic neighbours that influence its behaviour. The mean degree of the network is $\langle k \rangle$, where the angles stand for an average over nodes[1]: $\langle \cdot \rangle \equiv N^{-1} \sum_i (\cdot)$.

6.2.2 Network ensembles

When one wishes to consider a set of networks which are randomly wired while respecting certain constraints – that is, an *ensemble* – it is usually useful to define the expected value of the adjacency matrix[2], $E(\hat{a}) \equiv \hat{\epsilon}$. The element $\hat{\epsilon}_{ij}$ of this matrix is the mean value of $\hat{a}_{ij}$ obtained by averaging over the ensemble. For instance, in the Erdős-Rényi (ER) ensemble all elements (outside the diagonal) take the value $\hat{\epsilon}_{ij}^{ER} = \langle k \rangle / N$, which is the probability that a given pair of nodes be connected by an edge. For studying networks with a given degree sequence, $(k_1, ...k_N)$, it is common to assume the *configuration ensemble*, defined as

$$\epsilon_{ij}^{conf} = \frac{k_i k_j}{\langle k \rangle N}$$

This expression can usually be applied also when the constraint is a given degree distribution, $p(k)$, by integrating over $p(k_i)$ and $p(k_j)$ where appropriate. One way of deriving $\hat{\epsilon}^{conf}$ is to assume one has k_i dangling half-edges at each node i; we then randomly choose pairs of half-edges and join them together until the network is wired up. Each time we do this, the probability that we join i to j is $k_i k_j / (\langle k \rangle N)^2$, and we must perform the operation $\langle k \rangle N$ times. Bianconi showed that this is also the solution for Barabási-Albert evolved networks (Bianconi, 2002). However, we should bear in mind that this result is only strictly valid for networks constructed in certain particular ways, such as in these examples. It is often implicitly assumed that were we to average over all random networks with a given degree distribution, the mean adjacency matrix obtained would be $\hat{\epsilon}^{conf}$. However, as we discussed in Chapter 5, this

[1] In directed networks the mean *in* degree and the mean *out* degree necessarily coincide, whatever the forms of the *in* and *out* distributions.

[2] As in statistical physics, one can consider the *microcanonical* ensemble, in which each element (network) satisfies the constraints exactly, or the *canonical* ensemble, where the constraints are satisfied on average (Bianconi, 2009). Throughout this work, we shall refer to canonical ensembles.

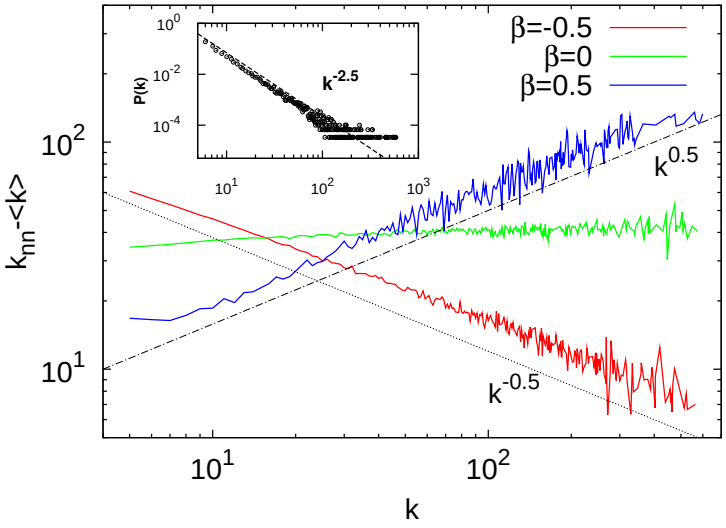

Figure 6.1: Mean-nearest-neighbour functions $\overline{k}_{nn}(k)$ for scale-free networks with $\beta = -0.5$ (disassortative), 0.0 (neutral), and 0.5 assortative, generated according to the algorithm described in Sec. 6.3.2. Inset: degree distribution (the same in all three cases). Other parameters are $\gamma = 2.5$, $\langle k \rangle = 12.5$, $N = 10^4$.

is not in fact necessarily true (Johnson et al., 2010b).

6.2.3 Correlated networks

In the configuration ensemble, the expected value of the mean degree of the neighbours of a given node is $\overline{k}_{nn,i} = k_i^{-1} \sum_j \hat{\epsilon}_{ij}^{conf} k_j = \langle k^2 \rangle / \langle k \rangle$, which is independent of k_i. However, as mentioned above, real networks often display degree-degree correlations, with the result that $\overline{k}_{nn,i} = \overline{k}_{nn}(k_i)$. If $\overline{k}_{nn}(k)$ increases with k, the network is said to be assortative – whereas it is disassortative if it decreases with k (see Fig. 6.1). This is from the more general nomenclature (borrowed form sociology) in which sets are assortative if elements of a kind group together, or assort. In the case of degree-degree correlated networks, positive assortativity means that edges are more than randomly likely to occur between nodes of a similar degree.

The ensemble of all networks with a given degree sequence $(k_1, ...k_N)$ contains a subset for all members of which $\overline{k}_{nn}(k)$ is constant (the configuration ensemble), but also subsets displaying other functions $\overline{k}_{nn}(k)$. We can identify each one of these subsets (regions of phase space) with an expected adjacency matrix $\hat{\epsilon}$ which simultaneously satisfies the following conditions: **i**)

$\sum_j k_j \hat{\epsilon}_{ij} = k_i \overline{k}_{nn}(k_i)$, $\forall i$ (by definition of $\overline{k}_{nn}(k)$), and **ii)** $\sum_j \hat{\epsilon}_{ij} = k_i$, $\forall i$ (for consistency). As we showed in Chapter 5, the general solution to this problem is a matrix of the form

$$\hat{\epsilon}_{ij} = \frac{k_i k_j}{\langle k \rangle N} + \int d\nu \frac{f(\nu)}{N} \left[\frac{(k_i k_j)^\nu}{\langle k^\nu \rangle} - k_i^\nu - k_j^\nu + \langle k^\nu \rangle \right], \tag{6.1}$$

where $\nu \in \mathbb{R}$ and the function $f(\nu)$ is determined by $\overline{k}_{nn}(k)$ (Johnson et al., 2010b). (If the network were directed, then $k_i = k_i^{\text{in}}$ and $k_j = k_j^{\text{out}}$ in this expression.) This yields

$$\overline{k}_{nn}(k) = \frac{\langle k^2 \rangle}{\langle k \rangle} + \int d\nu f(\nu) \sigma_{\nu+1} \left[\frac{k^{\nu-1}}{\langle k^\nu \rangle} - \frac{1}{k} \right] \tag{6.2}$$

(the first term being the result for the configuration ensemble), where $\sigma_{b+1} \equiv \langle k^{b+1} \rangle - \langle k \rangle \langle k^b \rangle$. This means that $\hat{\epsilon}$ is not just one possible way of obtaining correlations according to $\overline{k}_{nn}(k)$; rather, there is a two-way mapping between $\hat{\epsilon}$ and $\overline{k}_{nn}(k)$: every network with this particular function $\overline{k}_{nn}(k)$ and no other ones are contained in the ensemble defined by $\hat{\epsilon}$. Thanks to this, if we are able to consider random networks drawn according to this matrix (whether we do this analytically or computationally; see Section 6.3.2), we can be confident that we are correctly taking account of the whole ensemble of interest. In other words, whatever the reasons behind the existence of degree-degree correlations in a given network, we can study the effects of these with only information on $p(k)$ and $\overline{k}_{nn}(k)$ by obtaining the associated matrix $\hat{\epsilon}$. This is not to say, of course, that all topological properties are captured in this way: a particular network may have other features – such as higher order correlations, modularity, etc. – the consideration of which would require concentrating on a sub-partition of those with the same $p(k)$ and $\overline{k}_{nn}(k)$. But this is not our purpose here.

In many empirical networks, $\overline{k}_{nn}(k)$ has the form $\overline{k}_{nn}(k) = A + Bk^\beta$, with $A, B > 0$ (Boccaletti et al., 2006; Pastor-Satorras et al., 2001) – the mixing being assortative if β is positive, and disassortative when negative. Such a case is fitted by Eq. (6.2) if

$$f(\nu) = C \left[\frac{\sigma_2}{\sigma_{\beta+2}} \delta(\nu - \beta - 1) - \delta(\nu - 1) \right], \tag{6.3}$$

with C a positive constant, since this choice yields

$$\overline{k}_{nn}(k) = \frac{\langle k^2 \rangle}{\langle k \rangle} + C\sigma_2 \left[\frac{k^\beta}{\langle k^{\beta+1} \rangle} - \frac{1}{\langle k \rangle} \right]. \tag{6.4}$$

In Chapter 5 we discussed how the most likely configurations for networks with scale-free degree distributions ($p(k) \sim k^{-\gamma}$) and correlations given by Eq. (6.4) are generally disassortative. We also showed that the maximum entropy is usually obtained for values of C close to one. Here, we shall use this result to justify concentrating on correlated networks with $C = 1$, so that the only parameter we need to take into account is β. It is worth mentioning that Pastor-Satorras *et al.* originally suggested using this exponent as a way of quantifying correlations (Pastor-Satorras et al., 2001), since this seems to be the most relevant magnitude. Because β does not depend directly on $p(k)$ (as r does), and can be defined for networks of any size (whereas r, in very heterogeneous networks, always goes to zero for large N due to its normalization (Dorogovtsev et al., 2005)), we shall henceforth use β as our assortativity parameter.

So, after plugging Eq. (6.3) into Eq. (6.1), we find that the ensemble of networks exhibiting correlations given by Eq. (6.4) (and $C = 1$) is defined by the mean adjacency matrix

$$\begin{aligned} \hat{\epsilon}_{ij} &= \frac{1}{N}[k_i + k_j - \langle k \rangle] \\ &+ \frac{\sigma_2}{\sigma_{\beta+2}} \frac{1}{N} \left[\frac{(k_i k_j)^{\beta+1}}{\langle k^{\beta+1} \rangle} - k_i^{\beta+1} - k_j^{\beta+1} + \langle k^{\beta+1} \rangle \right]. \end{aligned} \tag{6.5}$$

6.3 Analysis and results

6.3.1 Mean field

Let us consider the single-pattern case ($P = 1$, $\xi_i = \xi_i^1$). Substituting the adjacency matrix $\hat{a}$ for its expected value $\hat{\epsilon}$ (as given by Eq. (6.5)) in the expression for the local field at i – which amounts to a mean-field approximation – we have

$$\begin{aligned} h_i &= \frac{1}{\langle k \rangle} \xi_i \left\{ \left[(k_i - \langle k \rangle) + \frac{\sigma_2}{\sigma_{\beta+2}} (\langle k^{\beta+1} \rangle - k_i^{\beta+1}) \right] \mu_0 \right. \\ &+ \left. \langle k \rangle \mu_1 + \frac{\sigma_2}{\sigma_{\beta+2}} (k_i^{\beta} - \langle k^{\beta+1} \rangle) \mu_{\beta+1} \right\}, \end{aligned}$$

where we have defined

$$\mu_\alpha \equiv \frac{\langle k_i^\alpha \xi_i s_i \rangle}{\langle k^\alpha \rangle}$$

for $\alpha = 0,\ 1,\ \beta + 1$. These order parameters measure the extent to which the system is able to recall information in spite of noise (Johnson et al., 2008).

For the first order we have $\mu_0 = m \equiv \langle \xi_i s_i \rangle$, the standard overlap measure in neural networks (analogous to magnetization in magnetic systems), which takes account of memory performance. However, μ_1, for instance, weighs the sum with the degree of each node, with the result that it measures information per synapse instead of per neuron. Although the overlap m is often assumed to represent, in some sense, the *mean firing rate* of neurological experiments, it is possible that μ_1 is more closely related to the empirical measure, since the total electric potential in an area of tissue is likely to depend on the number of synapses transmitting action potentials. In any case, a comparison between the two order parameters is a good way of assessing to what extent the performance of neurons depends on their degree – larger-degree model neurons can in general store information at higher temperatures than ones with smaller degree can (Torres et al., 2004).

Substituting s_i for its expected value according to the transition probability, $s_i \to \tanh(h_i/T)$, we have, for any α,

$$\langle k_i^\alpha \xi_i s_i \rangle = \langle k_i^\alpha \xi_i \tanh(h_i/T) \rangle;$$

or, equivalently, the following 3-D map of closed coupled equations for the macroscopic overlap observables μ_0, μ_1 and $\mu_{\beta+1}$ – which describes, in this mean-field approximation, the dynamics of the system:

$$\begin{aligned} \mu_0(t+1) &= \int p(k) \tanh[F(t)/(\langle k \rangle T)] \mathrm{d}k \\ \mu_1(t+1) &= \frac{1}{\langle k \rangle} \int p(k) k \tanh[F(t)/(\langle k \rangle T)] \mathrm{d}k \\ \mu_{\beta+1}(t+1) &= \frac{1}{\langle k^{\beta+1} \rangle} \int p(k) k^{\beta+1} \tanh[F(t)/(\langle k \rangle T)] \mathrm{d}k, \end{aligned} \tag{6.6}$$

with

$$\begin{aligned} F(t) &\equiv (k\mu_0(t) + \langle k \rangle \mu_1(t) - \langle k \rangle \mu_0(t)) \\ &+ \frac{\sigma_2}{\sigma_{\beta+2}} [k^{\beta+1}(\mu_{\beta+1}(t) - \mu_0(t)) \\ &+ \langle k^{\beta+1} \rangle (\mu_0(t) - \mu_{\beta+1}(t))]. \end{aligned}$$

This can be easily computed for any degree distribution $p(k)$. Note that taking $\beta = 0$ (the uncorrelated case) the system collapses to the 2-D map obtained by

Torres et al. (2004), while it becomes the typical 1-D case for a homogeneous $p(k)$ – say a fully-connected network (Hopfield, 1982). It is in principle possible to do similar mean-field analysis for any number P of patterns, but the map would then be $3P$-dimensional, making the problem substantially more complex.

At a critical temperature T_c, the system will undergo the characteristic second order phase transition from a phase in which it exhibits memory (akin to ferromagnetism) to one in which it does not (paramagnetism). To obtain this critical temperature, we can expand the hyperbolic tangent in Eqs. (6.6) around the trivial solution $(\mu_0, \mu_1, \mu_{\beta+1}) \simeq (0, 0, 0)$ and, keeping only linear terms, write

$$\begin{aligned}
\mu_0 &= \mu_1/T_c, \\
\mu_1 &= \frac{1}{\langle k\rangle^2 T_c}\left[\langle k\rangle^2\mu_1 + \sigma_2\mu_{\beta+1}\right], \\
\mu_{\beta+1} &= \frac{1}{T_c\langle k\rangle\langle k^{\beta+1}\rangle}\Big[\sigma_{\beta+2}\mu_0 \\
&+ \frac{\sigma_2}{\sigma_{\beta+2}}\left(\langle k^{\beta+1}\rangle^2 - \langle k^{2(\beta+1)}\rangle\right)\mu_0 \\
&+ \langle k\rangle\langle k^{\beta+1}\rangle\mu_1 - \frac{\sigma_2}{\sigma_{\beta+2}}\left(\langle k^{\beta+1}\rangle^2 - \langle k^{2(\beta+1)}\rangle\right)\mu_{\beta+1}\Big].
\end{aligned}$$

Defining

$$\begin{aligned}
A &\equiv \frac{\sigma_2}{\langle k\rangle^2}, \\
B &\equiv \frac{\sigma_2}{\sigma_{\beta+2}}\frac{\langle k^{2(\beta+1)}\rangle - \langle k^{\beta+1}\rangle^2}{\langle k\rangle\langle k^{\beta+1}\rangle}, \\
D &\equiv \frac{\sigma_{\beta+2}}{\langle k\rangle\langle k^{\beta+1}\rangle},
\end{aligned}$$

T_c will be the solution to the third order polynomial equation:

$$T_c^3 - (B+1)T_c^2 + (B-A)T_c + A(B-D) = 0. \tag{6.7}$$

Note that for neutral (i.e., uncorrelated) networks, $\beta = 0$, and so $A = B = D$. We then have $T_c = \langle k^2\rangle/\langle k\rangle^2$, as expected (Johnson et al., 2008).

6.3.2 Generating correlated networks

Given a degree distribution $p(k)$, the ensemble of networks compatible with this constraint and with degree-degree correlations according to Eq. (6.4) (with some exponent β) is defined by the mean adjacency matrix $\hat{\epsilon}$ of Eq. (6.5) – as described in Section 6.2.3 and by Johnson et al. (2010b). Therefore, although there will generally be an enormous number of possible networks in this volume of phase space, we can sample them correctly simply by generating them according to $\hat{\epsilon}$. To do this, first we have to assign to each node a degree drawn from $p(k)$. If the elements of $\hat{\epsilon}$ were probabilities, it would suffice then to connect each pair of nodes (i, j) with probability $\hat{\epsilon}_{ij}$ to generate a valid network. Strictly speaking, $\hat{\epsilon}$ is an expected value, which in certain cases can be greater than one. To get round this, we write a probability matrix $\hat{p} = \hat{\epsilon}/a$ with a some value such that all elements of $\hat{p}$ are smaller than one. If we then take random pairs of nodes (i, j) and, with probability $\hat{p}_{ij}$, place an edge between them, repeating the operation until $\frac{1}{2}\langle k\rangle N$ edges have been placed, the expected value of edges joining i and j will be $\hat{\epsilon}_{ij}$. This method is like the *hidden variable* technique (Boguñá and Pastor-Satorras, 2003) in that edges are placed with a predefined probability (which is why the resulting ensemble is canonical). The difference lies in the fact that in the method here described correlations only depend on the degrees of nodes.

We are interested here in neural networks, in which a given pair of nodes can be joined by several synapses, so we shall not impose the restriction of so-called simple networks of allowing only one edge at most per pair. We shall, however, consider networks with a *structural cutoff*: $k_i < \sqrt{\langle k\rangle N}$, $\forall i$ (Bianconi, 2008). This ensures that, at least for $\beta \leq 0$, all elements of $\hat{\epsilon}$ are indeed smaller than one.

Because we can expect effects due to degree-degree correlations to be largest when $p(k)$ is very broad, and since most networks in nature and technology seem to exhibit approximately power-law degree distributions (Newman, 2003c; Arenas et al., 2008a; Peretto, 1992; Barabási and Oltvai, 2004), we shall here test our general theoretical results against simulations of scale-free networks: $p(k) \sim k^{-\gamma}$. This means that a network (or the region of phase space to which it belongs) is characterized by the set of parameters $\{\langle k\rangle, N, \gamma, \beta\}$.

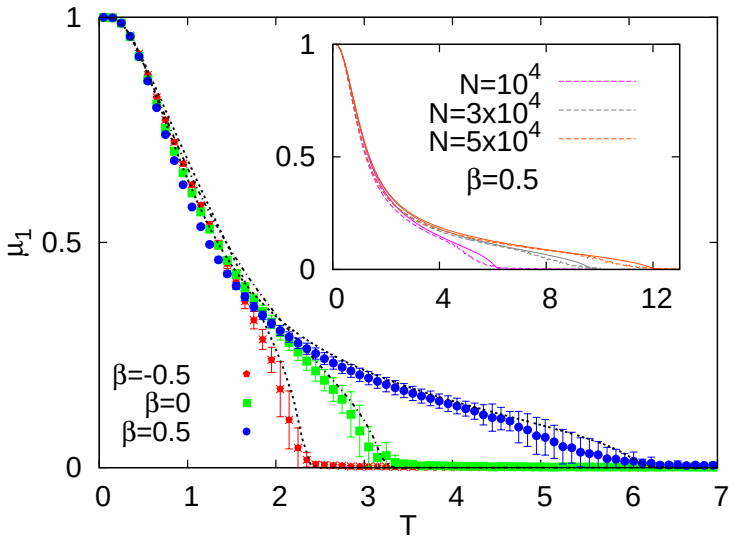

Figure 6.2: Stable stationary value of the weighted overlap μ_1 against temperature T for scale-free networks with correlations according to $\overline{k}_{nn} \sim k^{\beta}$, for $\beta = -0.5$ (disassortative), 0.0 (neutral), and 0.5 (assortative). Symbols from MC simulations, with errorbars representing standard deviations, and lines from Eqs. (6.6). Other network parameters as in Fig. 6.1. Inset: μ_1 against T for the assortative case ($\beta = 0.5$) and different system sizes: $N = 10^4$, $3 \cdot 10^4$ and $5 \cdot 10^4$.

6.3.3 Assortativity and dynamics

In Fig. 6.2 we plot the stationary value of μ_1 against the temperature T, as obtained from simulations and Eqs. (6.6), for disassortative, neutral and assortative networks. The three curves are similar at low temperatures, but as T increases their behaviour becomes quite different. The disassortative network is the least robust to noise. However, the assortative one is capable of retaining some information at temperatures considerably higher than the critical value, $T_c = \langle k^2 \rangle / \langle k \rangle$, of neutral networks. A comparison between μ_1 and μ_0 (see Fig. 6.3) shows that it is the high degree nodes that are mainly responsible for this difference in performance. This can be seen more clearly in Fig. 6.4, which displays the difference $\mu_1 - \mu_0$ against T for the same networks. It seems that, because in an assortative network a sub-graph of hubs will have more edges than in a disassortative one, it has a higher effective critical temperature. Therefore, even when most of the nodes are acting randomly, the set of nodes of sufficiently high degree nevertheless displays associative memory.

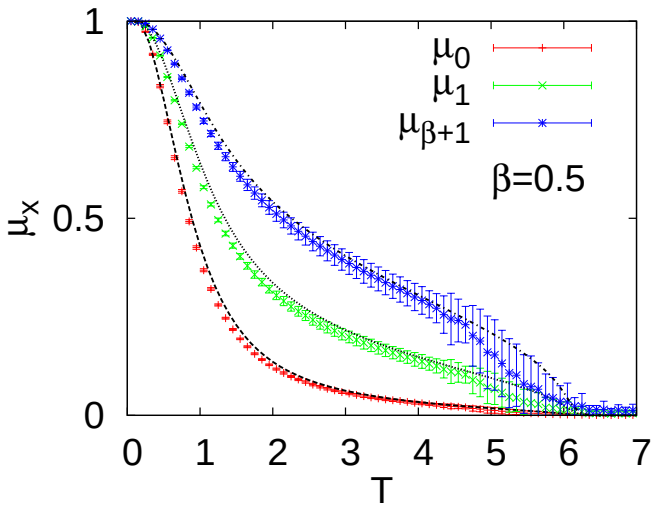

Figure 6.3: Stable stationary values of order parameters μ_0, μ_1 and $\mu_{\beta+1}$ against temperature T, for assortative networks according to $\beta = 0.5$. Symbols from MC simulations, with errorbars representing standard deviations, and lines from Eqs. (6.6). Other parameters as in Fig. 6.1.

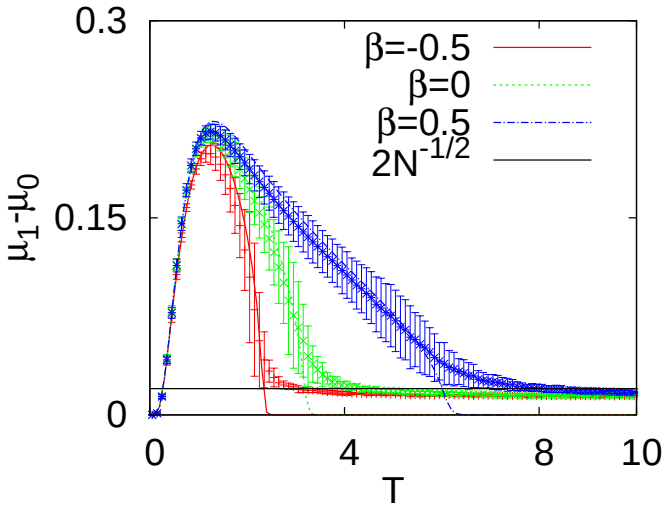

Figure 6.4: Difference between the stationary values μ_1 and μ_0 for networks with $\beta = -0.5$ (disassortative), 0.0 (neutral) and 0.5 (assortative), against temperature. Symbols from MC simulations, with errorbars representing standard deviations, and lines from Eqs. (6.6). Line shows the expected level of fluctuations due to noise, $\sim N^{-\frac{1}{2}}$. Other parameters as in Fig. 6.1.

The phase diagram if Fig. 6.5 shows the critical temperature, T_c, as obtained from Eq. (6.7). In addition to the effect reported by Torres et al. (2004) whereby the T_c of scale-free networks grows with degree heterogeneity (decreasing γ), it also increases very significantly with positive degree-degree correlations (increasing β).

At large values of N, the critical temperature scales as $T_c \sim N^b$, with $b \geq 0$ a constant. However, because the moments of k appearing in the coefficients of Eq. (6.7) can have different asymptotic behaviour depending on the values of γ and β, the scaling exponent b differs from one region to another in the space of these parameters. These are the seven regions shown in Fig. 6.6, along with the scaling behaviour exhibited by each one. This can be seen explicitely in Fig. 6.7, where T_c, as obtained from MC simulations, is plotted against N for cases in each of the regions with $\gamma < 3$. In each case, the scaling is as given by Eq. (6.7) and shown in Fig. 6.6. For the four regions with $\gamma < 3$, from lowest to highest assortativity we have scaling exponents which are dependent on: only γ (region I), only β (region II), both γ and β (region III), and, perhaps most interestingly, neither of the two (region IV) – with T_c scaling, in the latter case, as $\sqrt{N}$. As for the more homogeneous $\gamma > 3$ part, regions V and VI have a diverging critical temperature despite the fact that the second moment of $p(k)$ is finite, simply as a result of assortativity.

The case in which more than one pattern are stored ($P > 1$) can be explored numerically. Assuming there are P uncorrelated patterns, we have an order parameter μ_1^ν for each pattern ν. A global measure of the degree to which there is memory can be captured by the parameter ζ, where

$$\zeta^2 \equiv \frac{1}{1 + P/N} \sum_{\nu=1}^{P} (\mu_1^\nu)^2.$$

Notice that the normalization factor is due to the fact that if one pattern is *condensed* – i.e., $|\mu_1| \lesssim 1$ – the others have $|\mu_\nu| \sim 1/\sqrt{N}$, $\nu = 2, ..P$, and so $\zeta \simeq 1$. Figure 6.8 shows how ζ decreases with T in variously correlated networks for $P = 3$ (left panel) and $P = 10$ patterns (right panel). The behaviour is not qualitatively different from that observed for the single-pattern case in the main panel of Fig. 6.2, suggesting that the influence of assortativity we report is robust as to the number of patterns stored, P.

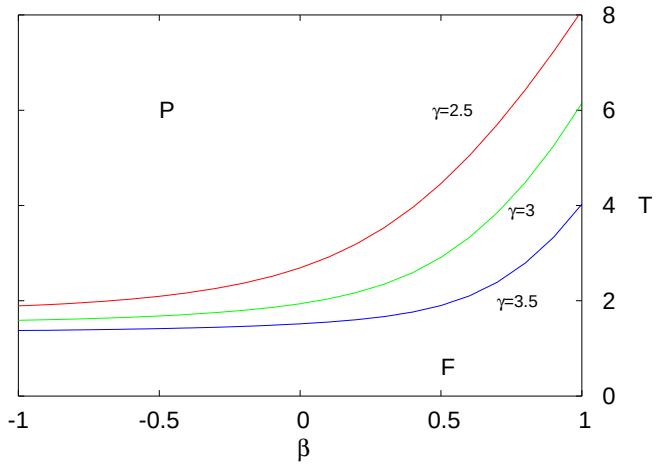

Figure 6.5: Phase diagrams for scale-free networks with $\gamma = 2.5$, 3, and 3.5. Lines show the critical temperature T_c marking the second-order transition from a memory (ferromagnetic) phase to a memoryless (paramagnetic) one, against the assortativity β, as given by Eq. (6.7). Other parameters as in Fig. 6.1.

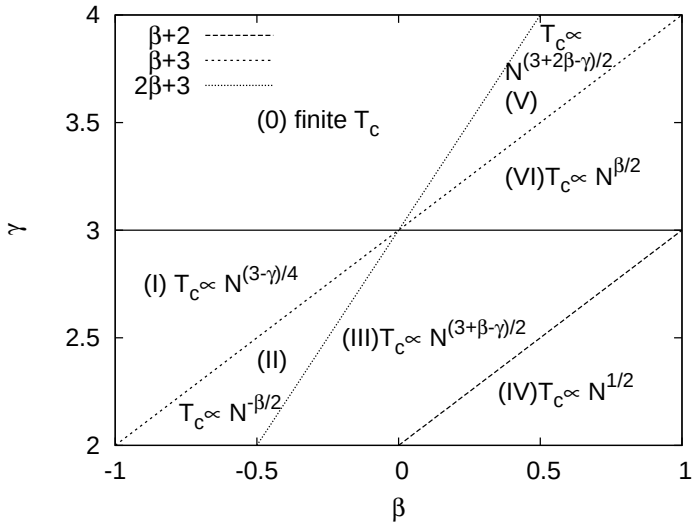

Figure 6.6: Parameter space $\beta - \gamma$ partitioned into the regions in which $b(\beta, \gamma)$ has the same functional form – where b is the scaling exponent of the critical temperature: $T_c \sim N^b$. Exponents obtained by taking the large N limit in Eq. (6.7).

6.4 Discussion

We have shown that assortative networks of simple model neurons are able to exhibit associative memory in the presence of levels of noise such that uncor-

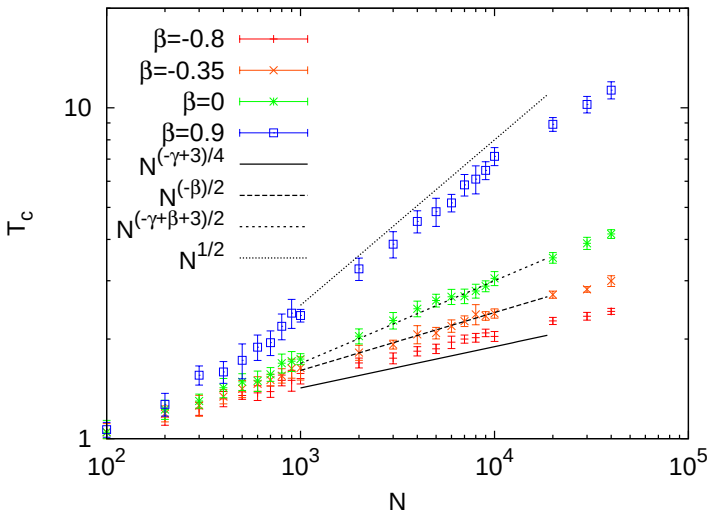

Figure 6.7: Examples of how T_c scales with N for networks belonging to regions I, II, III and IV of Fig. 6.6 ($\beta = -0.8$, -0.35, 0.0 and 0.9, respectively). Symbols from MC simulations, with errorbars representing standard deviations, and slopes from Eq. (6.7). All parameters – except for β and N – are as in Fig. 6.1.

related (or disassortative) networks cannot. This may appear to be in contradiction with a recent result obtained using spectral graph analysis – that synchronizability of a set of coupled oscillators is highest for disassortative networks (Brede and Sinha). A synchronous state of model oscillators and a memory phase of model neurons are both sets of many simple dynamical elements coupled via a network in such a way that a macroscopically coherent situation is maintained (Barahona and Pecora, 2002). Obviously both systems require the effective transmission of information among the elements. So why are opposite results as regards the influence of topology reported for each system? The answer is simple: whereas the definition of a synchronous state is that every single element oscillate at the same frequency, it is precisely when most elements are actually behaving randomly that the advantages to assortativity we report become apparent. In fact, it can be seen in Fig. 6.2 that at low temperatures disassortative networks perform the best, although the effect is small. This is reminiscent of percolation: at high densities of edges the giant component is larger in disassortative networks, but in assortative ones a non-vanishing fraction of nodes remain interconnected even at densities below the usual percolation threshold (Newman, 2002, 2003a). Because in the case

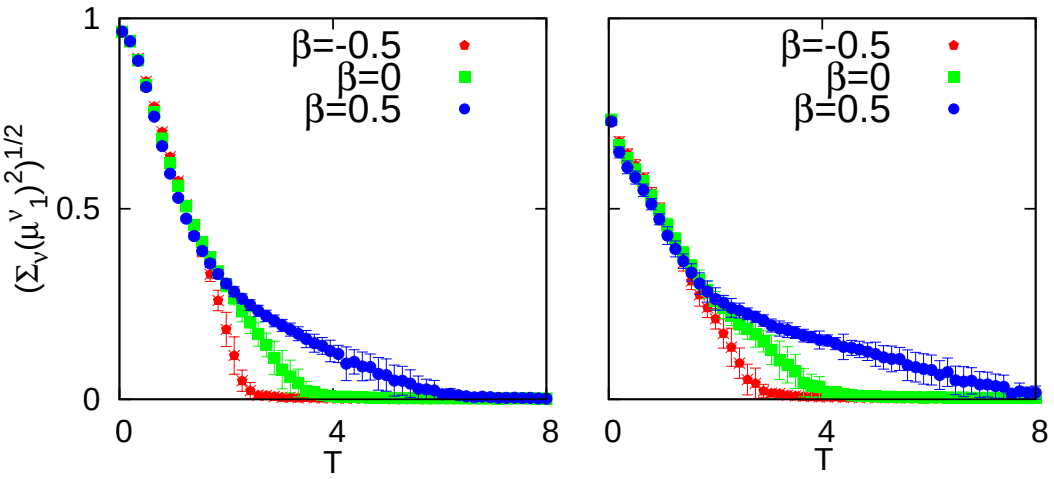

Figure 6.8: Global order parameter ζ for assortative ($\beta = 0.5$), neutral ($\beta = 0.0$) and disassortative ($\beta = -0.5$) networks with $P = 3$ (left panel) and $P = 10$ (right panel) stored patterns. Symbols from MC simulations, with errorbars representing standard deviations. All parameters are as in Fig. 6.1.

of targeted attacks it is this threshold which is taken as a measure of resilience, we say that assortative networks perform the best. The relevance of partial synchronization and the important role of hubs have already been noted for systems of (weakly) coupled oscillators (Gómez-Gardenes et al., 2007; Pereira, 2010) – for which, however, assortativity has not been expected to be of consequence (Pereira, 2010). In general, the optimal network for good conditions (i.e., complete synchronization, high density of edges, low levels of noise) is not necessarily the one which performs the best in bad conditions (partial synchronization, low density of edges, high levels of noise). It seems that optimality – whether in resilience or robustness – should thus be defined for particular conditions.

We have used the technique suggested by Johnson et al. (2010b) to study the effect of correlations on networks of model neurons, but many other systems of dynamical elements should be susceptible to a similar treatment. In fact, Ising spins (Bianconi, 2002), Voter Model agents (Suchecki et al., 2005), or Boolean nodes (Peixoto, 2010), for instance, are similar enough to binary neurons that we should expect similar results for these models. If a moral

can be drawn, it is that persistence of partial synchrony, or coherence of a subset of highly connected dynamical elements, can sometimes be as relevant (or more so) as the possibility of every element behaving in the same way. In the case of real brain cells, experiments suggest that hub neurons play key functional roles (Morgan and Soltesz, 2008; Bonifazi et al., 2009). From this point of view, there may be a selective pressure for brain networks to become assortative – although, admittedly, this organ engages in such complex behaviour that there must be many more functional constraints on its structure than just a high robustness to noise. Nevertheless, it would be interesting to investigate this aspect of biological systems experimentally. For this, it should be borne in mind that heterogeneous networks have a natural tendency to become disassortative, so it is against the expected value of correlations discussed by Johnson et al. (2010b) that empirical data should be contrasted in order to look for meaningful deviations towards assortativity. Similarly, it may be necessary to take into account the correlations that could emerge due to the spatial layout of neurons (Kaiser et al., 2007; Johnson et al., 2011). In any case, it would be in areas of the cortex specifically related to memory – such as the temporal (long-term memory) (Miyashita, 1988; Sakai and Miyashita, 1991) or prefrontal (short-term memory) (Camperi and Wang, 1998b; Compte et al., 2003) lobes – that this effect might be relevant. A curious fact that would seem to support our hypothesis is that whereas the vast majority of non-social networks are disassortative (Newman, 2003c), one that appears actually to be strongly assortative is the functional network of the human cortex (Eguíluz et al., 2005).

Chapter 7

Cluster Reverberation: A mechanism for robust short-term memory without synaptic learning

Short-term memory cannot in general be explained the way long-term memory can – as a gradual modification of synaptic conductances – since it takes place too quickly. Theories based on some form of cellular bistability, however, do not seem to be able to account for the fact that noisy neurons can collectively store information in a robust manner. We show how a sufficiently clustered network of simple model neurons can be instantly induced into metastable states capable of retaining information for a short time. Cluster Reverberation, as we call it, could constitute a viable mechanism available to the brain for robust short-term memory with no need of synaptic learning. Relevant phenomena described by neurobiology and psychology, such as power-law statistics of forgetting avalanches, emerge naturally from this mechanism.

7.1 Slow but sure, or fast and fleeting?

Of all brain phenomena, memory is probably one of the best understood (Amit, 1989; Abbott and Kepler, 1990; Torres and Varona, 2010). Consider a set of many neurons, defined as elements with two possible states (firing or not firing, one or zero) connected among each other in some way by synapses which carry a proportion of the current let off by a firing neuron to its neighbours; the probability that a given neuron has of firing at a certain time is then some

function of the total current it has just received. Such a simplified model of the brain is able to store and retrieve information, in the form of patterns of activity (i.e., particular configurations of firing and non-firing neurons) when the synaptic conductances, or weights, have been appropriately set according to a learning rule (Hebb, 1949). Because each of the stored patterns becomes an attractor of the dynamics, the system will evolve towards whichever of the patterns most resembles the initial configuration. Artificial systems used for tasks such as pattern recognition and classification, as well as more realistic neural network models that take into account a variety of subcellular processes, all tend to rely on this basic mechanism, known as Associative Memory (Amari, 1972; Hopfield, 1982).

Synaptic conductances in animal brains have indeed been found to become strengthened or weakened during learning, via the biochemical processes of long-term potentiation (LTP) and depression (LTD) (Malenka and Nicoll, 1999; Gruart et al., 2006; Roo et al., 2008; Rodríguez-Moreno and Paulsen, 2008; Kwag and Paulsen, 2009). Further support for the hypothesis that such a mechanism underlies long-term memory (LTM) comes from psychology, where it is being found more and more that so-called *connectionist* models fit in well with observed brain phenomena (Marcus and G.F., 2001; Frank, 1997). However, some memory processes take place on timescales of seconds or less and in many instances cannot be accounted for by LTP and LTD (Durstewitz et al., 2000), since these require at least minutes to be effected (Lee et al., 1980; Klintsova and Greenough, 1999). For example, Sperling found that visual stimuli are recalled in great detail for up to about one second after exposure (iconic memory) (Sperling, 1960); similarly, acoustic information seems to linger for three or four seconds (echoic memory) (Cowan, 1984). In fact, it appears that the brain actually holds and continually updates a kind of buffer in which sensory information regarding its surroundings is maintained (sensory memory) (Baddeley, 1999). This is easily observed by simply closing one's eyes and recalling what was last seen, or thinking about a sound after it has finished. Another instance is the capability referred to as *working* memory (Durstewitz et al., 2000; Baddeley and A.D., 2003): just as a computer requires RAM for its calculations despite having a hard drive for long term storage, the brain must continually store and delete information to perform almost any cognitive task. To some extent, working memory could consist in somehow labelling or bringing forward previously stored concepts, like when one is asked to remember a particular sequence of digits or familiar shapes.

But we are also able to manipulate – if perhaps not quite so well – shapes and symbols we have only just become acquainted with, too recently for them to have been learned synaptically. We shall here use *short-term* memory (STM) to describe the brain's ability to store information on a timescale of seconds or less[1].

Evidence that short-term memory is related to sensory information while long-term memory is more conceptual can again be found in psychology. For instance, a sequence of similar sounding letters is more difficult to retain for a short time than one of phonetically distinct ones, while this has no bearing on long-term memory, for which semantics seems to play the main role (Conrad, 1964a,b); and the way many of us think about certain concepts, such as chess, geometry or music, is apparently quite sensorial: we imagine positions, surfaces or notes as they would look or sound. Most theories of short-term memory – which almost always focus on working memory – make use of some form of previously stored information (i.e., of synaptic learning) and so can account for the labelling tasks referred to above but not for the instant recall of novel information (Wang, 2001; Barak and Tsodyks, 2007; Roudi and Latham; Mongillo et al., 2008; Mejias and Torres, 2009). Attempts to deal with the latter have been made by proposing mechanisms of *cellular bistability*: neurons are assumed to retain the state they are placed in (such as firing or not firing) for some period of time thereafter (Camperi and Wang, 1998a; Teramae and Fukai, 2005; Tarnow, 2008). Although there may indeed be subcellular processes leading to a certain bistability, the main problem with short-term memory depending exclusively on such a mechanism is that if each neuron must act independently of the rest the patterns will not be robust to random fluctuations (Durstewitz et al., 2000) – and the behaviour of individual neurons is known to be quite noisy (Compte et al., 2003). It is worth pointing out that one of the strengths of Associative Memory is that the behaviour of a given neuron depends on many neighbours and not just on itself, which means that robust global recall can emerge despite random fluctuations at an individual

[1]We should mention that sensory memory is usually considered distinct from STM – and probably has a different origin – but we shall use "short-term memory" generically since the mechanism we propose in this paper could be relevant for either or both phenomena. On the other hand, the recent flurry of research in psychology and neuroscience on working memory has lead to this term sometimes being used to mean short-term memory; strictly speaking, however, working memory is generally considered to be an aspect of cognition which operates on information stored in STM.

level.

Something that, at least until recently, most neural network models have failed to take into account is the structure of the network – its topology – it often being assumed that synapses are placed among the neurons completely at random, or even that all neurons are connected to all the rest (a mathematically convenient but unrealistic situation). Although relatively little is yet known about the architecture of the brain at the level of neurons and synapses, experiments have shown that it is heterogeneous (some neurons have very many more synapses than others), clustered (two neurons have a higher chance of being connected if they share neighbours than if not) and highly modular (there are groups, or modules, with neurons forming synapses preferentially to those in the same module) (Sporns et al., 2004; Johnson et al., 2010a). This chapter describes the main result of Ref. (Johnson et al., 2011) – namely, that it suffices to use a more realistic topology, in particular one which is modular and/or clustered, for a randomly chosen pattern of activity the system is placed in to be metastable. This means that novel information can be instantly stored and retained for a short period of time in the absence of both synaptic learning and cellular bistability. The only requisite is that the patterns be coarse grained versions of the usual patterns – that is, whereas it is often assumed that each neuron in some way represents one bit of information, we shall allocate a bit to a small group or neurons[2] (four or five can be enough).

The mechanism, which we call Cluster Reverberation, is very simple. If neurons in a group are more highly connected to each other than to the rest of the network, either because they form a module or because the network is significantly clustered, they will tend to retain the activity of the group: when they are all initially firing, they each continue to receive many action potentials and so go on firing, whereas if they start off silent, there is not usually enough input current from the outside to set them off. The fact that each neuron's state depends on its neighbours conferres to the mechanism a certain robustness in the face of random fluctuations. This robustness is particularly important for biological neurons, which as mentioned are quite noisy. Furthermore, not only does the limited duration of short-term memory states emerge naturally from this mechanism (even in the absence of interference from new stimuli) but this natural forgetting follows power-law statistics, as

[2]This does not, of course, mean that memories are expected to be encoded as bitmaps. Just as with individual neurons, positions or orientations, say, could be represented by the activation of particular sets of clusters.

in experimental settings (Wixted and Ebbesen, 1991, 1997; Sikström, 2002).

The process is reminiscent both of block attractors in ordinary neural networks (Dominguez et al., 2009) and of domains in magnetic materials (A. and R., 1998), while Muñoz et al. have recently highlighted a similarity with Griffiths phases on networks (Muñoz et al., 2010). It can also be interpreted as a multiscale phenomenon: the mesoscopic clusters take on the role usually played by individual neurons, yet make use of network properties. Although the mechanism could also work in conjunction with other ones, such as synaptic learning or cellular bistability, we shall illustrate it by considering the simplest model which has the necessary ingredients: a set of binary neurons linked by synapses of uniform weight according to a topology whose modularity or clustering we shall tune. As with Associative Memory, this mechanism of Cluster Reverberation appears to be simple and robust enough not to be qualitatively affected by the complex subcellular processes incorporated into more realistic neuron models – such as integrate-and-fire or Hodgkin-Huxley neurons. However, such refinements are probably needed to achieve graded persistent activity, since the mean frequency of each cluster could then be set to a certain value.

7.2 The simplest neurons on modular networks

We consider a network of N model neurons, with activities $s_i = \pm 1$. The topology is given by the adjacency matrix $\hat{a}_{ij} = \{1, 0\}$, each element representing the existence or absence of a synapse from neuron j to neuron i ($\hat{a}$ need not be symmetric). In this kind of model, each edge usually has a *synaptic weight* associated, $\omega_{ij} \in \mathbb{R}$; however, we shall here consider these to have all the same value: $\omega_{ij} = \omega \; \forall i, j$. Neurons are updated in parallel (Little dynamics) at each time step, according to the stochastic transition rule

$$P(s_i \to \pm 1) = \pm \frac{1}{2} \tanh\left(\frac{h_i}{T}\right) + \frac{1}{2},$$

where the *field* of neuron i is defined as

$$h_i = \omega \sum_j^N \hat{a}_{ij} s_j$$

and T is a parameter we shall call *temperature*.

First of all, we shall consider the network defined by $\hat{a}$ to be made up of M distinct modules. To achieve this, we can first construct M separate

random directed networks, each with $n = N/M$ nodes and mean degree (mean number of neighbours) $\langle k \rangle$. Then we evaluate each edge and, with probability λ, eliminate it, to be substituted for another edge between the original post-synaptic neuron and a new pre-synaptic neuron chosen at random from among any of those in other modules[3]. Note that this protocol does not alter the number of pre-synaptic neighbours of each node, $k_i^{in} = \sum_j \hat{a}_{ij}$ (although the number of post-synaptic neurons, $k_i^{out} = \sum_j \hat{a}_{ji}$, can vary). The parameter λ can be seen as a measure of *modularity* of the partition considered, since it coincides with the expected value of the proportion of edges that link different modules. In particular, $\lambda = 0$ defines a network of disconnected modules, while $\lambda = 1 - M^{-1}$ yields a random network in which this partition has no modularity. If $\lambda \in (1 - M^{-1}, 1)$, the partition is less than randomly modular – i.e., it is *quasi-multipartite* (or multipartite if $\lambda = 1$).

If the size of the modules is of the order of $\langle k \rangle$, the network will also be highly clustered. Taking into account that the network is directed, let us define the clustering coefficient C_i as the probability, given that there is a synapse from neuron i to a neuron j and from another neuron l to i, that there be a synapse from j to l: that is, that there exist a feedback loop $i \to j \to l \to i$. Then, assuming $M \gg 1$, the expected value of the clustering coefficient $C \equiv \langle C_i \rangle$ is

$$C \gtrsim \frac{\langle k \rangle - 1}{n - 1}(1 - \lambda)^3.$$

7.3 Cluster Reverberation

A memory pattern, in the form of a given configuration of activities, $\{\xi_i = \pm 1\}$, can be stored in this system with no need of prior learning. Imagine a pattern such that the activities of all n neurons found in any module are the same, i.e., $\xi_i = \xi_{\mu(i)}$, where the index $\mu(i)$ denotes the module that neuron i belongs to. This can be thought of as a coarse graining of the standard idea of memory patterns, in which each neuron represents one bit of information. In our scheme, each module represents – and stores – one bit. The system can be induced into this configuration via the application of an appropriate *stimulus* (see Fig. 7.1): the field of each neuron will be altered for just one time step

[3]We do not allow self-edges (although these can occur in reality) since they can be regarded as a form of cellular bistability.

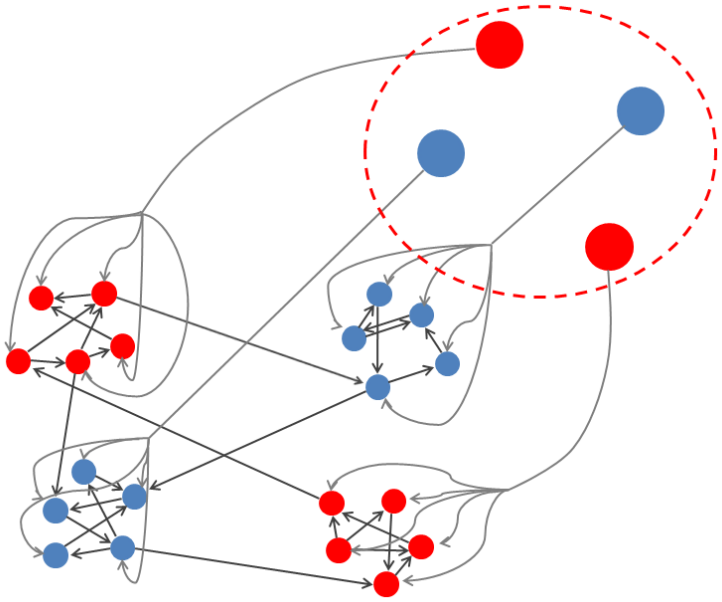

Figure 7.1: Diagram of a modular network composed of four five-neuron clusters. The four circles enclosed by the dashed line represent the stimulus: each is connected to a particular module, which adopts the input state (red or blue) and retains it after the stimulus has disappeared via Cluster Reverberation.

according to

$$h_i \longrightarrow h_i + \delta\xi_{\mu(i)}, \quad \forall i,$$

where the factor δ is the intensity of the stimulus. This mechanism for dynamically storing information will work for values of parameters such that the system is sensitive to the stimulus, acquiring the desired configuration, yet also able to retain it for some interval of time thereafter.

The two main attractors of the system are $s_i = 1\ \forall i$ and $s_i = -1\ \forall i$. These are the configurations of minimum energy (see the next section for a more detailed discussion on energy). However, the energy is locally minimised for any configuration in which $s_i = d_{\mu(i)}\ \forall i$ with $d_\mu = \pm 1$; that is, configurations such that each module comprises either all active or all inactive neurons. These are the configurations that we shall use to store information. We define the

mean activity[4] of each module,

$$m_\mu \equiv \frac{1}{n}\sum_{i\in\mu}^{n} s_i,$$

which is a mesoscopic variable, as well as the global mean activity,

$$m \equiv \frac{1}{N}\sum_{i}^{N} s_i = \frac{1}{M}\sum_{\mu}^{M} m_\mu$$

(these magnitudes change with time, but, where possible, we shall avoid writing the time dependence explicitely for clarity). The extent to which the network, at a given time, retains the pattern $\{\xi_i\}$ with which it was stimulated is measured with the *overlap* parameter

$$m_{stim} \equiv \frac{1}{N}\sum_{i}^{N} \xi_i s_i = \frac{1}{M}\sum_{\mu}^{M} \xi_\mu m_\mu.$$

Ideally, the system should be capable of reacting immediately to a stimulus by adopting the right configuration, yet also be able to retain it for long enough to use the information once the stimulus has disappeared. A measure of performance for such a task is therefore

$$\eta \equiv \frac{1}{\tau}\sum_{t=t_0+1}^{t_0+\tau} m_{stim}(t),$$

where t_0 is the time at which the stimulus is received and τ is the period of time we are interested in ($|\eta| \leq 1$) (Johnson et al., 2008). If the intensity of the stimulus, δ, is very large, then the system will always adopt the right pattern perfectly and η will only depend on how well it can then retain it. In this case, the best network will be one that is made up of unconnected modules. However, since the stimulus in a real brain can be expected to arrive via a relatively small number of axons, either from another part of the brain or directly from sensory cells, it is more realistic to assume that δ is of a similar order as the input a typical neuron receives from its neighbours, $\langle h\rangle \sim \omega\langle k\rangle$.

Fig. 7.2 shows the mean performance obtained when the network is repeatedly stimulated with different randomly generated patterns. For low enough values of the modularity λ and stimuli of intensity $\delta \gtrsim \omega\langle k\rangle$, the system can

[4]The mean activity in a neural network model is usually taken to represent the mean firing rate measured in experiments (Torres and Varona, 2010).

capture and successfully retain any pattern it is "shown" for some period of time, even though this pattern was in no way previously learned. For less intense stimuli ($\delta < \omega\langle k\rangle$), performance is nonmonotonic with modularity: there exists an optimal value of λ at which the system is sensitive to stimuli yet still able to retain new patterns quite well.

It is worth noting that performance can also break down due to thermal fluctuations. The two main attractors of the system ($s_i = 1\ \forall i$ and $s_i = -1\ \forall i$) suffer the typical second order phase transition of the Hopfield model (Hopfield, 1982), from a memory phase (one in which $m = 0$ is not stable and stable solutions $m \neq 0$ exist) to one with no memory (with $m = 0$ the only stable solution), at the critical temperature (Johnson et al., 2008)

$$T_c = \omega \frac{\langle k_{in}^2 \rangle}{\langle k \rangle}.$$

(Note that, in a directed network, $\langle k_{in}\rangle = \langle k_{out}\rangle \equiv \langle k\rangle$, although the other moments can in general be different.) The metastable states we are interested in, though, have a critical temperature

$$T_c' = (1 - \lambda)T_c$$

(assuming that the mean activity of the network is $m \simeq 0$). That is, the temperature at which the modules are no longer able to retain their individual activity is in general lower than that at which the the solution $m = 0$ for the whole network becomes stable.

7.4 Energy and topology

Each pair of nodes contributes a configurational energy $e_{ij} = -\omega\frac{1}{2}(\hat{a}_{ij}+\hat{a}_{ji})s_i s_j$; that is, if there is an edge from i to j and they have opposite activities, the energy is increased in $\frac{1}{2}\omega$, whereas it is decreased by the same amount if their activities are the same. Given a configuration, we can obtain its associated energy by summing over all pairs. We shall be interested in configurations with x neurons that have $s = +1$ (and $N - x$ with $s = -1$), chosen in such a way that one module at most, say μ, has neurons in both states simultaneously. Therefore, $x = n\rho + z$, where ρ is the number of modules with all their neurons in the positive state and z is the number of neurons with positive sign in module μ. We can write $m = (2x-1)/N$ and $m_\mu = (2z-1)/n$. The total configurational energy of the system will be $E = \sum_{ij} e_{ij} = \frac{1}{2}\omega(L_{\uparrow\downarrow} - \langle k\rangle N)$, where $L_{\uparrow\downarrow}$ is the number of edges linking nodes with opposite activities. By simply

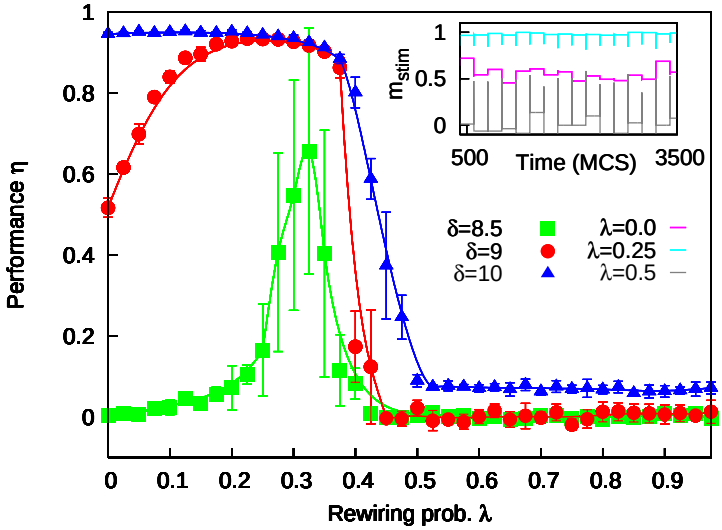

Figure 7.2: Performance η against λ for networks of the sort described in the main text with $M = 160$ modules of $n = 10$ neurons, $\langle k \rangle = 9$; patterns are shown with intensities $\delta = 8.5$, 9 and 10, and $T = 0.02$ (lines – splines – are drawn as a guide to the eye). Inset: typical time series of m_{stim} (i.e., the overlap with whichever pattern was last shown) for $\lambda = 0.0$, 0.25, and 0.5, and $\delta = \langle k \rangle = 9$.

counting over edges, we can obtain the expected value of $L_{\uparrow\downarrow}$ (which amounts to a mean-field approximation because we are substituting the number of edges between two neurons for its expected value), yielding:

$$\frac{E}{\omega\langle k\rangle} = (1-\lambda)\frac{z(n-z)}{n-1}$$
$$+\frac{\lambda n}{N-n}\left\{\rho[n-z+n(M-\rho-1)]+(M-\rho-1)(z+n\rho)\right\}-\frac{1}{2}N. \quad (7.1)$$

Fig. 7.3 shows the mean-field configurational energy curves for various values of the modularity on a small modular network. The local minima (metastable states) are the configurations used to store patterns. It should be noted that the mapping $x \to m$ is highly degenerate: there are C^M_{mM} patterns with mean activity m that all have the same energy.

7.5 Forgetting avalanches

In obtaining the energy we have assumed that the number of synapses rewired from a given module is always $\nu = \langle k \rangle n\lambda$. However, since each edge is evaluated

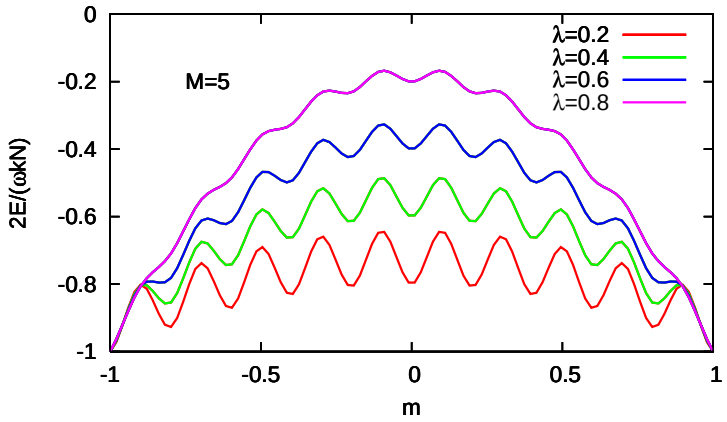

Figure 7.3: Configurational energy of a network composed of $M = 20$ modules of $n = 10$ neurons each, according to Eq. (7.1), for various values of the rewiring probability λ. The minima correspond to situations such that all neurons within any given module have the same sign.

with probability λ, ν will in fact vary somewhat from one module to another, being approximately Poisson distributed with mean $\langle\nu\rangle = \langle k\rangle n\lambda$. The depth of the energy well corresponding to a given module is then, neglecting all but the first term in Eq. (7.1) and approximating $n - 1 \simeq n$,

$$\Delta E \simeq \frac{1}{4}\omega(n\langle k\rangle - \nu).$$

The typical escape time τ from an energy well of depth ΔE at temperature T is $\tau \sim e^{\Delta E/T}$ (Levine and R.D., 2005). Using Stirling's approximation in the Poissonian distribution of ν and expressing it in terms of τ, we find that the escape times are distributed according to

$$P(\tau) \sim \left(1 - \frac{4T}{\omega n\langle k\rangle}\ln\tau\right)^{-\frac{3}{2}} \tau^{-\beta(\tau)}, \tag{7.2}$$

where

$$\beta(\tau) = 1 + \frac{4T}{\omega n\langle k\rangle}\left[1 + \ln\left(\frac{\lambda n\langle k\rangle}{1 - \frac{4T}{\omega n\langle k\rangle}\ln\tau}\right)\right]. \tag{7.3}$$

Therefore, at low temperatures, $P(\tau)$ will behave approximately like a power-law. The left panel of Fig. 7.4 shows the distribution of time intervals between events in which the overlap m_μ of at least one module μ changes sign. The power-law-like behaviour is apparent, and justifies talking about *forgetting avalanches* – since there are cascades of many forgetting events interspersed

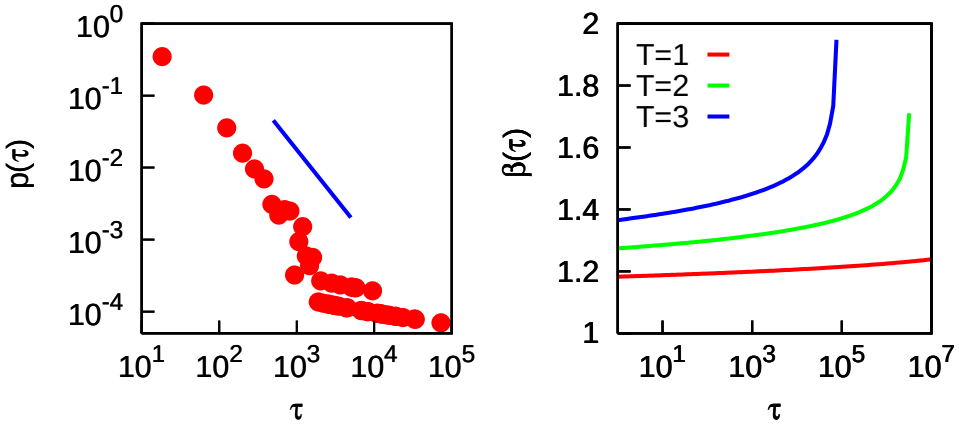

Figure 7.4: Left panel: distribution of escape times τ, as defined in the main text, for $\lambda = 0.25$ and $T = 2$. Slope is for $\beta = 1.35$. Other parameters as in Fig. 7.2. Symbols from MC simulations and line given by Eqs. (7.2) and (7.3). Right panel: exponent β of the quasi-power-law distribution $p(\tau)$ as given by Eq. (7.3) for temperatures $T = 1$ (red line), $T = 2$ (green line) and $T = 3$ (blue line).

with long periods of metastability. This is very similar to the behaviour observed in other nonequilibrium settings in which power-law statistics arise from the convolution of exponentials (Hurtado et al., 2008; Muñoz et al., 2010).

It is known from experimental psychology that forgetting in humans is indeed well described by power-laws (Wixted and Ebbesen, 1991, 1997; Sikström, 2002). The right panel of Fig. 7.4 shows the value of the exponent $\beta(\tau)$ as a function of τ. Although for low temperatures it is almost constant over many decades of τ – approximating a pure power-law – for any finite T there will always be a τ such that the denominator in the logarithm of Eq. (7.3) approaches zero and β diverges, signifying a truncation of the distribution.

7.6 Clustered networks

Although we have illustrated how the mechanism of Cluster Reverberation works on a modular network, it is not actually necessary for the topology to have this characteristic – only for the patterns to be in some way "coarse-grained," as described, and that each region of the network encoding one bit have a small enough parameter λ, defined as the proportion of synapses to other regions. For instance, for the famous Watts-Strogatz *small-world* model

(Watts and Strogatz, 1998) – a ring of N nodes, each initially connected to its k nearest neighbours before a proportion p of the edges are randomly rewired – we have $\lambda \simeq p$ (which is not surprising considering the resemblance between this model and the modular network used above). More precisely, the expected modularity of a randomly imposed box of n neurons is

$$\lambda = p - \frac{n-1}{N-1}p + \frac{1-p}{n}\left(\frac{k}{4} - \frac{1}{2}\right),$$

the second term on the right accounting for the edges rewired to the same box, and the third to the edges not rewired but sufficiently close to the border to connect with a different box.

Perhaps a more realistic model of clustered network would be a random network embedded in d-dimensional Euclidean space. For this we shall use the scheme laid out by Rozenfeld *et al.* (Rozenfeld et al., 2002), which consists simply in allocating each node to a site on a d-torus and then, given a particular degree sequence, placing edges to the nearest nodes possible – thereby attempting to minimise total edge length[5]. For a scale-free degree sequence (i.e., a set $\{k_i\}$ drawn from a degree distribution $p(k) \sim k^{-\gamma}$) according to some exponent γ, then, as shown in B, such a network has a modularity

$$\lambda \simeq \frac{1}{d(\gamma-2)-1}\left[d(\gamma-2)l^{-1} - l^{-d(\gamma-2)}\right], \tag{7.4}$$

where l is the linear size of the boxes considered.

Fig. 7.5 compares this expression with the value obtained numerically after averaging over many network realizations, and shows that it is fairly good – considering the approximations used for its derivation. It is interesting that even in this scenario, where the boxes of neurons which are to receive the same stimulus are chosen at random with no consideration for the underlying topology, these boxes need not have very many neurons for λ to be quite low (as long as the degree distribution is not too heterogeneous).

Carrying out the same repeated stimulation test as on the modular networks in Fig. 7.2, we find a similar behaviour for the scale-free embedded networks. This is shown in Fig. 7.6, where for high enough intensity of stimuli δ and scale-free exponent γ, performance can, as in the modular case, be $\eta \simeq 1$. We should point out that for good performance on these networks we require more neurons for each bit of information than on modular networks

[5]The authors also consider a cutoff distance, but we shall take this to be infinite here.

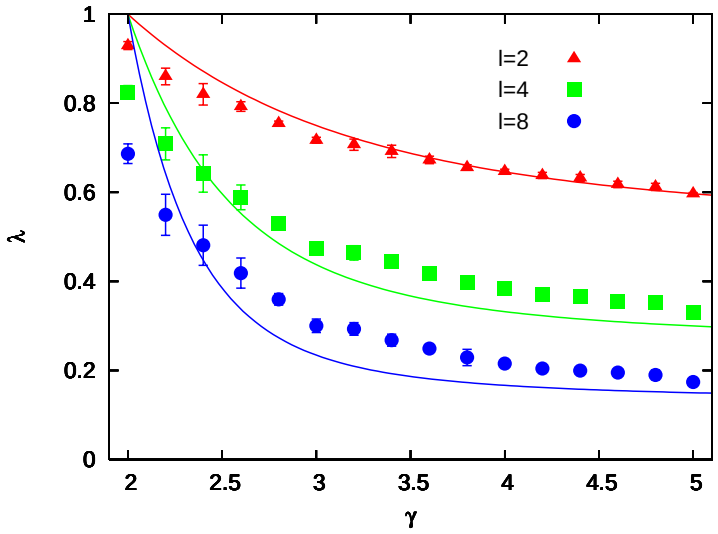

Figure 7.5: Proportion of outgoing edges, λ, from boxes of linear size l against exponent γ for scale-free networks embedded on $2D$ lattices. Lines from Eq. (7.4) and symbols from simulations with $\langle k \rangle = 4$ and $N = 1600$.

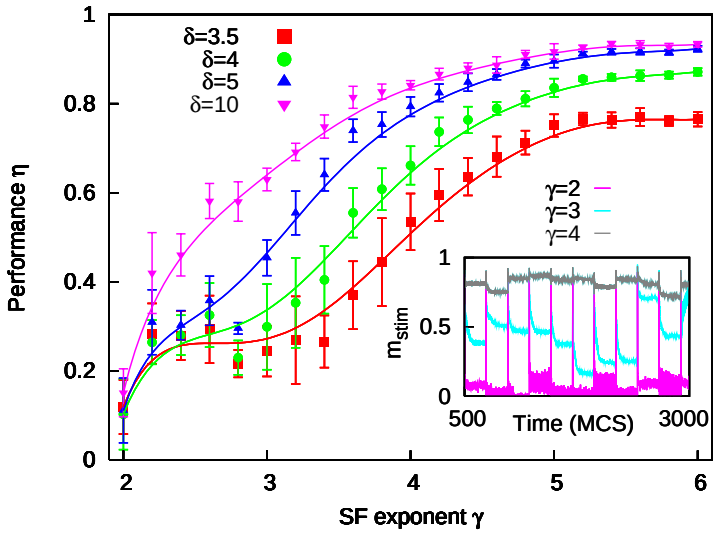

Figure 7.6: Performance η against exponent γ for scale-free networks, embedded on a 2D lattice, with patterns of $M = 16$ modules of $n = 100$ neurons each, $\langle k \rangle = 4$ and $N = 1600$; patterns are shown with intensities $\delta = 3.5$, 4, 5 and 10, and $T = 0.01$ (lines – splines – are drawn as a guide to the eye). Inset: typical time series for $\gamma = 2$, 3, and 4, with $\delta = 5$.

with the same λ (in Fig. 7.6 we use $n = 100$, as opposed to $n = 10$ in Fig. 7.2). However, that we should be able to obtain good results for such diverse network topologies underlines that the mechanism of Cluster Reverberation is robust and not dependent on some very specific architecture. In fact, we have recently shown that similar metastable memory states can also occur on networks which have random modularity and clustering, but a certain degree of *assortativity*[6] (de Franciscis et al., 2011).

7.7 Yes, but does it happen in the brain?

As we have shown, Cluster Reverberation is a mechanism available to neural systems for robust short-term memory without synaptic learning. To the best of our knowledge, this is the first mechanism proposed which has these characteristics – essential for, say, sensory memory or certain working-memory tasks. All that is needed is for the network topology to be highly clustered or modular, and for small groups of neurons to store one bit of information, as opposed to the conventional view which assumes one bit per neuron. Considering the enormous number of neurons in the brain, and the fact that real individual neurons are probably too noisy to store information reliably, these hypotheses do not seem farfetched. The mechanism is furthermore consistent both with what is known about the topology of the brain, and with experiments which have revealed power-law forgetting.

Since the purpose of this paper is only to describe the mechanism of Cluster Reverberation, we have made use of the simplest possible model neurons – namely, binary neurons with static, uniform synapses – for the sake of clarity and generality. However, there is no reason to believe that the mechanism would cease to function if more neuronal ingredients were to be incorporated. In fact, cellular bistability, for instance, would increase performance, and the two mechanisms could actually work in conjunction. Similarly, we have also used binary patterns to store information. But it is to be expected that patterns depending on any form of frequency coding, for instance, could also be maintained with more sophisticated neurons – such that different modules could be set to different mean frequencies.

Whether Cluster Reverberation would work for biological neural systems

[6]The assortativity of a network is here understood to mean the extent to which the degrees of neighbouring nodes are correlated (Johnson et al., 2010b).

could be put to the test by growing such modular networks *in vitro*, stimulating appropriately, and observing the duration of the metastable states. *In vivo* recordings of neural activity during short-term memory tasks, together with a mapping of the underlying synaptic connections, could be used to ascertain whether the brain does indeed make use of this mechanism – although for this it must be borne in mind that the neurons forming a module need not find themselves close together in metric space. We hope that experiments such as these will be carried out and eventually reveal something more about the basis of this puzzling emergent property of the brain's known as thought.

Chapter 8

Concluding remarks

"As long as the brain is a mystery, the universe will remain a mystery," claimed Santiago Ramón y Cajal. Our very essence seems to reside somehow in the workings of this organ, probably as a consequence of electro-chemical signalling that goes on among its hundred billion or so constituent neurons. Will this mystery ever be cleared up? We know of other objects that process information in highly sophisticated ways – electronic computers. Faced with a sudden blue screen, one may be forgiven for calling these devices incomprehensible and capricious, even malevolent. But in fact most educated people understand, on some level at least, what mechanisms and physical processes are behind the complex behaviour displayed by computers, and do not consider the issue a mystery. This is not to suggest that the analogy between brain and computer should be taken any further than to illustrate how a great many elements, each executing some fairly simple and obvious operation, can "cooperate" to yield astonishingly complicated yet functional behaviour; and that one can grasp how this occurs without having to know every detail. But we have not yet reached this point as regards the brain. Much progress has been made concerning aspects of physiology, while once unassailable mental disorders such as phobias can now be easily cured by psychology. Yet as far as what mechanisms relate these two levels of description goes, perhaps all we can safely say for now is that synaptic plasticity is responsible for long-term memory. The origins of even some well-defined and much studied cognitive abilities – such as probabilistic reasoning or short-term memory – remain somewhat elusive, while the nature of consciousness, say, is still truly a mystery. However, if instead of developing computers ourselves we had been given them by an alien species, we could still hope one day to unravel the mysteries of their magic. In much the same manner, by searching for ways in which collections of neurons

might perform tasks such as we know them to be capable of, we will some day understand not only how our stomachs digest and our hearts pump, but also how our brains think.

I cannot pretend that the work described here takes us more than, at best, a tiny step of the way along this path. The brain is, among other things, a network, and networks are a kind of mathematical object about which we now know much more than just a few years ago. In fact, they are a central element of what can arguably be called the most challenging frontier currently facing human understanding about the world – the nature of complex systems. So, from among the innumerable aspects likely to shape and determine the way neurons cooperate, the research presented here focuses on the structure of the underlying network. First of all it looks at how this structure can develop. Chapter 3 addressed this by formalizing as a stochastic process a situation governed by probabilistic events like synaptic growth and death. Such simple individual behaviour was shown to be enough to explain many statistical features of real neural systems. Furthermore, this Fokker-Planck description relating microscopic, stochastic actions to a macroscopic evolution of properties such as mean synaptic density, degree heterogeneity or assortativity may help to gain insights into the biochemical processes taking place.

The rest of the thesis is mostly devoted to how aspects of a neural network's topology might influence or even determine its ability to carry out certain tasks akin to those the brain undertakes. The fact that dynamical memory performance ensuing from synaptic depression is favoured by a highly heterogeneous degree distribution, laid out in Chapter 4, may help to explain why the brain seems to display such a topology at several levels of description – perhaps somehow maintaining itself close to a critical point. Similarly, the enhanced robustness to noise found for positively correlated networks in Chapter 6 suggests a functional advantage to a neural network being thus wired; a prediction also in agreement with some experimental findings.

As far as unearthing the mechanisms underpinning how neurons can perform cognitive tasks goes, though, perhaps the most interesting idea proposed is that of Cluster Reverberation, in Chapter 7, whereby thanks to modularity and/or clustering a neural network is able to store information instantly, without requiring biochemical changes in the synapses. Time will tell whether real neural systems do indeed harness this mechanism to perform certain short-term memory tasks.

A collateral but noteworthy aspect of this research is the potentiality for

application elsewhere of some of the mathematical techniques developed. Most of all, the method for studying correlated networks and dynamics thereon put forward in Chapter 5 for use in Chapter 6 can be expected to find widespread use. The answer to the question of why most networks are disassortative given in Chapter 5, or the relation between degree-degree correlations and nestedness described in Appendix C are examples of this.

Finally I must mention not just the answers I hope to have provided, or at least hinted at, to some unsolved problems, but also the questions that have been posed and challenges laid bare: Would a more detailed description of brain development still be possible with Fokker-Planck equations? Are these topological effects, found to be at work for the simplest neural models, indeed so relevant for real neurons? Can Cluster Reverberation be performed *in vitro*? The greatest function this thesis could perform would be to stimulate others to look into these or related issues in more depth than here. But I also hope it may serve to illustrate the sentiment, What matters how long the path to the final unravelling of the mysteries is, as long as the going is fun?

Chapter 9

Conclusiones en español

"Mientras el cerebro sea un misterio, el universo continuará siendo un misterio", dijo una vez Santiago Ramón y Cajal. Parece que nuestra misma esencia reside de alguna manera en el funcionamiento de este órgano, probablemente como consecuencia de las señales electro-químicas entre sus aproximadamente cien mil millones de neuronas. ¿Se resolverá algún día este misterio? Conocemos otros objetos capaces de procesar información de manera altamente sofisticada: los ordenadores electrónicos. Confrontados con un pantallazo azul, se nos podría perdonar el tildar este tipo de aparatos de incomprensibles y caprichosos, por no decir malévolos. Pero en realidad la mayor parte de la gente entiende, al menos en algún nivel, cuáles son los mecanismos y procesos físicos que subyacen el comportamiento complejo del que hacen gala los ordenadores, y no consideran que el tema sea un misterio. No es que la analogía entre cerebro y ordenador deba ser llevado más lejos que para ilustrar cómo muchos elementos, cada uno ejecutando alguna operación relativamente simple y obvia, pueden "cooperar" y mostrar un comportamiento colectivo asombrosamente complicado, pero funcional; y que se puede comprender cómo ocurre esto sin necesidad de conocer hasta el último detalle. Aún no hemos llegado a poder responder a esta pregunta en lo que respecta al cerebro. Hemos ampliado enormemente nuestro conocimiento de aspectos fisiológicos, y trastornos mentales antaño incurables, como las fobias, son fácilmente tratadas hoy en día por la psicología. En cuanto a los mecanismos que relacionan estos dos niveles de descripción, posiblemente lo único que podamos decir a ciencia cierta es que la plasticidad sináptica está detrás de la memoria a largo plazo. Los orígenes incluso de algunas habilidades cognitivas bien definidas y extensamente estudiadas, como el razonamiento probabilístico o la memoria a corto plazo, están aún por descifrar completamente; mientras que, por ejemplo, la naturaleza de

la consciencia es verdaderamente aún un misterio. Sin embargo, si en lugar de haber desarrollado los ordenadores nosotros mismos los hubiésemos recibido de una especie alienígena, aún así podríamos esperar algún día desenmarañar los misterios de su magia. Del mismo modo, buscando maneras de que conjuntos de neuronas puedan realizar el tipo de tareas de las que las sabemos capaces, algún día entenderemos no sólo cómo nuestros estómagos digieren y nuestros corazones laten, sino también cómo nuestros cerebros piensan.

Este trabajo, en el mejor de los casos, nos avanza un paso infinitesimal por este camino. El cerebro es, entre otras muchas cosas, una red, y las redes son objetos matemáticos sobre los que sabemos hoy mucho más que hace tan sólo unos años. De hecho, son un elemento fundamental para uno de los mayores retos con los que se enfrenta actualmente el conocimiento humano: la naturaleza de los sistemas complejos. Así que, de entre los innumerables aspectos susceptibles de modificar y determinar cómo las neuronas cooperan, esta investigación se centra en la estructura de la red subyacente. Primero analiza cómo dicha estructura puede desarrollarse. El Capítulo 3 enfoca esto formalizando mediante la teoría de los procesos estocásticos una situación gobernada por eventos probabilísticos tales como el crecimiento y la muerte sinápticas. Se demuestra que este tipo de comportamiento individual es suficiente para explicar muchas propiedades estadísticas de las redes de cerebros reales. Por otra parte, este marco teórico puede ser reducido a una descripción en términos de ecuaciones de Fokker-Planck, que relacionan acciones microscópicas estocásticas con la evolución macroscpica de propiedades como la densidad sináptica media, la heterogeneidad de la distribución de grados o la asortatividad, que quizás nos permita extraer información relevante acerca de los procesos bioquímicos involucrados.

La mayor parte del resto de la tesis trata de cómo aspectos de la topología de una red neuronal pueden influenciar o incluso determinar su habilidad para ejecutar ciertas tareas cognitivas como las que se describen en un cerebro o medio neuronal real. Por ejemplo, el hecho de que, en cuanto a la memoria dinámica que emerge gracias a la depresión sináptica, el rendimiento es mayor para una distribución de grados altamente heterogénea, como demuestra el Capítulo 4, podría ayudar a explicar por qué el cerebro parece mostrar una topología de este tipo en varios niveles de descripción, quizás incluso manteniéndo su actividad, de alguna manera todavía no comprendida del todo, cerca de un punto crítico. De igual modo, la mayor robustez durante los procesos cognitivos en presencia de ruido en el caso de redes con correlaciones

positivas como se ha descrito en el Capítulo 6 sugiere que existe una ventaja funcional para una red neuronal en adoptar esta propiedad; una predicción que también encaja con algunos hallazgos experimentales.

En lo que se refiere a desentrañar los mecanismos que permiten a las neuronas realizar colectivamente tareas cognitivas, quizás la idea más interesante aquí propuesta es la de *Cluster Reverberation* (Reverberación de Grupo), en el Capítulo 7, según la cual, gracias a la modularidad y/o el grado de "agrupamiento", una red neuronal es capaz de almacenar información instantáneamente, sin requerir para ello cambios bioquímicos de potenciación o depresión a largo plazo en las sinapsis. El tiempo dirá si el cerebro aprovecha realmente este mecanismo para realizar ciertas tareas de memoria de corto plazo.

Un aspecto colateral pero digno de mención de este trabajo es el de la potencialidad de algunas de las técnicas matemáticas desarrolladas de ser aplicadas para otras situaciones de interés. Sobre todo, es de esperar que el método para estudiar redes correlacionadas, y dinámicas sobre ellas, propuesto en el Capítulo 5 y utilizado en el Capítulo 6, sea útil para una amplia gama de problemas. La respuesta, en el Capítulo 5, a la pregunta de por qué la mayoría de las redes son disasortativas, o la relación entre correlaciones entre los nodos y el "anidamiento" descrita en el Apéndice C son ejemplos de aplicaciones.

Finalmente, hay que mencionar no sólo las respuestas que se han intentado dar, o al menos sugerir, con esta tesis para algunos problemas sin resolver, sino también las preguntas y los nuevos retos que han surgido: por ejemplo, ¿sería posible, también con ecuaciones de Fokker-Planck, una descripción más detallada del desarrollo cerebral? ¿Son estos efectos topológicos, descritos para los modelos neuronales más sencillos, realmente tan relevantes para neuronas de verdad? ¿Puede el mecanismo de *Cluster Reverberation* ocurrir *in vitro*? En definitiva, la mayor función que pudiera cumplir esta tesis sería la de estimular a otra/os para que indaguen en estos y otros temas más profundamente que aquí. Pero quizás también sirva para ilustrar el siguiente sentimiento: ¿qué más da cuán largo sea el camino hacia el desenmarañamiento último de los misterios, siempre que el trayecto sea divertido?

Appendix A

Nonlinear preferential rewiring in fixed-size networks as a diffusion process

We present an evolving network model in which the total numbers of nodes and edges are conserved, but in which edges are continuously rewired according to nonlinear preferential detachment and reattachment. Assuming power-law kernels with exponents α and β, the stationary states the degree distributions evolve towards exhibit a second order phase transition – from relatively homogeneous to highly heterogeneous (with the emergence of starlike structures) at $\alpha = \beta$. Temporal evolution of the distribution in this critical regime is shown to follow a nonlinear diffusion equation, arriving at either pure or mixed power-laws, of exponents $-\alpha$ and $1 - \alpha$.

Complex systems may often be described as a set of nodes with edges connecting some of them – the *neighbours* – (see, for instance, Refs.(Boccaletti et al., 2006; Arenas et al., 2008a; Marro et al., 2008)). The number of edges a particular node has is called its degree, k. The study of such large networks is usually made simpler by considering statistical properties, e.g., the degree distribution, $p(k)$ (probability of finding a node with a particular degree). It turns out that a high proportion of real-world networks follow power-law degree distributions, $p(k) \sim k^{-\gamma}$ – referred to as *scale-free* due to their lack of a characteristic size. Also, many of them have their edges placed among the nodes apparently in a random way – i.e., there is no correlation between the degree of a node and any other of its properties, such as the degrees of its neighbours. Barabási and Albert (Barabási and Albert, 1999) applied the mechanism of *preferential attachment* to an evolving network model and

showed how this resulted in the degree distributions becoming scale-free for long enough times. For this to work, attachment had to be linear – i.e., the probability a node with degree k has of receiving a new edge is $\pi(k) \sim k + q$. This results in scale-free stationary degree distributions with an exponent $\gamma = 3 - q$.

Preferential attachment seems to be behind the emergence of many real-world, continuously growing networks. However, not all networks in which some nodes at times gain (or loose) new edges have a continuously growing number of nodes. For example, a given group of people may form an evolving social network (Kossinets and Watts, 2006) in which the edges represent friendship. Preferential attachment may be relevant here – the more people you know, the more likely it is that you will be introduced to someone new – but probabilities are not expected to depend linearly on degree. For instance, there may be saturations (highly connected people might become less accessible), threshold effects (hermits may be prone to antisocial tendencies), and other non-linearities. The brain may also be a relevant case. Once formed, the number of neurons does not seem to continually augment, and yet its structural topology is dynamic (Klintsova and Greenough, 1999). Synaptic growth and dendritic arborization have been shown to increase with electric stimulation (Lee et al., 1980; Roo et al., 2008) – and, in general, the more connected a neuron is, the more current it receives from the sum of its neighbours.

Barabási and Albert showed that both (linear) preferential attachment and an ever-growing number of nodes are needed for scaling to emerge in their model. In a fixed population, their mechanism would result in a fully-connected network. However, this is not normally observed in real systems. Rather, just as some new edges sprout, others disappear – less used synapses suffer atrophy, unstimulating friendships wither. Often, the numbers of both nodes and edges remain roughly constant. The same authors did therefore extend their model so as to include the effects of *preferential rewiring* (which could be applied to fixed-size networks), although again probabilities depended linearly on node degree (Albert and Barabási, 2000). Another mechanism which (roughly) maintains constant the numbers of nodes and edges is node fusing (Thurner et al., 2007), once more according to linear probabilities. As to nonlinear preferential attachment, the (growing) BA model was extended to take power-law probabilities into account (Krapivsky et al., 2000), although the solutions are only scale free for the linear case.

In this note we present an evolving network model with preferential rewiring

according to nonlinear (power-law) probabilities. The number of nodes and edges is conserved but the topology evolves, arriving eventually at a macroscopically (nonequilibrium) stationary state – as described by global properties such as the degree distribution. Depending on the exponents chosen for the rewiring probabilities, the final state can be either fairly homogeneous, with a typical size, or highly heterogeneous, with the emergence of starlike structures. In the critical case marking the transition between these two regimes, the degree distribution is shown to follow a nonlinear diffusion equation. This describes a tendency towards stationary states that are characterized either by scale-free or by mixed scale-free distributions, depending on parameters.

Our model consists of a random network with N nodes of respective degree k_i, $i = 1, 2, ..., N$, and $\frac{1}{2}N\langle k\rangle$ edges. Initially, the degrees have a given distribution $p(k, t = 0)$. At each time step, one node is chosen with a probability which is a function of its degree, $\rho(k_i)$. One of its edges is then chosen randomly and removed from it, to be reconnected to another node j chosen according to a probability $\pi(k_j)$. That is, an edge is broken and another one is created, and the total number of edges, as well as the total number of nodes, is conserved. The functions $\pi(k)$ and $\rho(k)$ are arbitrary, but we shall explicitly illustrate here $\pi(k_i) \sim k_i^{\alpha}$ and $\rho(k_i) \sim k_i^{\beta}$ that capture the essence of a wide class of nonlinear monotonous response functions and are easy to handle analytically.

The probabilities π and ρ a given node has, at each time step, of increasing or decreasing its degree can be interpreted as transition probabilities between states. The expected value of the increment in a given $p(k, t)$ at each time step, $\Delta p(k, t)$, may then be written as

$$\begin{aligned}\frac{\partial p(k,t)}{\partial t} &= (k-1)^{\alpha}\,\bar{k}_{\alpha}^{-1}p(k-1,t)\\ &+ (k+1)^{\beta}\,\bar{k}_{\beta}^{-1}\,p(k+1,t)\\ &- \left(k^{\alpha}\,\bar{k}_{\alpha}^{-1} + k^{\beta}\,\bar{k}_{\beta}^{-1}\right)\,p(k,t),\end{aligned} \tag{A.1}$$

where $\bar{k}_a = \bar{k}_a(t) = \sum_k k^a p(k, t)$. If it exists, any stationary solution must satisfy the condition $p_{\rm st}(k+1)\,(k+1)^{\beta}\,\bar{k}_{\alpha}^{\rm st} = p_{\rm st}(k)\,k^{\alpha}\,\bar{k}_{\beta}^{\rm st}$ which, for $k \gg 1$, implies that

$$\frac{\partial p_{\rm st}(k)}{\partial k} = \left(\frac{\bar{k}_{\alpha}^{\rm st}}{\bar{k}_{\beta}^{\rm st}}\frac{k^{\alpha}}{(k+1)^{\beta}} - 1\right)p_{\rm st}(k). \tag{A.2}$$

Therefore, the distribution will have an extremum at $k_e = \left(\bar{k}_{\beta}^{\rm st}/\bar{k}_{\alpha}^{\rm st}\right)^{\frac{1}{\alpha-\beta}}$ (where we have approximated $k_e \simeq k_e + 1$). If $\alpha < \beta$, this will be a maximum,

signalling the peak of the distribution. On the other hand, if $\alpha > \beta$, k_e will correspond to a minimum. Therefore, most of the distribution will be broken in two parts, one for $k < k_e$ and another for $k > k_e$. The critical case for $\alpha = \beta$ will correspond to a monotonously decreasing stationary distribution, but such that $\lim_{k\to\infty} \partial p_{st}(k)/\partial k = 0$. In fact, Eq. (A.1) is for this situation ($\alpha = \beta$) the discretized version of a nonlinear diffusion equation,

$$\frac{\partial p(k,\tau)}{\partial \tau} = \frac{\partial^2}{\partial k^2}[k^\alpha p(k,\tau)], \tag{A.3}$$

after dynamically modifying the time scale according to $\tau = t/\bar{k}_\alpha\,(t)$. Ignoring, for the moment, border effects, the solutions of this equation are of the form

$$p_{\rm st}(k) \sim Ak^{-\alpha} + Bk^{-\alpha+1}, \tag{A.4}$$

with A and B constants. If $\alpha > 2$, then given A we can always find a B which allows $p_{\rm st}(k)$ to be normalized in the thermodynamic limit [1]. For example, if the lower limit is $k \geq 1$, then $B = (\alpha - 2)\,[1 - A/(\alpha - 1)]$. However, if $1 < \alpha \leq 2$, then only A can remain non-zero, and $p_{\rm st}(k)$ will be a pure power law. For $\alpha \leq 1$, both constants must tend to zero as $N \to \infty$. In finite networks, no node can have a degree larger than $N - 1$ or lower than 0. In fact, one would usually wish to impose a minimum nonzero degree, e.g. $k \geq 1$. The temporal evolution of the degree distribution is illustrated in Fig. A.1. This shows the result of integrating Eq. (A.1) for $k \geq 1$, different times, $\beta = 1$, and three different values of α, along with the respective values obtained from Monte Carlo simulations.

The main result may be summarized as follows. For $\alpha < \beta$, the network will evolve to have a characteristic size, centred around $\langle k \rangle$. At the critical case $\alpha = \beta$, all sizes appear, according either to a pure or a composite power law, as detailed above.

If we impose, say, $k \geq 1$, then starlike structures will emerge, with a great many nodes connected to just a few hubs [2].

Figure A.2 illustrates the second order phase transition undergone by the variance of the final (stationary) degree distribution, depending on the exponent α, where β is set to unity. It should be mentioned that this particular

[1] Although all moments of k will diverge unless $B = 0$.

[2] There is a finite-size effect not taken into account by the theory – but relevant when $\alpha > \beta$ – which provides a natural lower cutoff for $p_{st}(k)$: if there are, say, m nodes which are connected to the whole network, then the minimum degree a node can have is m.

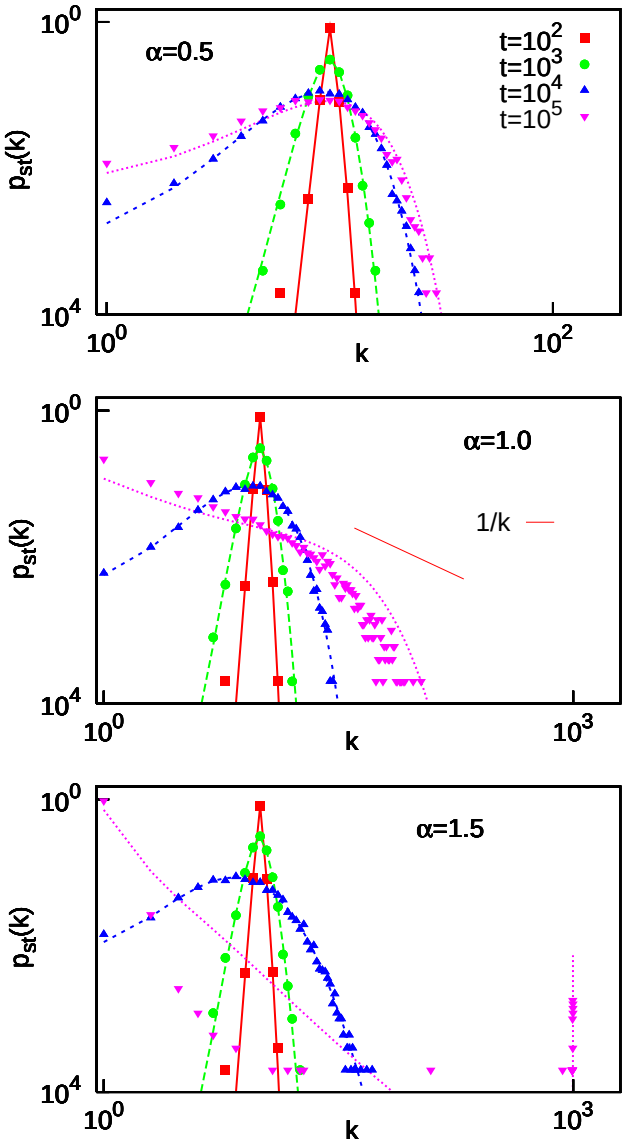

Figure A.1: Degree distribution $p(k,t)$ at four different stages of evolution: $t = 10^2$ [(yellow) squares], 10^3 [(blue) circles], 10^4 [(red) triangles)] and 10^5 MCS [(black) diamonds]. From top to bottom panels, subcritical ($\alpha = 0.5$), critical ($\alpha = 1$) and supercritical ($\alpha = 1.5$) rewiring exponents. Symbols from MC simulations and corresponding solid lines from numerical integration of Eq. (A.1). $\beta = 1$, $\langle k \rangle = 10$ and $N = 1000$ in all cases.

case, $\beta = 1$, corresponds to edges being chosen at random for disconnection, since the probability of a random edge belonging to node i is proportional to k_i.

This topological phase transition is similar to the ones that have been

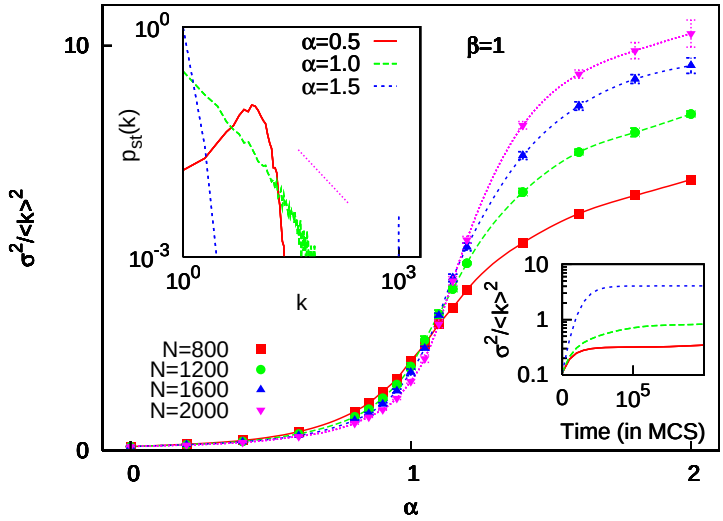

Figure A.2: Adjusted variance $\sigma^2/\langle k\rangle^2$ of the degree distribution after 2×10^5 MCS against α, as obtained from MC simulations, for system sizes $N = 800$ [(yellow) squares], 1200 [(blue) circles], 1600 [(red) triangles] and 2000 [(black) diamonds]. Top left inset shows final degree distributions for $\alpha = 0.5$ [light gray (blue)], 1 [dark gray (red)] and 1.5 (black), with $N = 1000$. Bottom right inset shows typical time series of $\sigma^2/\langle k\rangle^2$ for the same three values of α and $N = 1200$. In all cases, $\beta = 1$ and $\langle k\rangle = 10$.

described in equilibrium network ensembles defined via an energy function, in the so-called *synchronic* approach to network analysis (Farkas et al., 2004; Park and Newman, 2004; Burda et al., 2004; Derényi et al., 2004). However, our (nonequilibrium) model does not come within the scope of this body of work, since the rewiring rates cannot, in general, be derived from a potential. Furthermore, we are here concerned with the time evolution rather than the stationary states, making our approach *diachronic*.

Summing up, in spite of its simplicity, our model captures the essence of many real-world networks which evolve while leaving the total numbers of nodes and edges roughly constant. The grade of heterogeneity of the stationary distribution obtained is seen to depend crucially on the relation between the exponents modelling the probabilities a node has of obtaining or loosing a new edge. It is worth mentioning that the heterogeneity of the degree distribution of a random network has been found to determine many relevant behaviours and magnitudes such as its clustering coefficient and mean minimum path (Newman, 2003c), critical values related to the dynamics of

excitable networks (Johnson et al., 2008), or the synchronizability for systems of coupled oscillators (since this depends on the spectral gap of the Laplacian matrix) (Barahona and Pecora, 2002).

The above shows how scale-free distributions, with a range of exponents, may emerge for nonlinear rewiring, although only in the critical situation in which the probabilities of gaining or loosing edges are the same. We believe that this non-trivial relation between the microscopic rewiring actions (governed in our case by parameters α and β) and the emergent macroscopic degree distributions could shed light on a class of biological, social and communications networks.

Appendix B

Effective modularity of highly clustered networks

The number of nodes within a radius r is $n(r) = A_d r^d$, with A_d a constant. We shall therefore assume a node with degree k to have edges to all nodes up to a distance $r(k) = (k/A_d)^{1/d}$, and none beyond (note that this is not necessarily always feasible in practice). To estimate λ, we shall first calculate the probability that a randomly chosen edge have length x. The chance that the edge belong to a node with degree k is $\pi(k) \sim kp(k)$ (where $p(k)$ is the degree distribution). The proportion of edges that have length x among those belonging to a node with degree k is $\nu(x|k) = dA_d x^{d-1}/k$ if $A_d x^d < k$, and 0 otherwise. Considering, for example, scale-free networks (as in Ref. (Rozenfeld et al., 2002)), so that the degree distribution is $p(k) \sim k^{-\gamma}$ in some interval $k \in [k_0, k_{max}]$ (Barabási and Albert, 1999), and integrating over $p(k)$, we have the distribution of lengths,

$$P(x) = (Const.) \int_{\max(k_0, Ax^d)}^{k_{max}} \pi(k)\nu(k|x)dk = d(\gamma - 2)x^{-[d(\gamma-2)+1]},$$

where we have assumed, for simplicity, that the network is sufficiently sparse that $\max(k_0, Ax^d) = Ax^d$, $\forall x \geq 1$, and where we have normalised for the interval $1 \leq x < \infty$; strictly, $x \leq (k_{max}/A)^{1/d}$, but we shall also ignore this effect. Next we need the probability that an edge of length x fall between two compartments of linear size l. This depends on the geometry of the situation as well as dimensionality; however, a first approximation which is independent of such considerations is

$$P_{out}(x) = \min\left(1, \frac{x}{l}\right).$$

We can now estimate the modularity λ as

$$\lambda = \int_1^\infty P_{out}(x)P(x)dx = \frac{1}{d(\gamma-2)-1}\left[d(\gamma-2)l^{-1} - l^{-d(\gamma-2)}\right].$$

Fig. 7.5 shows how λ depends on γ for $d = 2$ and various box sizes.

Appendix C

Nestedness of networks

The property of *nestedness* has for some time aroused a fair amount of interest as regards ecological networks – especially since a high nestedness in mutualistic systems has been shown to enhance biodiversity. However, because it is usually estimated with software, no analytical work has been done relating nestedness with other network characteristics, and consequently comparisons of experimental data with null-models can only be done computationally. We suggest a slightly refined version of the measure recently defined by Bastolla *et al.* and go on to study the effect of the degree distribution and degree correlations (assortativity). Our work provides a benchmark against which empirical networks can be contrasted.

C.1 Introduction

The intense study that complex networks have undergone over the past decade or so has shown how important topological features can be for properties of complex systems, such as dynamical behaviour, spreading of information, resilience to attacks, etc. (Newman, 2003c; Boccaletti et al., 2006). A paradigmatic case is that of ecosystems. The solution to May's paradox (May, 1973) – the fact that large ecosystems seem to be especially stable, when theory predicts the contrary – is still not clear, but it is widely suspected that there is some structural feature of ecological networks which as yet eludes us. One aspect of such networks, which has been studied for some time by ecologists and may be related to this problem, is called *nestedness*. Loosly speaking, a network – say of species and islands, linked whenever the former inhabit the latter – is said to be highly nested if the species which exist on scarcely populated islands tend always to be found also on those islands inhabited by many

Figure C.1: Maximally packed matrix representing a network of plants and islands off Perth (Abbott and Black, 1980) (because the network is bipartite, the adjacency matrix is composed of four blocks: two identical to this matrix, the other two composed of zeros). Data, image and line obtained from *NESTEDNESS CALCULATOR*, which returns a "temperature" of $T = 0.69^o$ for this particular network.

different species. This can be most easily seen by graphically representing a matrix such that animals are columns and islands are files, with elements equal to one whenever two nodes are linked and zero if not. If, after ordering each kind of node by degree (number of neighbours), all the ones can be quite neatly packed into one corner, the network is considered highly nested. This is done in Fig. C.1 for a network of plants inhabiting islands off Perth. This rather vague concept is usually measured with software for the purpose. For Fig. C.1, we have used *NESTEDNESS CALCULATOR*, which estimates a curve of equal density of ones and zeros, calculates how many ones and zeros are on the "wrong" side and by how much, and returns a number between 0 and 100 called "temperature" by analogy with some system such as a subliming solid. A low temperature indicates high nestedness. To determine how significantly nested a given network is, the usual procedure is to generate equivalent random networks computationally (with sone constraint such as the number of edges or the degree of each node being conserved) and estimate how likely it is that such a network be "colder" than that of the data.

Bastolla *et al.* (Bastolla et al., 2009) have recently shown how symbiotic interactions can reduce the effective competition between two species, say of insect, via common symbiotic hosts – such as plants they pollinate. These authors define a measure to take into account the average number of shared partners in these *mutualistic* networks, and call it "nestedness" because it would seem to be related to the concept referred to above. They go on to show

evidence of how the nestedness of empirical mutualistic networks is correlated with the biodiversity of the corresponding ecosystems. This beneficial effect "enemy" nodes can gain from sharing "friendly" partners is not confined to ecosystems. It is expected also to play a role, for instance, in financial networks or other economic systems (Sugihara and Ye, 2009). The principle is simple. Say nodes A and B are in competition with each other. An increase in A will be to B's detriment, and viceversa; but if both A and B engage in a symbiotic relationship with node C, then A's thriving will stimulate C, which in turn will be helpful to B. Thus, the effective competition between A and B is reduced, and the whole system becomes more stable and capable of sustaining more nodes (Domínguez-Chibetín et al., 2011).

In Ref. (Johnson and Muñoz) we take up this idea of shared neighbours (though characterised with a slightly different measure, for reasons we shall explain in Section C.2) and study analytically the effect of other topological properties, such as the degree distribution and degree-degree correlations. This allows us to contrast empirical data with null-models and thus test for statistical significance with no need of computer randomisations. We also comment on how mutual-neighbour structure could develop in systems of interdependent networks (such as competition and symbiosis) so as to minimise the risk of a "cascade of failures" (Buldyrev et al., 2010). Although we are not here concerned specifically with neural systems, a description of this work is included as an appendix since it serves as an example application of the method put forward in Ref. (Johnson et al., 2010b) and presented in Chapter 5.

C.2 Definition

Consider a network with N nodes defined by the adjacency matrix $\hat{a}$: the element $\hat{a}_{ij}$ is equal to the number on links, or edges, from node j to node i (typically considered to be either one or zero). If $\hat{a}$ is symmetric, then the network is undirected and each node i can be characterised by a degree $k_i = \sum_j \hat{a}_{ij}$. (If it is directed, i has both an *in* degree, $k_i^{\text{in}} = \sum_j \hat{a}_{ij}$, and an *out* degree, $k_i^{\text{out}} = \sum_j \hat{a}_{ji}$; we shall focus here on undirected networks, although most of the results could be easily extended to directed ones.).

Bastolla *et al.* (Bastolla et al., 2009) have shown that the effective competition between two species (say two species of insect) can be reduced if they have common neighbours with which they are in symbiosis (for instance, if they both pollinate the same plant). Therefore, in mutualistic networks (net-

works of symbiotic interactions) it is beneficial to the species at two nodes i and j for the number of shared symbiotic partners, $n_{ij} = \sum_l \hat{a}_{il}\hat{a}_{lj} = (\hat{a}^2)_{ij}$, to be high. Going on this, and assuming the network is undirected, the authors suggest taking into account the following measure:

$$\eta_B = \frac{\sum_{i<j} \hat{n}_{ij}}{\sum_{i<j} \min(k_i, k_j)}, \tag{C.1}$$

which they call *nestedness* because it would seem to be highly correlated with the measures returned by nestedness software. Note that, although the authors were considering only bipartite graphs, this characteristic is not imposed in the above definition. In this work, we shall take up the idea of the importance of n_{ij}, but use a slightly different measure of nestedness, for several reasons. One is that η_B has a serious shortcoming. If we commute the sums[1] in the numerator of Eq. (C.1), we find that the result only depends on the heterogeneity of the degree distribution: $\sum_{ij} \hat{n}_{ij} = \sum_l \sum_i \hat{a}_{il} \sum_j \hat{a}_{lj} = N\langle k^2 \rangle$. Also, although the maximum value $\hat{n}_{ij}$ can take is $\min(k_i, k_j)$, this is not necessarily the best normalisation factor, since the expected number of paths of length 2 connecting nodes i and j depends on both k_i and k_j (as we show explicitely in Section C.3). Furthermore, it can sometimes be convenient to have a local measure of nestedness. For these reasons, we shall use

$$\eta_{ij} \equiv \frac{n_{ij}}{k_i k_j} = \frac{(\hat{a}^2)_{ij}}{k_i k_j}, \tag{C.2}$$

which is defined for every pair of nodes (i, j). This allows for the consideration of a nestedness per node, $\eta_i = N^{-1} \sum_j \eta_{ij}$, or of the global measure

$$\eta = \frac{1}{N^2} \sum_{ij} \eta_{ij}. \tag{C.3}$$

C.3 The effect of the degree distribution

Most networks have quite broad degree distributions $p(k)$, most notably the fairly ubiquitous scale-free networks, for which they follow power-laws, $p(k) \sim k^{-\gamma}$. Since this heterogeneity tends to have an importante influence on any network measure, it will be useful to take this effect into account analytically. As is standard, the null-model we shall use to do this is the *configurational*

[1] In an undirected network, $\sum_{i<j} = \frac{1}{2} \sum_{ij}$; we shall always sum over all i and j, since it is easier to generalise to directed networks and often avoids writing factors 2.

model (Newman, 2003c): the set of random networks wired according to the constraints that a given degree sequence $(k_1, ..., k_N)$ is respected, and also that there be no degree-degree correlations. The expected value of an element of the adjacency matrix for networks belonging to this ensemble is

$$\overline{\hat{a}_{ij}} \equiv \hat{\epsilon}^c_{ij} = \frac{k_i k_j}{\langle k \rangle N}. \tag{C.4}$$

We shall use a line, $\overline{(\cdot)}$, to represent expected values given certain constraints, and angles, $\langle \cdot \rangle$, for averages over nodes of a given network[2]. For the case of the adjacency matrix, we use the notation $\hat{\epsilon}^c_{ij} = \overline{\hat{a}_{ij}}$ for clarity and coherence with previous work. Plugging Eq. (C.4) into Eq. (C.2), we have the expected value in the configuration ensemble,

$$\overline{\eta_{ij}} = \frac{\langle k^2 \rangle}{\langle k \rangle^2 N} \equiv \eta_{conf}. \tag{C.5}$$

Since η_c is independent of i and j, it coincides with the expected value for the global measure, $\overline{\eta} = \eta_{conf}$ – a fact that justifies the normalisation chosen in Eq. (C.2). It is obvious from Eq. (C.5) that degree heterogeneity will have an important effect on η. Therefore, if we are to capture aspects of network structure other than those directly induced by the degree distribution, it will in general be useful to consider the nestedness normalised to this expected value,

$$\tilde{\eta} \equiv \frac{\eta}{\eta_{conf}} = \frac{\langle k \rangle^2}{\langle k^2 \rangle N} \sum_{ij} \frac{(\hat{a}^2)_{ij}}{k_i k_j}. \tag{C.6}$$

Although $\tilde{\eta}$ is unbounded, it has the advantage that it is equal to unity for any uncorrelated random network, independently of its degree heterogeneity, thereby making it possible to detect non-trivial structure in a given empirical network without the need for computational randomisations.

C.4 Nestedness and assortativity

In the configuration ensemble, the expected value of the mean degree of the neighbours of a given node is $\overline{k_{nn,i}} = k_i^{-1} \sum_j \hat{\epsilon}^c_{ij} k_j = \langle k^2 \rangle / \langle k \rangle$, which is independent of k_i. However, real networks usually display degree-degree correlations, with the result that $\overline{k_{nn,i}} = \overline{k_{nn}}(k_i)$. If $\overline{k_{nn}}(k)$ increases (decreases) with k, the

[2]In this case, for instance, the network considered for $\langle k \rangle$ is any of the members of the ensemble, since they all have the same mean degree by definition.

network is assortative (disassortative). A measure of this phenomenon is Pearson's coefficient applied to the edges (Newman, 2003c, 2002, 2003a; Boccaletti et al., 2006): $r = ([k_l k'_l] - [k_l]^2)/([k_l^2] - [k_l]^2)$, where k_l and k'_l are the degrees of each of the two nodes belonging to edge l, and $[\cdot] \equiv (\langle k \rangle N)^{-1} \sum_l (\cdot)$ is an average over edges. Writing $\sum_l (\cdot) = \sum_{ij} \hat{a}_{ij}(\cdot)$, r can be expressed as

$$r = \frac{\langle k \rangle \langle k^2 \overline{k_{nn}}(k) \rangle - \langle k^2 \rangle^2}{\langle k \rangle \langle k^3 \rangle - \langle k^2 \rangle^2}. \tag{C.7}$$

The ensemble of all networks with a given degree sequence $(k_1, ...k_N)$ contains a subset for all members of which $\overline{k_{nn}}(k)$ is constant (the configuration ensemble), but also subsets displaying other functions $\overline{k_{nn}}(k)$.

In Chapter 5 (Johnson et al., 2010b) we showed that there is a one-to-one mapping between any mean-nearest-neighbour function $\overline{k_{nn}}(k)$ and its corresponding mean-adjacency-matrix $\hat{\epsilon}$, which is as follows: writing $\overline{k_{nn}}(k)$ as

$$\overline{k_{nn}}(k) = \frac{\langle k^2 \rangle}{\langle k \rangle} + \int d\nu f(\nu) \sigma_{\nu+1} \left[\frac{k^{\nu-1}}{\langle k^\nu \rangle} - \frac{1}{k} \right] \tag{C.8}$$

with $\sigma_{\nu+1} \equiv \langle k^{\nu+1} \rangle - \langle k \rangle \langle k^\nu \rangle$ (which can always be done), the corresponding matrix $\hat{\epsilon}$ takes the form

$$\hat{\epsilon}_{ij} = \frac{k_i k_j}{\langle k \rangle N} + \int d\nu \frac{f(\nu)}{N} \left[\frac{(k_i k_j)^\nu}{\langle k^\nu \rangle} - k_i^\nu - k_j^\nu + \langle k^\nu \rangle \right]. \tag{C.9}$$

In many empirical networks, $\overline{k_{nn}}(k)$ has the form $\overline{k_{nn}}(k) = A + Bk^\beta$, with $A, B > 0$ (Boccaletti et al., 2006; Pastor-Satorras et al., 2001) – the mixing being assortative (disassortative) if β is positive (negative). Such a case is fitted by Eq. (C.8) if $f(\nu) = C[\delta(\nu - \beta - 1)\sigma_2/\sigma_{\beta+2} - \delta(\nu - 1)]$, with C a positive constant, since this choice yields

$$\overline{k_{nn}}(k) = \frac{\langle k^2 \rangle}{\langle k \rangle} + C\sigma_2 \left[\frac{k^\beta}{\langle k^{\beta+1} \rangle} - \frac{1}{\langle k \rangle} \right]. \tag{C.10}$$

After plugging Eq. (C.10) into Eq. (C.7), one obtains:

$$r = \frac{C\sigma_2}{\langle k^{\beta+1} \rangle} \left(\frac{\langle k \rangle \langle k^{\beta+2} \rangle - \langle k^2 \rangle \langle k^{\beta+1} \rangle}{\langle k \rangle \langle k^3 \rangle - \langle k^2 \rangle^2} \right). \tag{C.11}$$

It turns out that the configurations most likely to arise naturally (those with maximum entropy) usually have $C \simeq 1$ (Johnson et al., 2010b) (c.f. Chapter 5). Therefore, and for the sake of analytical tractability, we shall do

as in Chapter 6 and consider this particular case[3] – that is, we shall use

$$\hat{\epsilon}_{ij} = \frac{1}{N}\left\{\frac{\sigma_2}{\sigma_{\beta+2}}\left[\frac{(k_i k_i)^{\beta+1}}{\langle k^{\beta+1}\rangle} - k_i^{\beta+1} - k_j^{\beta+1} + \langle k^{\beta+1}\rangle\right] + k_i + k_j - \langle k\rangle\right\}. \tag{C.12}$$

Substituting the adjacency matrix for this expression in the definition of $\tilde{\eta}$ (Eq. (C.6)), we obtain its expected value as a function of the remaining parameter β:

$$\overline{\tilde{\eta}}_\beta = \frac{\langle k\rangle^2}{\langle k^2\rangle}\left[1 + (\sigma_2 - \alpha_\beta^2\rho_\beta)\left(2\frac{\langle k^\beta\rangle\langle k^{-1}\rangle}{\langle k^{\beta+1}\rangle} - \langle k^{-1}\rangle^2\right) + \alpha_\beta^2\rho_\beta\left(\frac{\langle k^\beta\rangle}{\langle k^{\beta+1}\rangle}\right)^2\right], \tag{C.13}$$

where $\alpha_\beta \equiv \sigma_2/\sigma_{\beta+2}$ and $\rho_\beta \equiv \langle k^{2(\beta+1)}\rangle - \langle k\rangle^{2(\beta+1)}$. Note that $\overline{\tilde{\eta}}_0 = 1$.

Fig. C.2 shows the value of $\overline{\tilde{\eta}}_\beta$ given by Eq. (C.13) against the assortativity r for various scale-free networks. Nestedness is seen to grow very fast with increasing disassortativity (decreasing negative r), while in general slightly assortative networks are less nested than neutral ones. However, highly heterogeneous networks ($\gamma \to 2$) show an increase in $\overline{\tilde{\eta}}_\beta$ for large positive r. Fig. C.3 shows a plot of nestedness against assortativity for the selection of empirical networks listed in Table C.4. Although these networks are highly disparate as regards size, density, degree distribution, etc., it is apparent from the similarity to Fig. C.2 that the main contribution to $\tilde{\eta}_\beta$ comes indeed from the assortativity.

C.5 Bipartite networks

Mutualistic networks are usually bipartite: two sets of nodes exist such that all edges are between nodes in one set and those of another. The ones considered in Ref. (Bastolla et al., 2009), for instance, are composed of animals and plants which interact in symbiotic relations of feeding-pollination; these interactions only take place between animals and plants. Let us therefore consider a bipartite network and call the sets Γ_1 and Γ_2, with n_1 and n_2 nodes, respectively ($n_1 + n_2 = N$). Using the notation $\langle\cdot\rangle_i$ for averages over set Γ_i, the total number of edges is $\langle k\rangle_1 n_2 = \langle k\rangle_2 n_1 = \frac{1}{2}\langle k\rangle N$. Assuming that the network is defined by the configuration ensemble, though with the additional

[3]Note that $C = 1$ corresponds to removing the linear term, proportional to $k_i k_j$, in Eq. (C.9), and leaving the leading non-linearity, $(k_i k_j)^{\beta+1}$, as the dominant one.

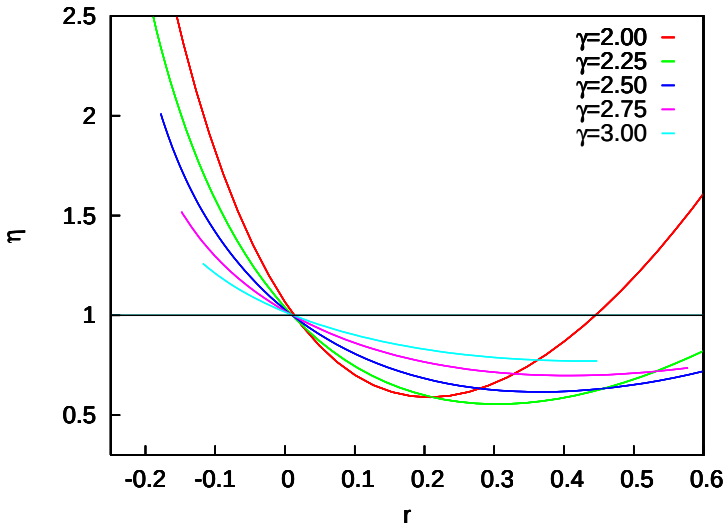

Figure C.2: Nestedness against assortativity (as measured by Pearson's correlation coefficient) for scale-free networks as given by Eq. (C.13). $\langle k \rangle = 10$, $N = 1000$.

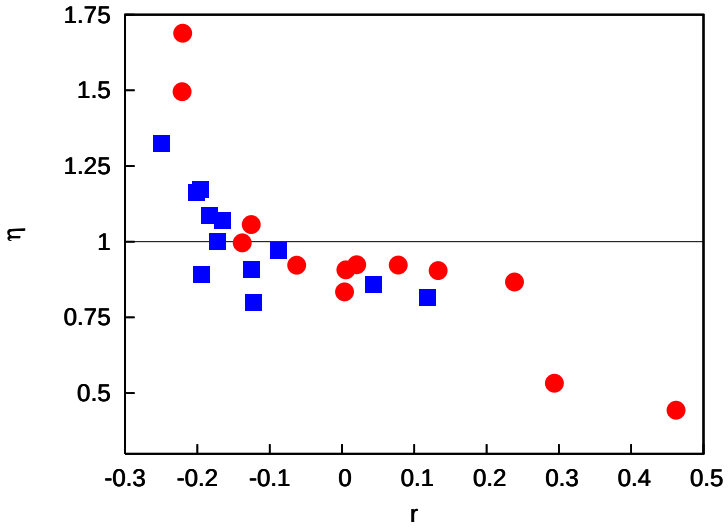

Figure C.3: Nestedness against assortativity (as measured by Pearson's correlation coefficient) for data on a variety of networks. Blue squares are food webs (Table C.4) and red circles are networks of all other types (Table C.4).

constraint of being bipartite, the probability of node l being connected to node i is

$$\hat{\epsilon}_{il} = 2\frac{k_i k_l}{\langle k \rangle N}$$

Food web	r	ν	$\langle k \rangle$	N	$\sigma/\langle k \rangle$
Little Rock lake	-0.343	1.219	20.4	92	0.73
Ythan Estuary (w/p)	-0.249	1.323	8.9	82	0.93
Stony Stream	-0.201	1.163	14.7	109	0.75
Canton Creek	-0.196	1.171	13.5	102	0.69
Skipwith Pond	-0.194	0.891	14.2	25	0.37
El Verde	-0.183	1.088	18.4	155	0.88
Caribbean Reef (small)	-0.172	1.000	19.7	50	0.49
St. Martin Island	-0.165	1.071	9.3	42	0.56
UK Grassland	-0.125	0.907	2.8	61	0.82
Chesapeake Bay	-0.123	0.801	4.1	31	0.60
NE US Shelf	-0.088	0.971	34.3	79	0.45
Coachella Valley	0.043	0.857	14.6	29	0.41
St. Mark's Estuary	0.118	0.816	8.5	48	0.55

Table C.1: Food webs appearing in Fig. C.3 (listed from least to most assortative) : r is the assortativity and ν the nestedness. The origins of all data cited in Ref. (Dunne et al., 2004), and kindly provided to us by Jennifer Dunne.

if they belong to different sets, and zero if they are in the same one. Proceeding as before, we find that the expected value of the nestedness for a bipartite network is

$$\eta_{bip} = \frac{1}{N^2}\left[\sum_{i,j\in\Gamma_1}\frac{1}{k_i k_j}\sum_{l\in\Gamma_2}\frac{k_i k_l}{\langle k\rangle_1 n_2}\frac{k_l k_j}{\langle k\rangle_2 n_1} + \sum_{i,j\in\Gamma_2}\frac{1}{k_i k_j}\sum_{l\in\Gamma_1}\frac{k_i k_l}{\langle k\rangle_1 n_2}\frac{k_l k_j}{\langle k\rangle_2 n_1}\right] = \frac{n_1\langle k^2\rangle_2 + n_2\langle k^2\rangle_1}{\langle k\rangle_1\langle k\rangle_2(n_1+n_2)^2}. \quad \text{(C.14)}$$

Interestingly, if $n_1 = n_2$, the fact that the network is bipartite has no effect on the nestedness: $\eta_{bip} = \eta_{conf}$.

C.6 Overlapping networks

If the adjacency matrix $\hat{a}$ describes a mutualistic network, the benefit to its being nested resides in a counteraction of the competition matrix $\hat{c}$, which takes into account the extent to which one species is detrimental to another

Network	r	ν	$\langle k \rangle$	N	$\sigma/\langle k \rangle$	Ref.
Political blogs	-0.221	1.496	22.4	1490	1.62	(Adamic and Glance, 2005)
Metabolic	-0.220	1.688	9.0	453	1.87	(Duch and Arenas, 2005)
Political books	-0.138	0.996	8.4	104	0.65	(Krebs)
Adjectives and nouns	-0.125	1.057	7.6	111	0.89	(Newman, 2006)
Dolphins	-0.063	0.922	5.1	61	0.58	(Lusseau et al., 2003)
Power grid	0.003	0.834	2.7	4940	0.67	(Watts and Strogatz, 1998)
Neural	0.005	0.907	5.9	306	0.81	(Watts and Strogatz, 1998)
Jazz musicians	0.020	0.924	27.6	198	0.63	(P.Gleiser and Danon, 2003)
Email	0.078	0.923	9.6	1133	0.97	(Guimerà et al., 2003)
American football	0.133	0.904	10.6	114	0.08	(Girvan and Newman, 2002)
PGP	0.239	0.867	4.6	10680	1.77	(Bogñá et al., 2004)
High-energy arXiv	0.294	0.533	3.8	8360	1.14	(Newman, 2001)
Net-science arXiv	0.462	0.443	3.45	1588	1.00	(Newman, 2006)

Table C.2: Empirical networks appearing in Fig. C.3 (listed from least to most assortative) : r is the assortativity and ν the nestedness. All data available on the personal Web pages of Álex Arenas, Mark Newman and Duncan Watts.

due to predation, sharing of resources, etc. From this point of view, it may be interesting to study to what extent matrices $\hat{c}$ and $\hat{a}^2$ overlap (note that both networks have the same nodes, but different edges). Presumably, if ecological networks are assembled in such a way that effective competition is minimised, this overlap should be higher than randomly expected. On the other hand, a certain degree of overlap may also arise from the fact that species interacting symbiotically with the same host are perhaps more than averagely likely to be phylogenetically close and/or phenotypically similar, leading (as Darwin noted) to a higher competition element.

In any case, a measure of this overlap is

$$r \equiv \frac{1}{\langle k \rangle_c N} \sum_{ij} \hat{c}_{ij} (\hat{a}^2)_{ij}, \tag{C.15}$$

where $\langle \cdot \rangle_c$ represents an average over the competion network; similarly, $\langle \cdot \rangle_a$ will stand for an average over the mutualistic network. If the two networks

are mutually uncorrelated[4] – i.e., if the existence of an edge in one provides no information as to whether there is a corresponding one in the other – we can write

$$r \simeq \frac{1}{\langle k\rangle_c N}\sum_{ij}\hat{c}_{ij}\frac{1}{N^2}\sum_{ij}(\hat{a}^2)_{ij} \equiv r_{unc}. \tag{C.16}$$

Using $\sum_{ij}(\hat{a}^2)_{ij} = \langle k^2\rangle_a N$, and assuming that $\hat{c}$ is normalised so that $\sum_{ij}\hat{c}_{ij} = \langle k\rangle_c N$, we have[5]

$$r_{unc} \simeq \frac{\langle k^2\rangle_a}{N}, \tag{C.17}$$

which only depends on the heterogeneity of the degree distribution of the mutualistic network. Again, it may be useful to consider the overlap normalised to this value,

$$\tilde{r} \equiv \frac{r}{r_{unc}} = \frac{1}{\langle k\rangle_c\langle k^2\rangle_a}\sum_{ij}\hat{c}_{ij}(\hat{a}^2)_{ij}. \tag{C.18}$$

This measure will equal unity when there is no statistical relation between the competition matrix and the mutualistic one, but can be expected to be greater if indeed such an overlap were contributing to a reduction in effective competition.

It has recently been shown that interconnected networks are prone to dangerous "cascades of failures" (Buldyrev et al., 2010). It seems that the northen half of Italy was once left temporarily with no electric supply due to failures in the power-grid closing down dependent internet servers, which in turn further disrupted the grid, until many nodes of both networks were rendered dysfunctional. If two inter-dependent networks were to coincide perfectly ($r = 1$), the resilience of the system to node removal would be the same as that of just one network; however, lower overlap leads to increased vulnerability to such cascades of failures. Since the extinction of a species can result in its host species also going extinct, such cascades of failures may be a threat to mutualistic systems. In such a case, it would seem that a high overlap r, as defined here, between the competition matrix and the mutualistic one would minimise this possibility. It would be interesting to test this experimentally.

[4]Note that we are saying nothing of the internal correlations that each network may display.

[5]The competition matrix will in general be weighted, as could be the mutualistic one; we shall treat both as though they were not, but using weighted networks would only influence results by a normalisation factor.

C.7 Discussion

Whether or not the topological feature here described should be considered a measure of nestedness as it is usually understood in ecology is not clear. What is certain is that interactions between dynamical elements that are mediated by third parties, or common neighbours, can be relevant in a wide variety of settings. We have mentioned the paradigmatical case of ecosystems as well as financial and communications networks. But other examples spring easily to mind. For instance, two excitatory neighbouring neurons might have their mutual effect dampened if they share inhibitory neighbours. Genetic networks are riddled with motifs such that switches activate or inactivate each other indirectly, via common neighbours. As we have shown, there are nontrivial relationships between nestedness, as it is here defined, and other topological features. If it turns out that this network property is indeed relevant for many complex systems, then we hope the null models we have laid out and analysed will prove useful in assessing its functional significance.

Appendix D

Publications derived from the thesis

D.1 Journals and book chapters (the most relevant ones marked with an asterisk)

1. * *Cluster Reverberation: A mechanism for robust short-term memory without synaptic learning*, S. Johnson, J. Marro, and JJ. Torres, submitted, arXiv:1007.3122

2. * *Enhancing neural-network performance via assortativity*, S. de Franciscis, S. Johnson, and J.J. Torres, *Physical Review E* **83**, 036114 (2011)

3. *Why are so many networks disassortative?* S. Johnson, J.J. Torres, J. Marro, and M.A. Muñoz, *AIP Conf. Proc.* **1332**, 249–50 (2011)

4. *Shannon entropy and degree-degree correlations in complex networks*, S. Johnson, J.J. Torres, J. Marro, and M.A. Muñoz, "Nonlinear Systems and Wavelet Analysis", Ed. R. López-Ruiz, WSEAS Press, pp. 31–35 (2010)

5. * *Entropic origin of disassortativity in complex networks*, S. Johnson, J.J. Torres, J. Marro, and M.A. Muñoz, *Physical Review Letters* **104**, 108702 (2010)

6. * *Evolving networks and the development of neural systems*, S. Johnson, J. Marro, and J.J. Torres, *Journal of Statistical Mechanics* (2010) P03003

7. *Excitable networks: Nonequilibrium criticality and optimum topology*, J.J. Torres, S. de Franciscis, S. Johnson, and J. Marro, *International Journal of Bifurcation and Chaos* **20**, 869–875 (2010)

8. *Nonequilibrium behavior in neural networks: criticality and optimal performance*, J.J. Torres, S. Johnson, J.F. Mejias, S. de Franciscis, and J. Marro, "Advances in Cognitive Neurodynamics (II)" Eds. R. Wang and F. Gu, pp 597–603, Springer, 2011, ISBN: 978-90-481-9694-4, Proceedings of Second International Conference on Cognitive Neurodynamics (ICCN2009), Hangzhou 15-19 November 2009.

9. *Development of neural network structure with biological mechanisms*, S. Johnson, J. Marro, J.F. Mejias, and J.J. Torres, *Lecture Notes in Computer Science* **5517**, 228–235 (2009)

10. *Switching dynamics of neural systems in the presence of multiplicative colored noise*, J.F. Mejias, J.J. Torres, S. Johnson, and H.J. Kappen, *Lecture Notes in Computer Science* **5517**, 17–23 (2009)

11. * *Nonlinear preferential rewiring in fixed-size networks as a diffusion process*, S. Johnson, J.J. Torres, and J. Marro, *Physical Review E* **79**, 050104(R) (2009)

12. * *Functional optimization in complex excitable networks*, S. Johnson, J.J. Torres, and J. Marro, *EPL* **83**, 46006 (2008)

13. *Excitable networks: Non-equilibrium criticality and optimum topology*, J.J. Torres, S. de Franciscis, S. Johnson, and J. Marro, "Modelling and Computation on Complex Networks and Related Topics", Eds. Criado, Gonzalez-Vias, Mancini and Romance. Proceedings of the conference "Net-Works 2008", 185–192, ISBN:978-84-691-3819-9.

14. *Topology-induced instabilities in neural nets with activity-dependent synapses*, S. Johnson, J. Marro, and J. J. Torres, "New Trends and Tools in Complex Networks", Eds. Criado, Pello and Romance. Proceedings of the conference "Net-Works 2007", 59–71, ISBN:978-84-690-6890-8.

D.2 Abstracts

1. *Network topology and dynamical task performance*, S. Johnson, J. Marro, and J.J. Torres, AIP Conf. Proc. **1091**, 280 (2009)

2. *Constructive chaos in excitable networks with tuneable topologies*, S. Johnson, J. Marro, and J.J. Torres, XV Congreso de Fsica Estadstica FisEs08, 104 (2008)

3. *The effect of topology on neural networks with unstable memories*, S. Johnson, J. Marro, and J.J. Torres, *AIP Conf. Proc.* **887** 261 (2006)

4. *Relationship between the solar wind and the upper-frequency limit of Saturn Kilometric Radiation*, M.Y. Boudjada, P.H.M. Galopeau, H.O. Rucker, A. Lecacheux, W.S. Kurth, D.A. Gurnett, U. Taubencshuss, J.T. Steinberg, S. Johnson, and W. Vollerr, European Geosciences Union (2006)

References

H. A. and S. R. *Magnetic Domains*. Springer, Berlin, 1998.

I. Abbott and R. Black. Changes in species composition of floras on islets near perth, western australia. *Journal of Biogeography*, 7:399–410, 1980.

L. Abbott and T. Kepler. *From Hodgkin-Huxley to Hopfield, in Statistical mechanics of neural networks*. Springer-Verlag, Berlin, 1990.

L. Abbott, J. Varela, K. Sen, and S. Nelson. Synaptic depression and cortical gain control. *Science*, 275:220, 1997.

L. Adamic and N. Glance. The political blogosphere and the 2004 US Election. *Proceedings of the WWW-2005 Workshop on the Weblogging Ecosystem*, 2005.

R. Albert and A.-L. Barabási. Topology of evolving networks: Local events and universality. *Phys. Rev. Lett.*, 85(24):5234–5237, 2000.

R. Albert and A.-L. Barabási. Statistical mechanics of complex networks. *Rev. Mod. Phys.*, 74:47–97, 2002.

L. Amaral, A. Scala, M. Barthélèmy, and H. Stanley. Classes of small-world networks. *Proc. Natl. Acad. Sci. USA*, 97:11149–52, 2000.

S. Amari. Characteristics of random nets of analog neuron-like elements. *IEEE Trans. Syst. Man. Cybern.*, 2:643–657, 1972.

D. Amit. The Hebbian paradigm reintegraged: Local reverberations as internal representations. *Behavioral and Brain Sciences*, 18:617–57, 1995.

D. J. Amit. *Modeling Brain Function: The World of Attractor Neural Networks*. Cambridge University Press, Cambridge, UK, 1989.

K. Anand and G. Bianconi. Entropy measures for networks: Toward an information theory of complex topologies. *Phys. Rev. E*, 80:045102, 2009.

L. Antiqueira, F. Rodrigues, and L. Costa. Letter: Modeling connectivity in terms of network activity. *Journal of Statistical Mechanics: Theory and Experiment*, 9, 2009.

A. Arenas, A. Díaz-Guilera, and C. Pérez-Vicente. Synchronization reveals topological scales in complex networks. *Phys. Rev. Lett.*, 96:114102, 2006.

A. Arenas, A. Díaz-Guilera, J. Kurths, Y. Y. Moreno, and C. Zhou. Synchronization in complex networks. *Phys. Rep.*, 469:93–153, 2008a.

A. Arenas, A. Fernández, and S. G. S. A complex network approach to the determination of functional groups in the neural system of c. elegans. *Lect. Notes Comp. Sci.*, 5151:9–18, 2008b.

Baddeley and A.D. Working memory: looking back and looking forward. *Nature Reviews Neuroscience*, 4:829–39, 2003.

A. Baddeley. *Essentials of Human Memory*. Psychology Press, East Sussex, UK, 1999.

P. Bak, K. Chen, and C. Tang. A forest-fire model and some thoughts on turbulence. *Phys. Lett. A*, 147:297, 1990.

A. Barabási and Z. Oltvai. Network biology: understanding the cell's functional organization. *Nature Reviews Genetics*, 5:101–3, 2004.

A.-L. Barabási and R. Albert. Emergence of scaling in random networks. *Science*, 286:509–512, 1999.

M. Barahona and L. Pecora. Synchronization in small-world systems. *Phys. Rev. Lett.*, 89:054101, 2002.

O. Barak and M. Tsodyks. Persistent activity in neural networks with dynamic synapses. *PLoS Comput. Biol.*, 3(2):e35, 2007.

J. Barrie, J. Freeman, and M. Lenhart. Spatiotemporal analysis of prepyriform, visual, auditory, and somesthetic surface EEGs in trained rabbits. *J. Neurophysiol.*, 76:520, 1996.

U. Bastolla, M. Fortuna, A. Pascual-García, A. Ferrera, B. Luque, and J. Bascompte. *Nature*, 458:1018–21, 2009.

R. Baxter. *Exactly Solved Models in Statistical Mechanics*. Academic Press, London, 1982.

N. Bertschinger and T. Natschläger. Real-time computation at the edge of chaos in recurrent neural networks. *Neural Comp.*, 16:1413, 2004.

G. Bianconi. Entropy of network ensembles. *Phys. Rev. E*, 79(3):036114, 2009.

G. Bianconi. The entropy of randomized network ensembles. *EPL*, 81:28005, 2008.

G. Bianconi. Mean-field solution of the Ising model on a Barabási-Albert network. *Phys. Lett. A*, 303:166–8, 2002.

G. Bianconi and A.-L. Barabási. Competition and multiscaling in evolving networks. *EPL*, 54:436–442, 2001.

V. Blondel, J.-L. Guillaume, R. Lambiotte, and E. Lefebvre. Fast unfolding of community hierarchies in large networks. *J. Stat. Mech.*, P10008, 2008.

S. Boccaletti, V. Latora, Y. Moreno, M. Chavez, and D. Hwang. Complex networks: Structure and dynamics. *Physics Reports*, 424:175–308, 2006.

M. Bogñá, R. Pastor-Satorras, A. Díaz-Guilera, and A. Arenas. Models of social networks based on social distance attachment. *Phys. Rev. E*, 70: 056122, 2004.

M. Boguñá and R. Pastor-Satorras. Class of correlated random networks with hidden variables. *Phys. Rev. E*, 68:036112, 2003.

M. Boguñá, F. Papadopoulos, and D. Krioukov. Sustaining the internet with hyperbolic mapping. *Nature Communications*, 1:62, 2010.

B. Bollobás. *Random Graphs*. Cambridge University Press, Cambridge, 2001.

J. Bonachela, S. de Franciscis, J. Torres, and M. Muñoz. Self-organization without conservation: Are neuronal avalanches generically critical? *J. Stat. Mech.*, page P02015, 2010.

P. Bonifazi, M. Goldin, M. Picardo, I. Jorquera, A. Cattani, G. Bianconi, A. Represa, Y. Ben-Ari, and R. Cossart. Gabaergic hub neurons orchestrate synchrony in developing hippocampal networks. *Science*, 326:1419, 2009.

M. Brede and S. Sinha. Assortative mixing by degree makes a network more unstable. *arXiv:cond-mat/0507710*.

S. Brush. History of the Lenz-Ising model. *Rev. Mod. Phys.*, 39:883–93, 1967.

S. Buldyrev, R. Parshani, G. Paul, H. Stanley, and S. Havlin. Catastrophic cascade of failures in interdependent networks. *Nature*, 464:1025–8, 2010.

E. Bullmore and O. Sporns. Complex brain networks: graph theoretical analysis of structural and functional systems. *Nature Reviews Neuroscience*, 10: 186–98, 2009.

Z. Burda, J. Jurkiewicz, and A. Krzywicki. Statistical mechanics of random graphs. *Physica A: Statistical Mechanics and its Applications*, 344:56–61, 2004.

G. Caldarelli, A. Capocci, P. D. L. Rios, and M. M. oz. Scale-free networks from varying vertex intrinsic fitness. *Phys. Rev. Lett.*, 89:258702, 2002.

M. Camperi and X.-J. Wang. A model of visuospatial working memory in prefrontal cortex: recurrent network and cellular bistability. *J. Comp. Neurosci.*, 5:383–405, 1998a.

M. Camperi and X.-J. Wang. A model of visuospatial working memory in prefrontal cortex: recurrent network and cellular bistability. *J. Comp. Neurosci.*, 5:383–405, 1998b.

A. Capocci and F. Colaiori. Mixing properties of growing networks and simpson's paradox. *Phys. Rev. E.*, 74:026122, 2006.

M. Chavez, D.-U. Hwang, A. Amann, H. Hentschel, and S. Boccaletti. Synchronization is enhanced in weighted complex networks. *Phys. Rev. Lett.*, 94:218701, 2005.

G. Chechik, I. Meilijson, and E. Ruppin. Neuronal regulation: a biologically plausible mechanism for efficient synaptic pruning in development. *Neurocomputing*, 26:633, 1999.

G. Chechik, I. Meilijson, and E. Ruppin. Synaptic pruning in development: A computational account. *Neural Computation*, in press.

D. Chialvo. Critical brain networks. *Physica A: Statistical Mechanics and its Applications*, 340:756–765, 2004.

D. Chialvo. Psychophysics: Are our senses critical? *Nature Physics*, 2:301–2, 2006.

D. Chialvo, P. Balenzuela, and D. Fraiman. The brain: What is critical about it? In . E. P. L. M. Ricciardi, A. Buonocore, editor, *Collective Dynamics: Topics on Competition and Cooperation in the Biosciences*, volume 1028 of *American Institute of Physics Conference Series*, pages 28–45, 2008.

A. Compte, C. Constantinidis, J. Tegner, S. Raghavachari, M. Chafee, and *et al.* Temporally irregular mnemonic persistent activity in prefrontal neurons of monkeys during a delayed response task. *J. Neurophysiol.*, 90:3441–54, 2003.

R. Conrad. Acoustic confusion in immediate memory. *B. J. Psychol.*, 55: 75–84, 1964a.

R. Conrad. Information and acoustic confusion and memory span. *B. J. Psychol.*, 55:429–32, 1964b.

J. Cortes, P. Garrido, H. Kappen, J. Marro, C. Morilla, D. Navidad, and J. Torres. Algorithms for identification and categorization. *AIP Conf. Proc.*, 779:178, 2005.

J. Cortes, J. Torres, J. Marro, P. Garrido, and H. Kappen. Effects of fast presynaptic noise in attractor neural networks. *Neural Comp.*, 18:614, 2006.

N. Cowan. On short and long auditory stores. *Psychological Bulletin*, 96: 341–70, 1984.

V. de Assis and M. Copelli. Dynamic range of hypercubic stochastic excitable media. *Phys. Rev. E*, 77:011923, 2008.

S. de Franciscis, S. Johnson, and J. Torres. Enhancing neural-network performance via assortativity. *Phys. Rev. E*, in press, 2011.

D. J. de S. Price. Networks of scientic papers. *Science*, 149:510–5, 1965.

I. Derényi, I. Farkas, G. Palla, and T. Vicsek. Topological phase transitions of random networks. *Physica A: Statistical Mechanics and its Applications*, 334:583–590, 2004.

D. Dominguez, M. González, E. Serrano, and F. Rodríguez. Structured information in small-world neural networks. *Phys. Rev. E*, 79:021909, 2009.

V. Domínguez-Chibetín, S. Johnson, and M. Muñoz. Hidden interactions in food-webs: Unearthing the missing links. *in preparation*, 2011.

L. Donetti and M. A. Muñoz. Detecting network communities: a new systematic and powerful algorithm. *J. Stat. Mech.: Theor. Exp.*, page P10012, 2004.

S. Dorogovtsev and J. Mendes. *Evolution of networks: From biological nets to the Internet and WWW*. Oxford Univ. Press, Oxford, 2003.

S. Dorogovtsev, A. Ferreira, A. Goltsev, and J. Mendes. Zero pearson coefficient for strongly correlated growing trees. *Phys. Rev. E*, 81:031135, 2005.

J. Duch and A. Arenas. Community identification using Extremal Optimization. *Phys. Rev. E*, 72:027104, 2005.

J. Dunne, R. Williams, and N. Martinez. Network structure and robustness of marine food webs. *Mar. Ecol. Prog. Ser.*, 273:291–302, 2004.

D. Durstewitz, J. Seamans, and T. S. and. Neurocomputational models of working memory. *Nature Neuroscience*, 3:1184–91, 2000.

V. Eguíluz, D. Chialvo, G. Cecchi, M. Baliki, and A. Apkarian. Scale-free brain functional networks. *Phys. Rev. Lett.*, 94:018102, 2005.

P. Erdös and A. Rényi. On random graphs I. *Publ. Math. Debrecen*, 6:290–7, 1959.

L. Euler. Solutio problematis ad geometriam situs pertinentis. *Acad. Sci. U. Petrop.*, 8:128–40, 1736.

I. Farkas, I. Derényi, G. Palla, and T. Vicsek. *Lect. Notes in Phys.*, 650:163, 2004.

E. Frank. Synapse elimination: For nerves it's all or nothing. *Science*, 275: 324–325, 1997.

A. Fronczak and P. Fronczak. Networks with given two-point correlations: hidden correlations from degree correlations. *Phys. Rev. E*, 74:026121, 2006.

G. G. Bianconi and A.-L. Barabási. Bose-Einstein condensation in complex networks. *Phys. Rev. Lett.*, 86:5632–5635, 2001.

M. Garey and D. Johnson. *Computers and Intractability: A Guide to the Theory of NP-Completeness*. W.H. Freeman and Company, USA, 1979.

E. Gilbert. Random graphs. *Annals of Mathematical Statistics*, 30:1141–4, 1959.

M. Girvan and M. Newman. Community structure in social and biological networks. *Proc. Natl. Acad. Sci. USA*, 99:7821–6, 2002.

J. Gómez-Gardenes, Y. Moreno, and A. Arenas. Paths to synchronization on complex networks. *Phys. Rev. Lett.*, 98:034101, 2007.

A. Gruart, M. Muñoz, and J. Delgado-García. Involvement of the ca3-ca1 synapse in the acquisition of associative learning in behaving mice. *J. Neurosci.*, 26:1077–87, 2006.

R. Guimerà, L. Danon, A. Díaz-Guilera, F. Giralt, and A. Arenas. Self-similar community structure in a network of human interactions. *Phys. Rev. E*, 68: 065103(R), 2003.

D. Hebb. *The Organization of Behavior*. Wiley, New York, 1949.

S. Hilfiker, V. Pieribone, H.-T. Kao, A. Czernik, G. Augustine, and P. Greengard. Synapsins as regulators of neurotransmitter release. *Phil. Trans. R. Soc. London B*, 354:269–79, 1999.

A. Hodgkin and A. Huxley. A quantitative description of membrane current and its application to conduction and excitation in nerve. *J. Physiol.*, 117: 500–44, 1952.

H. Holcman and M. Tsodyks. The emergence of Up and Down states in cortical networks. *PLoS Comput. Biol.*, 2:e23, 2006.

P. Holme and J. Zhao. Exploring the assortativity-clustering space of a network's degree sequence. *Phys. Rev. E*, 75:046111, 2007.

J. Hopfield. Neural networks and physical systems with emergent collective computational abilities. *Proc. Natl. Acad. Sci. USA*, 79:2554–8, 1982.

P. Hurtado, J. Marro, and P. Garrido. Demagnetization via nucleation of the nonequilibrium metastable phase in a model of disorder. *J. Stat. Phys.*, 133: 29–58, 2008.

P. R. Huttenlocher and A. S. Dabholkar. Regional differences in the synaptogensis in human cerebral cortex. *The Journal of Comparative Neurology*, 387:167–178, 1997.

E. M. Izhikevich. *Dynamical Systems in Neuroscience: The Geometry of Excitability and Bursting*. MIT Press, Cambridge MA, 2007.

E. Jaynes. Information theory and statistical mechanics. *Phys. Rev.*, 106(4): 620–630, 1957.

S. Johnson and M. Muñoz. Nestedness of networks: Null models and topological effects. *in preparation.*

S. Johnson, J. Torres, and J. Marro. Functional optimization in complex excitable networks. *EPL*, 83:46006, 2008.

S. Johnson, J. Marro, and J. Torres. Development of neural network structure with biological mechanisms. *Lecture Notes in Computer Science*, 5517:228–35, 2009a.

S. Johnson, J. Torres, and J. Marro. Nonlinear preferential rewiring in fixed-size networks as a diffusion process. *Phys. Rev. E*, 79:050104, 2009b.

S. Johnson, J. Marro, and J. Torres. Evolving networks and the development of neural systems. *J. Stat. Mech.*, P03003, 2010a.

S. Johnson, J. Torres, J. Marro, and M. Muñoz. Entropic origin of disassortativity in complex networks. *Physical Review Letters*, 104:108702, 2010b.

S. Johnson, J. Marro, and J. Torres. Cluster Reverberation: A mechanism for robust short-term memory without synaptic learning. *submitted. arXiv:1007.3122*, 2011.

M. Kaiser and C. Hilgetag. Spatial growth of real-world networks. *Phys. Rev. E*, 69:036103, 2004.

M. Kaiser, R. Martin, P. Andras, and M. Young. Simulation of robustness against lesions of cortical networks. *Eur. J. Neurosci.*, 25:3185–92, 2007.

O. Kinouchi and M. Copelli. Optimal dynamical range of excitable networks at criticality. *Nature Physics*, 2(5):348–351, 2006.

A. Klintsova and W. Greenough. Synaptic plasticity in cortical systems. *Current Opinion in Neurobiology*, 9:203, 1999.

H. Korn and P. Faure. Is there chaos in the brain? II. Experimental evidence and related models. *C. R. Biol.*, 326:787, 2003.

G. Kossinets and D. Watts. *Science*, 311:88–90, 2006.

P. L. Krapivsky, S. Redner, and F. Leyvraz. Connectivity of growing random networks. *Phys. Rev. Lett.*, 85:4629–4632, 2000.

V. Krebs. *unpublished, http://www.orgnet.com/*.

A. Kwag and O. Paulsen. The timing of external input controls the sign of plasticity at local synapses. *Nat Neurosci.*, 12:1219–21, 2009.

J. D. L. Danon, A. Díaz-Guilera, and A. Arenas. Comparing community structure identification. *J. Stat. Mech.*, P09008, 2005.

K. Lee, F. Schottler, M. Oliver, and G. Lynch. Brief bursts of high-frequency stimulation produce two types of structural change in rat hippocampus. *J. Neurophysiol.*, 44:247, 1980.

Levine and R.D. *Molecular Reaction Dynamics*. Cambridge University Press, Cambridge, 2005.

B. Lindner, J. García-Ojalvo, A. Neiman, and L. Schimansky-Geier. Effects of noise in excitable systems. *Phys. Rep.*, 392:321, 2004.

D. Lusseau, K. Schneider, O. J. Boisseau, P. Haase, E. Slooten, and S. Dawson. The bottlenose dolphin community of doubtful sound features a large proportion of long-lasting associations. *Behavioral Ecology and Sociobiology*, 54:396–405, 2003.

P. J. Magistretti. Neuroscience. low-cost travel in neurons. *Science*, 325:1349–51, 2009.

R. Malenka and R. Nicoll. Long-term potentiation – a decade of progress? *Science*, 285:1870–4, 1999.

Marcus and G.F. *The Algebraic Mind: Integrating Connectionism and Cognitive Science*. MIT Press, Cambrigde and MA, 2001.

J. Marro and R. Dickman. *Nonequilibrium Phase Transitions in Lattice Models*. Cambridge.

J. Marro, J. Torres, and J. Cortes. Complex behavior in a network with time-dependent connections and silent nodes. *J. Stat. Mech.*, page P02017, 2008.

S. Maslov, K. Sneppen, and A. Zaliznyak. Pattern detection in complex networks: correlation profile of the internet. *Physica A*, 333:529–40, 2004.

R. May. *Stability and Complexity in Model Ecosystems*. Princeton University Press, Princeton, 1973.

W. McCulloch and W. Pitts. A logical calculus of the ideas immanent in nervous activity. *Bulletin of Mathematical Biophysics*, 7:115–33, 1943.

J. Mejias and J. Torres. Maximum memory capacity on neural networks with short-term synaptic depression and facilitation. *Neural Comput.*, 21:851–71, 2009.

J. Mejias, H. Kappen, and J. Torres. Irregular dynamics in up and down cortical states. *PLoS ONE*, 5 (11):e13651, 2010.

E. Meron. Pattern formation in excitable media. *Phys. Rep.*, 218:1, 1992.

S. Milgram. The Small World problem. *Psychology Today*, 1:61–67, 1967.

Y. Miyashita. Neuronal correlate of visual associative long-term memory in the primate temporal cortex. *Nature*, 335:817–20, 1988.

G. Mongillo, O. Barak, and M. Tsodyks. Synaptic theory of working memory. *Science*, 319:1543–6, 2008.

R. Morgan and I. Soltesz. Nonrandom connectivity of the epileptic dentate gyrus predicts a major role for neuronal hubs in seizures. *Proc. Nat. Acad. Sci. USA*, 105:6179, 2008.

A. Motter, C. Zhou, and J. Kurths. Network synchronization, diffusion, and the paradox of heterogeneity. *Phys. Rev. E*, 71:016116, 2005.

M. Muñoz, R. Juhasz, C. Castellano, and G. Odor. Griffiths phases on complex networks. *Phys. Rev. Lett.*, 105:128701, 2010.

M. Newman. Mixing patterns in networks. *Phys. Rev. E*, 67:026126, 2003a.

M. Newman. Assortative mixing in networks. *Phys. Rev. Lett.*, 89:208701, 2002.

M. Newman. Power laws, Pareto distributions and Zipf's law. *Contemporary Physics*, 46:323, 2005.

M. Newman. *Random graphs as models of networks, in Handbook of Graphs and Networks, S. Bornholdt and H.G. Schuster (eds.)*. Wiley-VCH, Berlin, 2003b.

M. Newman. The structure and function of complex networks. *SIAM Review*, 45:167–256, 2003c.

M. Newman. The structure of scientific collaboration networks. *Proc. Natl. Acad. Sci. USA*, 98:404–9, 2001.

M. Newman and J. Park. Why social networks are different from other types of networks. *Phys. Rev. E*, 68:036122, 2003.

M. E. J. Newman. Finding community structure in networks using the eigenvectors of matrices. *Preprint physics/0605087*, 2006.

T. Nishikawa, A. Motter, Y.-C. Lai, and F. Hoppensteadt. Heterogeneity in oscillator networks: Are smaller worlds easier to synchronize? *Phys. Rev. Lett.*, 91:014101, 2003.

L. Onsager. Crystal statistics. I. A two-dimensional model with an order-disorder transition. *Phys. Rev.*, (2) 65:117–49, 1944.

L. Pantic, J. Torres, H. Kappen, and S. Gielen. Associative memory with dynamic synapses. *Neural Comp.*, 14:2903, 2002.

J. Park and M. Newman. Origin of degree correlations in the internet and other networks. *Phys. Rev. E*, 68:026112, 2003.

J. Park and M. E. J. Newman. Statistical mechanics of networks. *Phys. Rev. E*, 70:066117, 2004.

K. Park, Y.-C. Lai, and N. Ye. Self-organized scale-free networks. *Phys. Rev. E*, 72:026131, 2005.

R. Pastor-Satorras and A. Vespignani. *Evolution and structure of the Internet: A statistical physics approach*. Cambridge Univ. Press, Cambridge, 2004.

R. Pastor-Satorras, A. Vázquez, and A. Vespignani. Dynamical and correlation properties of the internet. *Phys. Rev. Lett.*, 87:258701, 2001.

T. Peixoto. Redundancy and error resilience in boolean networks. *Phys. Rev. Lett.*, 104:048701, 2010.

T. Pereira. Hub synchronization in scale-free networks. *Phys. Rev. E*, 82: 036201, 2010.

P. Peretto. *An Introduction to the Modeling of Neural Networks*. Cambridge Univ. Press, Cambridge, 1992.

P.Gleiser and L. Danon. Community structure in Jazz. *Adv. Complex Syst.*, 6:565, 2003.

J. Poncela, J. Gmez-Gardees, L. Floría, A. Sánchez, and Y. Moreno. Complex cooperative networks from evolutionary preferential attachment. *PLoS ONE*, 3(6):e2449, 2008.

S. Ree. Generation of scale-free networks using a simple preferential-rewiring dynamics. *Physica A: Statistical Mechanics and its Applications*, 376:692–698, 2007.

J. Reichardt and S. Bornholdt. Statistical mechanics of community detection. *Phys. Rev. E*, 74:016110, 2006.

A. Rodríguez-Moreno and O. Paulsen. Spike timing-dependent long-term depression requires presynaptic nmda receptors. *Nat Neurosci.*, 11:744–5, 2008.

M. D. Roo, P. Klauser, P. Mendez, L. Poglia, and D. Muller. Activity-dependent PSD formation and stabilization of newly formed spines in hippocampal slice cultures. *Cerebral Cortex*, 18:151–161, 2008.

Y. Roudi and P. Latham. A balanced memory network. *PLoS Comput. Biol.*, 3.

A. Rozenfeld, R. Cohen, D. ben Avraham, and S. Havlin. Scale-free networks on lattices. *Phys. Rev. Lett.*, 89:218701, 2002.

K. Sakai and Y. Miyashita. Neuronal organization for the long-term memory of paired associates. *Nature*, 354:152–5, 1991.

I. Sendina-Nadal, J. Buldú, I. Leyva, and S. Boccaletti. Phase locking induces scale-free topologies in networks of coupled oscillators. *PLoS ONE*, 3:e2644, 2008.

D. Sherrington and S. Kirkpatrick. Solvable model of a spin-glass. *Phys. Rev. Lett.*, 35:1792–6, 1975.

S. Sikström. Forgetting curves: implications for connectionist models. *Cognitive Psychology*, 45:95–152, 2002.

H. A. Simon. On a class of skew distribution functions. *Biometrika*, 42:425–40, 1955.

B. Söderberg. General formalism for inhomogeneous random graphs. *Phys. Rev. E*, 66:066121, 2002.

G. Sperling. The information available in brief visual persentation. *Psychological Monographs: General and Applied*, 74:1–30, 1960.

O. Sporns, D. R. Chialvo, M. Kaiser, and C. C. Hilgetag. Organization, development and function of complex brain networks. *Trends in Cognitive Sciences*, 8:418–425, 2004.

K. Suchecki, V. Eguíluz, and M. S. Miguel. Conservation laws for the voter model in complex networks. *EPL*, 69:228–34, 2005.

G. Süel, J. Garcia-Ojalvo, L. Liberman, and M. Elowitz. An excitable gene regulatory circuit induces transient cellular differentiation. *Nature*, 440:545–50, 2006.

G. Sugihara and H. Ye. Complex systems: Cooperative network dynamics. *Nature*, 458:979–80, 2009.

E. Tarnow. Short term memory may be the depletion of the readily releasable pool of presynaptic neurotransmitter vesicles. *Cognitive Neurodynamics*, 3: 263–9, 2008.

J.-N. Teramae and T. Fukai. A cellular mechanism for graded persistent activity in a model neuron and its implications for working memory. *J. Comp. Neurosci.*, 18:105–21, 2005.

S. Thurner, F. Kyriakopoulos, and C. Tsallis. *Phys. Rev. E.*, 76:036111, 2007.

J. Torres and P. Varona. *Modeling Biological Neural Networks, in Handbook of Natural Computing, ed. G. Rozenberg et al.* Springer Verlag, Berlin, Germany, 2010.

J. Torres, M. Muñoz, J. Marro, and P. L. Garrido. Influence of topology on the performance of a neural network. *Neurocomputing*, 58-60:229–234, 2004.

J. Torres, J. Cortes, J. Marro, and H. Kappen. Competition between synaptic depression and facilitation in attractor neural networks. *Neural Computation*, 19:2739–55, 2007.

J. Torres, J. Marro, J. M. Cortes, and B. Wemmenhove. Instabilities in attractor networks with fast synaptic fluctuations and partial updating of the neurons activity. *Neural Nets.*, 21:1272–77, 2008.

J. Torres, J. Marro, and S. de Franciscis. Chaos in heterogeneous networks with temporally inert nodes. *Int. J. Bifur. Chaos*, 19:677–86, 2009.

M. Tsodyks, K. Pawelzik, and H. Markram. Neural networks with dynamic synapses. *Neural Comp.*, 10:821–35, 1998.

N. van Kampen. *Stochastic Processes in Physics and Chemistry.* Elsevier Science, Amsterdam, 1992.

F. Vazquez, V. Eguíluz, and M. S. Miguel. Generic absorbing transition in coevolution dynamics. *Phys. Rev. Lett.*, 100:108702, 2008.

T. Vogels, K. Rajan, and L. Abbott. Neural network dynamics. *Annu. Rev. Neurosci.*, 28:357–76, 2005.

X.-J. Wang. Synaptic reverbaration underlying mnemonic presistent activity. *TRENDS in Neurosci.*, 24:455–63, 2001.

D. J. Watts and S. H. Strogatz. Collective dynamics of 'small-world' networks. *Nature*, 393:440–442, 1998.

J. White, E. Southgate, J. N. Thomson, and S. Brenner. The structure of the nervous system of the nematode c. elegans. *Philosophical transactions Royal Society London*, 314:1–340, 1986.

J. Wixted and E. Ebbesen. On the form of forgetting. *Psychological Science*, 2:409–15, 1991.

J. Wixted and E. Ebbesen. Genuine power curves in forgetting: A quantitative analysis of individual subject forgetting functions. *Memory & Cognition*, 25: 731–9, 1997.

S. R. y Cajal. *Histology of the Nervous System of Man and Vertebrates.* Oxford University Press, Oxford, 1995.

C. Zhou, A. Motter, and J. Kurths. Universality in the synchronization of weighted random networks. *Phys. Rev. Lett.*, 96:034101, 2006a.

C. Zhou, L. Zemanová, G. Zamora, C. Hilgetag, and J. Kurths. Hierarchical organization unveiled by functional connectivity in complex brain networks. *Phys. Rev. Lett.*, 97:238103, 2006b.